1976

Analytical and Experimental Investigation of Thermosyphon Solar Hot Water Systems

William E. Clark
University of Central Florida

ANALYTICAL AND EXPERIMENTAL INVESTIGATION OF THERMOSYPHON SOLAR HOT WATER SYSTEMS

BY

WILLIAM E. CLARK
B.S.E., Florida Technological University, 1975

THESIS

Submitted in partial fulfillment of the requirements
for the degree of Master of Science in Engineering
in the Graduate Studies Program of
Florida Technological University

Orlando, Florida
1976

ABSTRACT

A computer simulation of a thermosyphon system allowing load drawoff and non-ideal weather conditions has been developed. The model is restricted to the more common single cover, flat plate collector system. Using an analysis based on the present literature, this model calculates the energy absorbed by the collector, the temperature distribution through the system, and the corresponding flow rate.

Experimental data for a non-ideal day is compared to the computer simulation. Results of this comparison indicate that the desired parameters, flow rate, collector inlet and outlet temperatures, and the mean tank temperature can be predicted by this model to within 10 percent.

ACKNOWLEDGEMENTS

Since this work would not have resulted if it were not for the work of many people, I would like to acknowledge those who have been so helpful. Special thanks is extended to my thesis advisor, Dr. Bruce Nimmo, for allowing me the opportunity to become involved in solar research and for lending his moral and academic support in the development of the following analysis. Certainly, Jeff Pearce is owed a great deal for offering his expert assistance in computer programming and the confirmation of many of the equations used in this text. As a fellow student, he has also made the "trip up the river without a paddle" a more enjoyable one. The work of Mike Hackathorn and Rick Larsen in assisting me to obtain experimental data is greatly appreciated.

Thanks is also given my thesis committee members, Dr. Ronald Evans, Dr. Richard Rapson, and Dr. Harold Klee for their time spent evaluating this report.

Much gratitude is extended to Peggy Semo for the many hours she spent typing this paper.

Finally, I wish to offer a special thank you to my wife, Fran, for bearing with me through the preparation of this paper.

TABLE OF CONTENTS

LIST OF FIGURES

LIST OF VARIABLES

A_c	collector surface area
A_i	circumferential area of node i of storage tank
B	distance between tube centers
C	convection coefficient
C_a	lumped capacitance of absorber and fluid per unit area
c_a	lumped capacitance of absorber and fluid
c_p	specific heat of working fluid
d	inside tube diameter
d_o	outside tube diameter
E_{LOAD}	energy supplied by the storage tank to the load
ΔE_{TANK}	daily energy increase of storage tank
F	fin efficiency
F'	collector efficiency factor
F_{i-j}	configuration factor
f	friction factor
g	gravitation constant
H_f	total friction head around flow circuit
H_T	total thermosyphon head
h_f	film coefficient on inside of tubes
h_i	friction head contributed by section i of collector tube

h_{cij}	convection coefficient from node i to node j
h_{rij}	radiation coefficient from node i to node j
h_w	wind convection coefficient
I	incident radiation on collector surface
I_o	incident radiation normal to the collector surface
I_T	energy transmitted through the cover plate
K	extinction coefficient of cover plate ;
	conductivity of collector absorber sheet
K_T	conductivity of storage tank insulation
K_3	conductivity of collector back insulation
k_i	friction loss coefficient
L	thickness of cover plate ;
	total length of tubing in collector
l_i	length of section i of collector tube
M_L	mass of fluid supplied to the load
M_T	mass of fluid in storage tank
$\dot{m}$	system flow rate
$\dot{m}_a$	system flow rate averaged over a time interval
$\dot{m}_L$	load flow rate from storage tank
$(mc)_i$	capacitance of node i
n_1	refractive index of air
n_2	refractive index of cover plate
Q_u	useful energy gain
Q_{BACK}	energy loss from back of absorber sheet

Q_{EDGE}	energy loss from absorber through edges of collector
Q_{TOP}	energy loss from top of absorber
Q_{LOSS}	total energy loss from absorber
Q_{si}	energy stored in node i of collector
Q_{cij}	energy convected from node i to node j
Q_{kij}	energy conducted from node i to node j
Q_{rij}	energy radiated from node i to node j
Re	Reynold's number
r_t	radius of tank
S	total energy absorbed by absorber plate
S_g	total energy absorbed by cover plate
S_1	energy absorbed by cover plate due to internal reflections
S_2	energy absorbed by cover plate due to multiple reflections between cover and absorber
T	local fluid temperature in collector
T_a	ambient temperature
T_{OLD}	last known value of local fluid temperature
ΔT_{avg}	temperature rise across the collector averaged over a time interval
ΔT_{LOAD}	temperature difference between hot fluid supplied to load and cold return fluid
ΔT_{TANK}	rise in mean tank temperature for the day
T_i	temperature of node i in collector
TS_i	temperature of node i in storage tank

t	optical path length through cover plate ;
	time
U_L	loss coefficient of collector
U_T	loss coefficient of storage tank
u_i	velocity in section i of collector tube
v	kinematic viscosity
W	average fin width
x	optical distance in cover plate ;
	distance along tube in collector
Δx	thickness of storage tank insulation
Δx_3	thickness of collector back insulation
y	vertical position in system
α	absorptance of absorber sheet
α_g	effective absorptance of cover plate
β	angle of refraction
γ	specific gravity
δ	thickness of absorber sheet
ε_i	emissivity of node i of collector
η	collector efficiency
η_s	system efficiency
η_{day}	daily collector efficiency
θ	angle of incidence
ρ	reflectance at incident angle θ
ρ_o	reflectance at normal incidence

ρ_i	density in section i of collector tube
ρ_s	standard value of density
σ	Stephan-Boltzman constant
τ	transmittance of cover plate
$\Delta\tau$	length of time interval

I

INTRODUCTION

Solar energy systems used for heating water primarily in residences can be categorized as either pumped or thermosyphon types. As the classification implies, pumped systems are those employing a mechanical device for circulating the working fluid. Thermosyphon types have no such devices and operate on the principle of natural circulation of the working fluid. Since no electrical power is required, the thermosyphon system is ideal for use in rural areas. A typical unit is shown in Figure 1.

Considerable work has been done in developing useful computer simulations of solar energy systems.[1-6] Compared to thermosyphon units, pumped systems analyses have received much more attention since the latter type is presently in widespread use. In order to provide a capability for transient analysis of in-service thermosyphon units, a simulation model, herein referred to as the TSP, is developed.

General thermosyphon analyses are complicated not only by a varying flow rate but by the non-ideal conditions of transient effects and load drawoff. By generating a model which accounts for these conditions, a basis for several other system simulations is

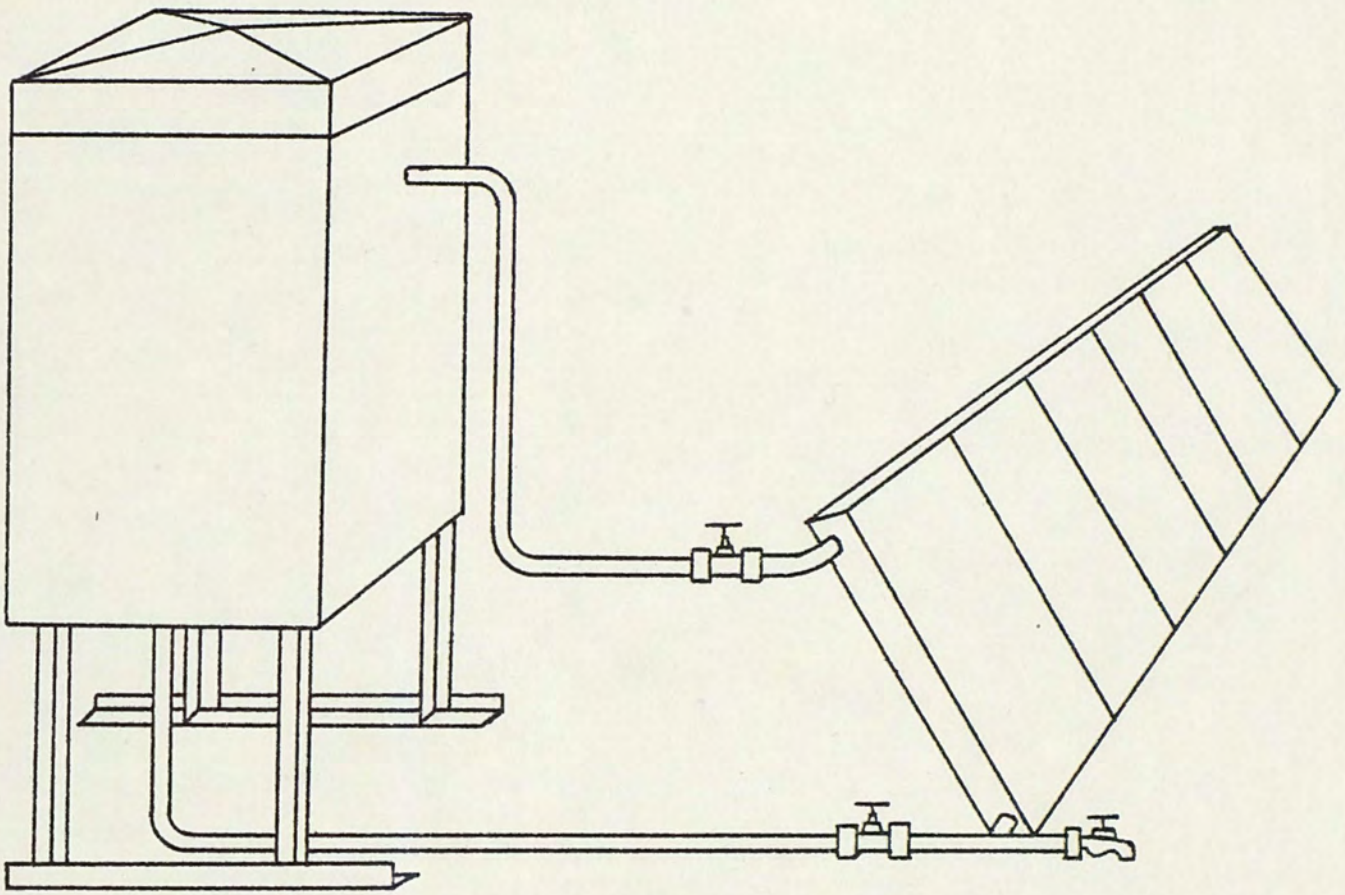

Figure 1. A Typical Thermosyphon System

established. For example, a steady state pumped system model is readily derived from the TSP by neglecting the transient effects and setting the flow rate to a constant.

Development of the equations used in the computer simulation is contained in the following four chapters. Much of the material presented is based on equations presently available in the literature, notably references 7, 8, 9. However, the overall approach to the problem is believed to be unique to this analysis.

Chapters VI and VII discuss the computer model itself and its validation. Chapter VI discusses the basic working of the model. The output parameters of the model are also presented. Chapter VII deals with verification of the TSP. Verification includes a comparison between the TSP and experimental data and a model existing in the literature.

II

SOLAR ENERGY INPUT

This chapter presents an analysis of the radiation input to a collector with a single cover plate. The energy absorbed by the primary absorber surface and the cover plate is considered.

The performance of any solar energy unit is dependent on the amount of energy it absorbs. For this analysis, it is assumed that solar radiation data is available for the tilted surface of the collector and that this data contains both direct and diffuse values. As a result of this assumption, complications arising from diffuse radiation reflected from surroundings are eliminated. The problem of obtaining the system energy input reduces to establishing the fraction of incident energy absorbed by the collector plate and the cover plate.

The cover plate on a collector serves to reduce energy losses from the primary absorber surface to the environment. In addition, if the cover material is transparent to the incoming short wavelength radiation, the cover plate will cause the collector to behave as a trap for solar radiation. There may be several covers on a collector. An increase in the number of covers reduces the energy losses. However, there is an accompanying decrease in the amount of

energy reaching the primary surface. For the sake of simplicity, this report is concerned only with a single cover system. However, analyses of energy transmission through several cover plates exist in the present literature.[10]

The transmittance of the cover plate to incident radiation can be obtained by the use of Bouguer's absorption law and reflection concepts for optically smooth surfaces.

According to Bouguer,[11] the absorption of radiation in a partially transparent medium is described as

$$\text{II.1} \qquad dI = IK\,dx$$

where I = intensity of incident light

K = extinction coefficient

x = optical thickness

Assuming the extinction coefficient is a constant throughout the material for the solar spectrum, an integration along the optical path (refer to Figure 2) yields:

$$\text{II.2} \qquad \frac{I_2}{I_1} = e^{-Kt}$$

where I_1 = radiation intensity at point 1

I_2 = radiation intensity at point 2

t = optical path length from point 1 to point 2

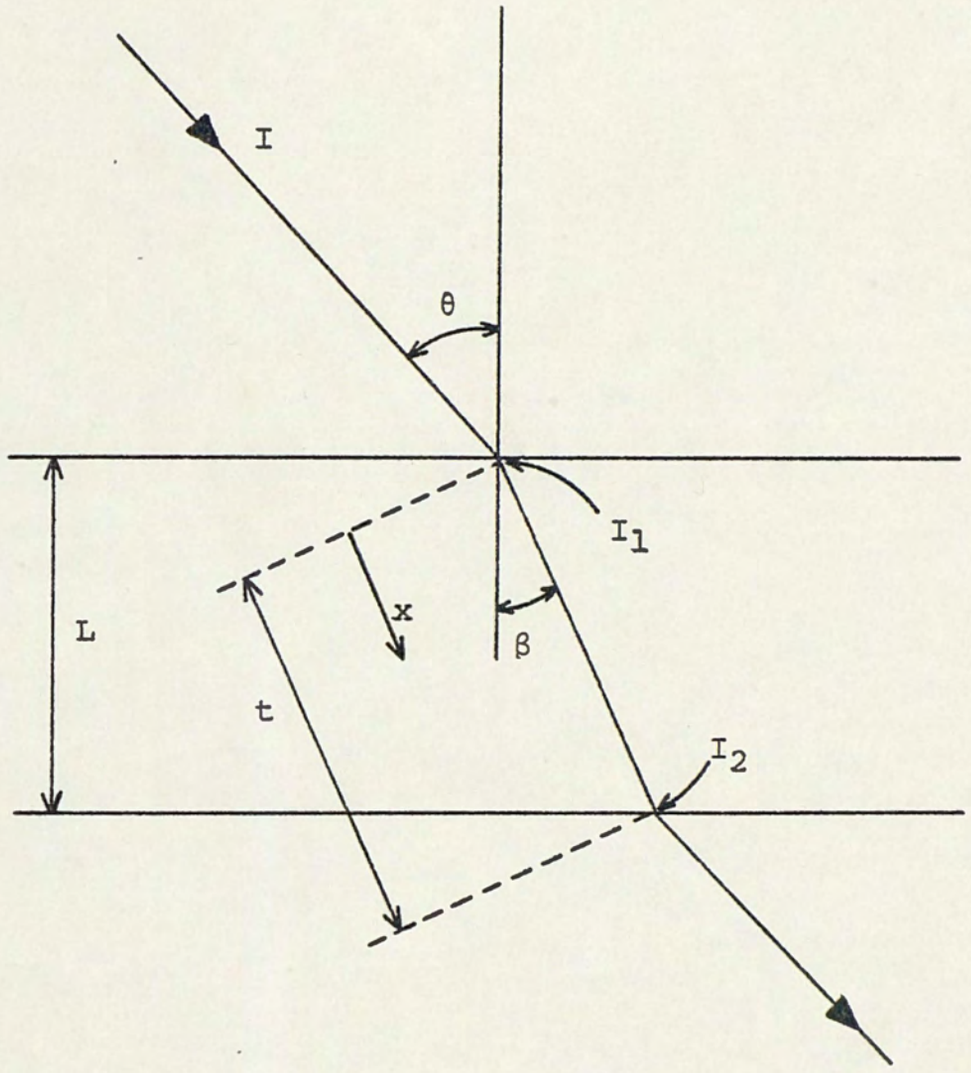

Figure 2. Transmission through Cover Plate

From Snell's law,

$$\text{II.3} \qquad \frac{\sin \beta}{\sin \theta} = \frac{n_1}{n_2}$$

where n_1 = refractive index of air

n_2 = refractive index of cover

θ = angle of incidence

β = angle of refraction

so that

$$\text{II.4} \qquad \beta = \sin^{-1}\left[\left(\frac{n_1}{n_2}\right) \sin \theta\right]$$

The optical path length, t, can now be calculated as

$$\text{II.5} \qquad t = \frac{L}{\cos \beta}$$

It now becomes obvious that the optical path length is dependent on the angle of incidence, θ. Duffie and Beckman[12] present this angle as a function of the earth's declination to the sun, the time of day, and the collector orientation. To simplify calculations, it is assumed that the optical path length remains constant. Since the measured radiation data is assumed normal to the collector surface, the path length, t, through the cover is assumed to be L, the cover thickness. This is equivalent to allowing the angles

β and θ to remain zero and considering only normal radiation values. Thus, equation II.2 becomes

$$\text{II.6} \qquad \frac{I_2}{I_1} = e^{-KL}$$

In addition to the absorption effect, there exists an effect due to reflection. We can employ Fresnel's relation for the reflection of radiation passing from medium one to medium two if we assume

1. the cover plate is optically smooth
2. incident radiation is composed of two linearly polarized components.

For an incident angle θ

$$\text{II.7} \qquad \rho = \frac{1}{2}\left[\frac{\sin^2(\beta - \theta)}{\sin^2(\beta + \theta)} + \frac{\tan^2(\beta - \theta)}{\tan^2(\beta + \theta)}\right]$$

where β is defined by equation II.3

ρ = reflectance at incident angle θ

Under the assumption that radiation data is for the plane of the collector surface, θ and β will again be considered zero for this analysis. Equations II.7 and II.3 can be combined to yield the reflectance for normal incidence, ρ_o,

$$\text{II.8} \qquad \rho_o = \left[\frac{n_1 - n_2}{n_1 + n_2}\right]^2$$

This is the reflection of normal incidence for one interface of the cover plate. There is also a reflection at the second interface. Neglecting absorption, the amount of energy transmitted into the material from the first interface is proportional to $(1 - \rho)$ as shown in Figure 3. Of this, an amount proportional to $(1 - \rho)\rho$ is reflected back into the material at the second interface. At the same surface, a quantity proportional to $(1 - \rho)(1 - \rho)$ leaves the material. There are an infinite number of these reflections occuring at the two surfaces.

Applying equation II.6 to each of these reflected components, the radiation component transmitted through the cover material can be calculated (refer to Figure 4). Summing all terms representing transmission of energy through the cover material and considering only the normal reflectance yields

$$\text{II.9} \qquad I_T = (I - \rho_o)^2 e^{-KL} I_o + (1 - \rho_o)^2 \rho_o^2 e^{-3KL} I_o +$$

$$(I - \rho_o)^2 \rho_o^4 e^{-5KL} I_o + \ldots$$

where I_T = transmitted energy

I_o = incident energy normal to the collector

$$\text{or} \qquad I_T = (1 - \rho_o)^2 I_o \sum_{n=0}^{\infty} \rho_o^{2n} e^{-(2n+1)KL}$$

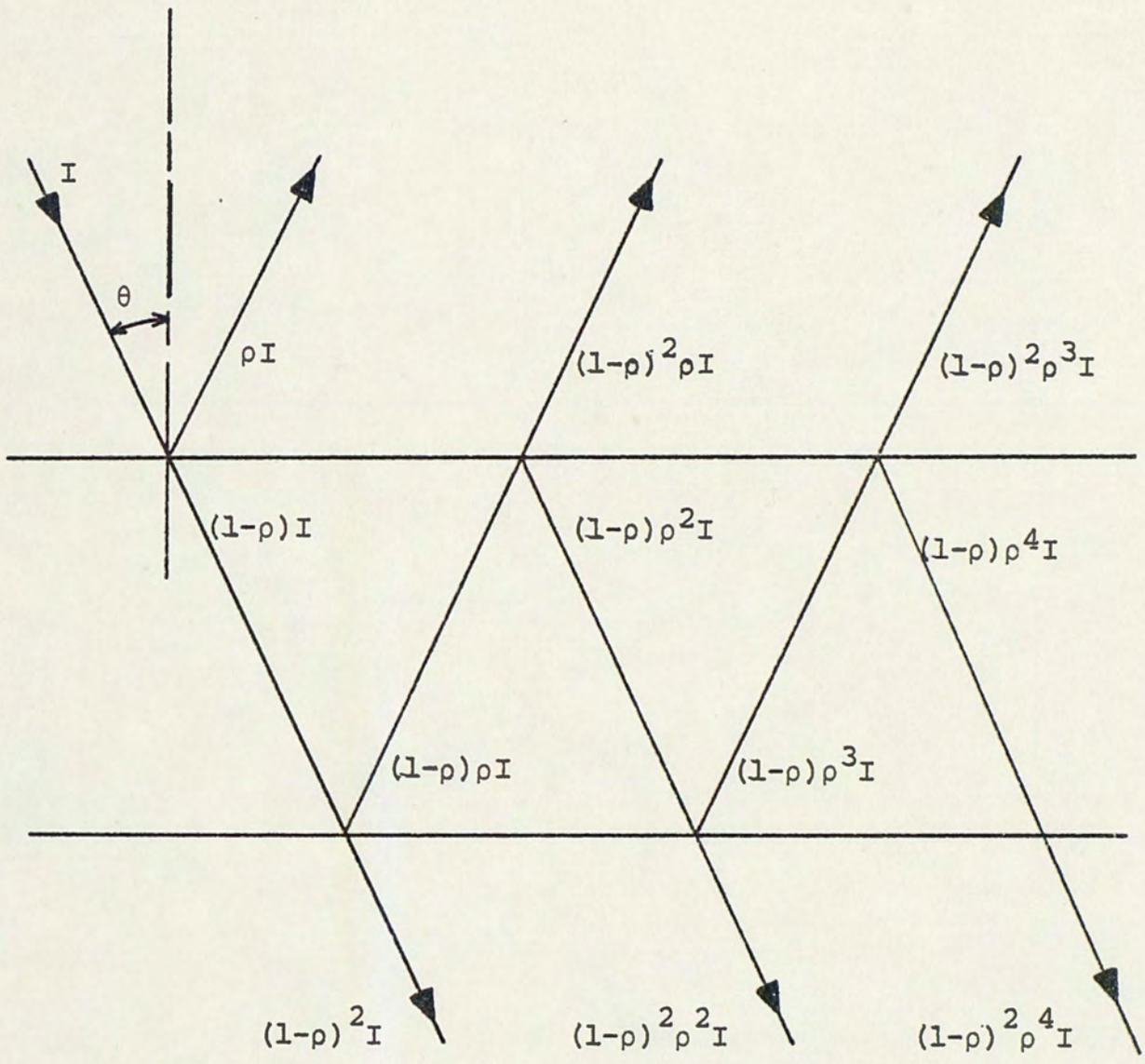

Figure 3. Transmission through Cover Plate due to Reflectance

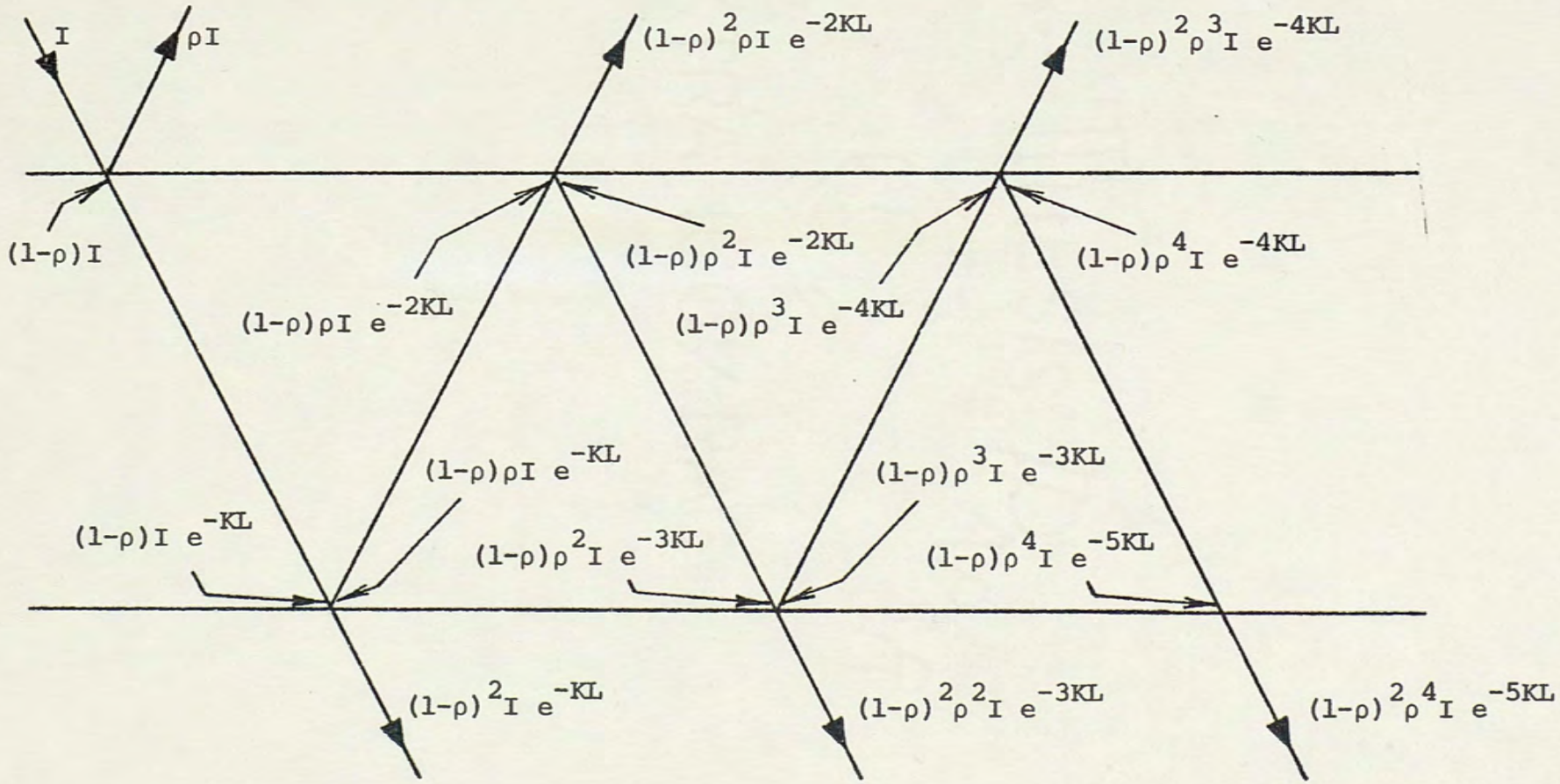

Figure 4. Transmission through Cover Plate due to Reflectance and Absorptance

This can be rearranged to yield

$$I_T = (1 - \rho_o)^2 I_o e^{-KL} \sum_{n=0}^{\infty} (\rho_o e^{-KL})^{2n}$$

For positive values of K and L, the quantity $(\rho_o e^{-KL})$ is always less than one. Therefore, this sum can be expanded to yield

$$\text{II.10} \qquad I_T = \left[\frac{(1 - \rho_o)^2 e^{-KL}}{1 - (\rho_o e^{-KL})^2}\right] I_o = \tau I_o$$

where τ represents the transmittance of the cover plate to incident radiation I_o.

The energy transmitted through the cover plate, I_T, strikes the absorber plate. Some of this energy is absorbed by the plate and some is reflected back to the cover material. Multiple reflections occur between the absorber and the cover as shown in Figure 5. Assuming the primary absorber surface absorbs a fixed fraction, α , of all incident radiation, and considering only normal reflectance, the total energy it absorbs becomes the sum

$$\text{II.11} \qquad S = \tau\alpha I_o + \tau\alpha(1 - \alpha)\rho_o I_o + \tau\alpha(1 - \alpha)^2 \rho_o^2 I_o + \ldots$$

or $$S = \tau\alpha I_o \sum_{n=0}^{\infty} (1 - \alpha)^n \rho_o^n$$

Since α and ρ_o are less than one, then the quantity $(1 - \alpha)\rho_o$ is less than one. Therefore, the above sum can be expanded to yield

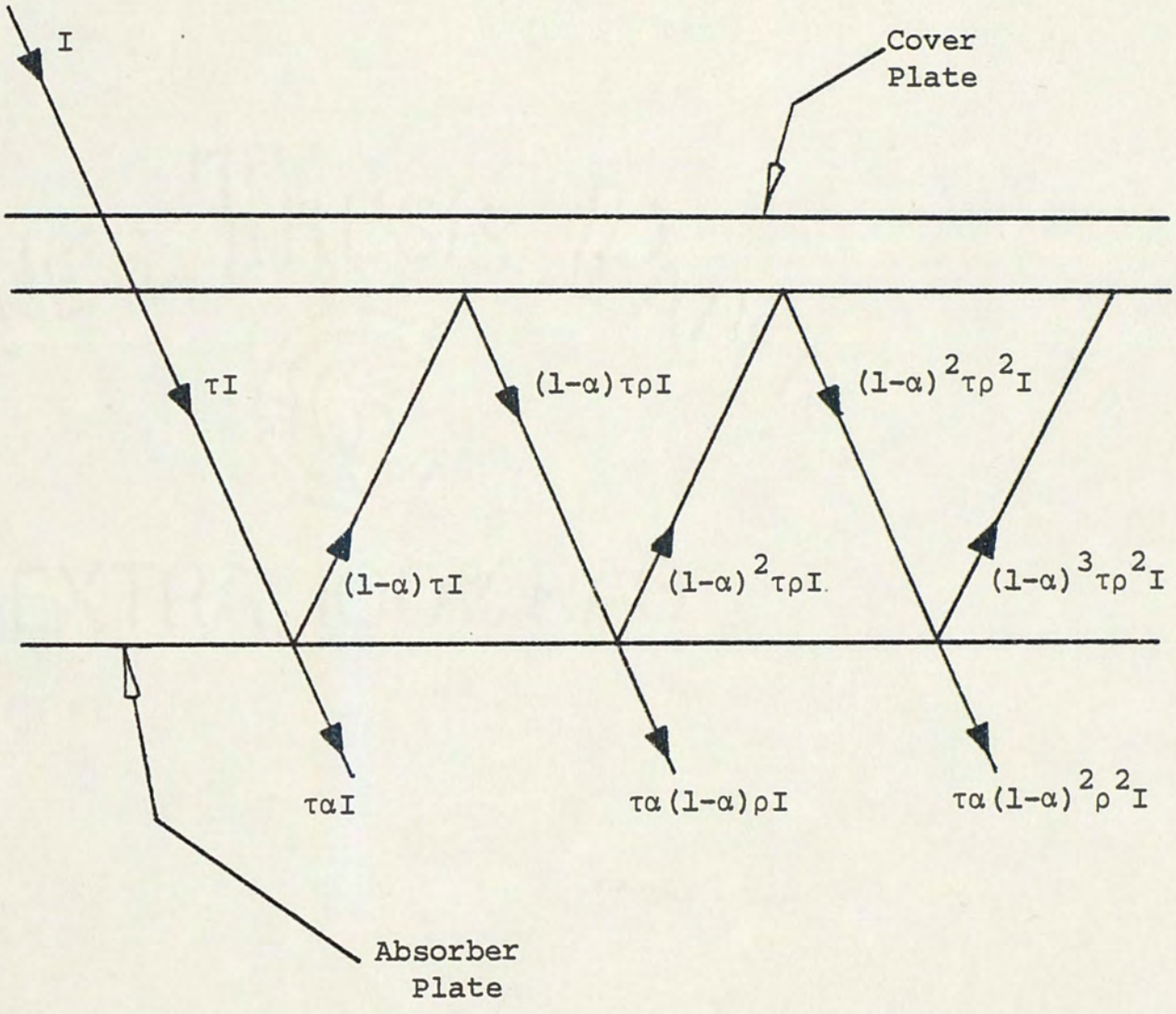

Figure 5. Absorption of Solar Radiation by Primary Absorber

$$\text{II.12} \qquad S = \left[\frac{\tau\alpha}{1 - (1 - \alpha)\rho_o}\right] I_o$$

Another quantity required for the analysis is the energy absorbed by the cover plate. Consider Figure 4. Employing only normal reflectance, the amount of energy absorbed in the cover plate due to multiple reflections within the cover is the sum

$$\text{II.13} \qquad S_1 = (1-\rho_o)I_o - (1-\rho_o)e^{-KL}I_o + (1-\rho_o)\rho_o e^{-KL}I_o -$$

$$(1-\rho_o)\rho_o e^{-2KL}I_o + (1-\rho_o)\rho_o^2 e^{-2KL} - (1-\rho_o)$$

$$\rho_o^2 e^{-3KL}I_o + (1-\rho_o)\rho_o^3 e^{-3KL}I_o - (1-\rho_o)\rho_o^3 e^{-4KL}$$

$$I_o + \ldots$$

or $$S_1 = (1-\rho_o)I_o \sum_{n=0}^{\infty} \rho_o^n e^{-nKL} - (1-\rho_o)I_o \sum_{n=0}^{\infty} \rho_o^n e^{-(n+1)KL}$$

Factoring yields

$$S_1 = (1-\rho_o)I_o \sum_{n=0}^{\infty} \left[\rho_o^n (e^{-nKL} - e^{-(n+1)KL})\right]$$

This can be simplified to

$$S_1 = (1-\rho_o)(1-e^{-KL})I_o \sum_{n=0}^{\infty} (\rho_o e^{-KL})^n$$

The above sum can be expanded to yield

$$\text{II.14} \qquad S_1 = \left[\frac{(1 - \rho_o)(1 - e^{-KL})}{(1 - \rho_o e^{-KL})} \right] I_o = \alpha_g I_o$$

where α_g represents the "absorptance" of the cover plate due to the single input I_o.

Consider the energy reflected from the collector plate (refer to Figure 5) as an additional input. For normal reflectance, this additional input is the sum

$$\text{II.15} \qquad S_2' = (1 - \alpha)\tau I_o - (1 - \alpha)\tau\rho_o I_o + (1 - \alpha)^2\tau\rho_o I_o -$$

$$(1 - \alpha)^2\tau\rho_o^2 I_o + (1 - \alpha)^3\tau\rho_o^2 I_o - (1-\alpha)^3\tau\rho_o^3 I_o + \ldots$$

or

$$S_2' = \left[(1 - \alpha)\tau I_o \sum_{n=0}^{\infty} (1 - \alpha)^n \rho_o^n \right] -$$

$$\left[\tau I_o \sum_{n=0}^{\infty} (1 - \alpha)^n \rho_o^n \right] + \tau I_o$$

This can be factored to yield

$$S_2' = \left[(1 - \alpha)\tau I_o - \tau I_o \right] \left[\sum_{n=0}^{\infty} (1 - \alpha)^n \rho_o^n \right] + \tau I_o$$

The above sum can be expanded to yield

$$\text{II.16} \qquad S_2' = \left[\tau - \frac{\tau\alpha}{1 - \rho_o(1 - \alpha)}\right] I_o$$

This represents an energy input to the cover plate in addition to the direct input I_o. As such, the cover plate will absorb a fraction, α_g, of this additional energy, so that

$$\text{II.17} \qquad S_2 = \alpha_g S_2'$$

where α_g is defined in equation II.14.

The total energy absorbed by the cover plate is the sum of equations II.17 and II.14.

$$\text{II.18} \qquad S_g = S_1 + S_2$$

Making the appropriate substitutions for S_1 and S_2 and simplifying yields

$$\text{II.19} \qquad S_g = \frac{(1 - \rho_o)(1 - e^{-KL})}{1 - \rho_o e^{-KL}} \left[1 + \tau - \frac{\tau\alpha}{1 - \rho_o(1 - \alpha)}\right] I_o$$

Equations II.12 and II.19 represent the energy absorbed by the solar collector, that is, the energy absorbed by the cover plate and the absorber plate. The preceeding analysis is based on the assumption that the radiation data input is for the collector surface. By assuming the incident angle to remain zero for this type

of data, we have approximated the energy absorbed by the collector to be a fixed fraction of the incident energy.

III

COLLECTOR MODEL

The simulation of a thermosyphon solar energy system usually includes some kind of model for the collector. Performance of this model will depend on the rate of useful energy removal which, in turn, depends on the flow rate of the circulating fluid. As opposed to pumped systems, thermosyphon system analyses usually involve unknown flow rates. As will be discussed later, the solution to the flow problem is heavily dependent on the temperature distribution of the circulating fluid. Therefore, a collector model which yields such a temperature distribution through its tubes is needed. In the following analysis, a capacitance model is developed to simulate collector performance. The particular collector used for this analysis is the common tube over sheet type shown in Figure 6.

An expression for the fluid temperature distribution can be derived from a consideration of an element of the absorber plate and fluid. If the capacitance of the fluid, tube and plate are lumped into a single value, an energy balance on a tube element (refer to Figure 7) yields:

Energy in = Energy out + Energy stored

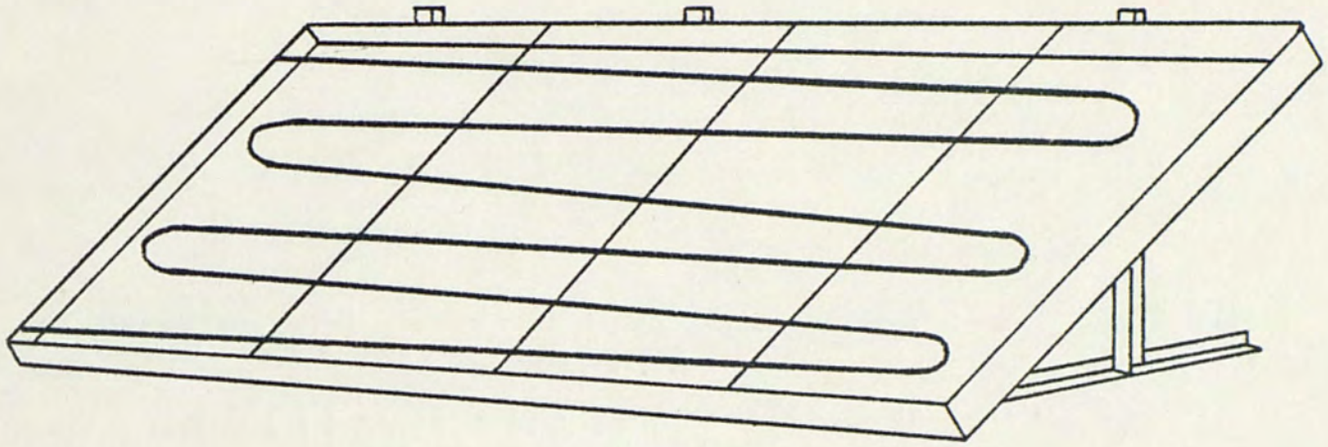

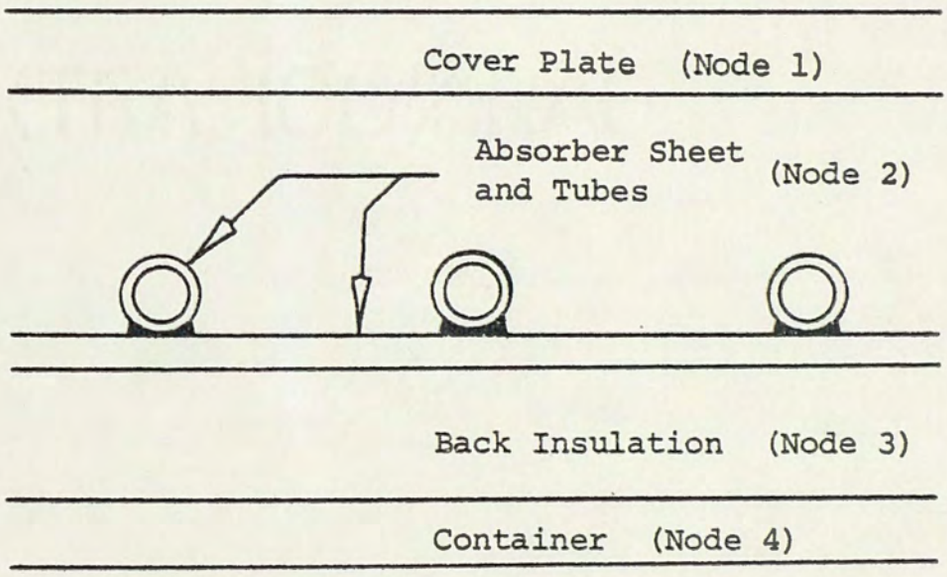

Figure 6. Tube Over Sheet Construction

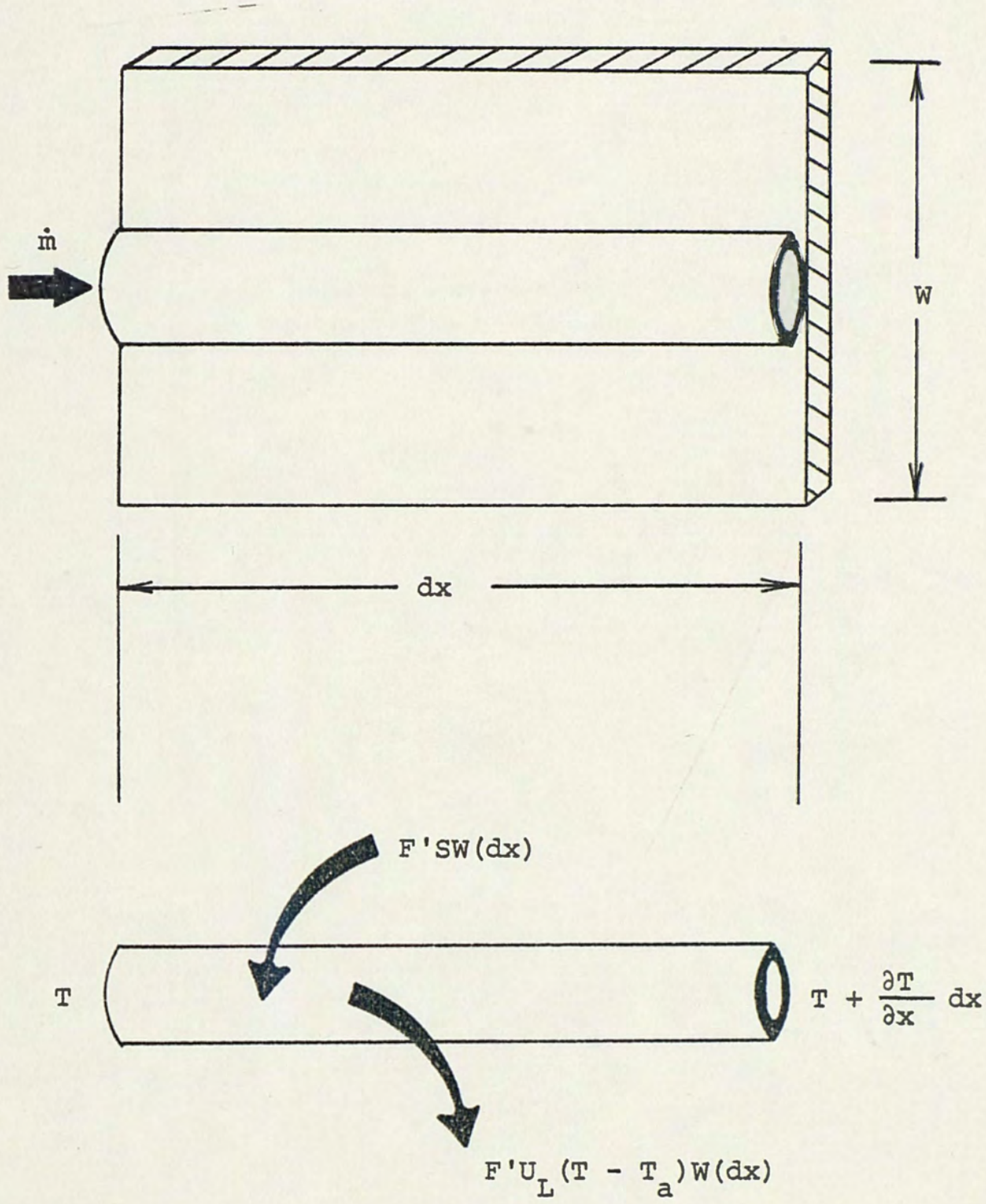

Figure 7. Energy Balance on Tube Element

III.1 $$F'SW\,dx = F'U_L(T - T_a)W\,dx + \dot{m}c_p \frac{\partial T}{\partial x}\,dx + mc_a \frac{\partial T}{\partial t}\,dx$$

where F' = collector efficiency factor

S = radiation absorbed on collector plate

W = average fin length associated with each tube

U_L = loss coefficient from plate to its surroundings

m = mass of absorber plate per unit length

$\dot{m}$ = circulating fluid flow rate

c_a = lumped capacitance value of plate + tube + fluid

x = length in flow direction

c_p = specific heat of fluid

T_a = ambient temperature

T = local fluid temperature

Letting $$W = \frac{\text{collector area}}{\text{total exposed tube length}} = \frac{A_c}{L}$$

then W becomes an averaged value of fin length associated with the tube. We can rearrange the lumped capacity value, mc_a as

$$mc_a = \frac{\text{total absorber mass}}{L} \cdot \frac{A_c C_a}{\text{total absorber mass}}$$

or $$mc_a = WC_a$$

where C_a = lumped capacitance of absorber and fluid per unit area

Rewriting and condensing equation III.1 gives the equation reported by Klein:[13]

$$\text{III.2} \qquad \dot{m}c_p \frac{\partial T}{\partial x} + WC_a \frac{\partial T}{\partial t} = F'W \left[S - U_L(T - T_a) \right]$$

The collector efficiency factor, F', represents the heat transfer resistance from the collector plate to ambient air. The development of this factor can be found in the literature. Bliss has calculated several efficiency factors for flat plate collectors.[14] For the tube over sheet case

$$\text{III.3} \qquad F' = \frac{1}{\frac{BU_L}{\pi d h_f} + \frac{1}{\frac{d_o}{B} + \frac{1}{\frac{BU_L}{U_c} + \frac{B}{(B-d_o)F}}}}$$

where B, d, d_o are shown in Figure 8

h_f = film coefficient on inside of tube

F = fin efficiency factor defined by

$$\text{III.4} \qquad F = \frac{\text{Tanh}\left[(U_L/K\delta)^{\frac{1}{2}} (B - d_o)/2\right]}{\left[(U_L/K\delta)^{\frac{1}{2}} (B - d_o)/2\right]}$$

where K = conductivity of collector sheet

δ = thickness of collector sheet

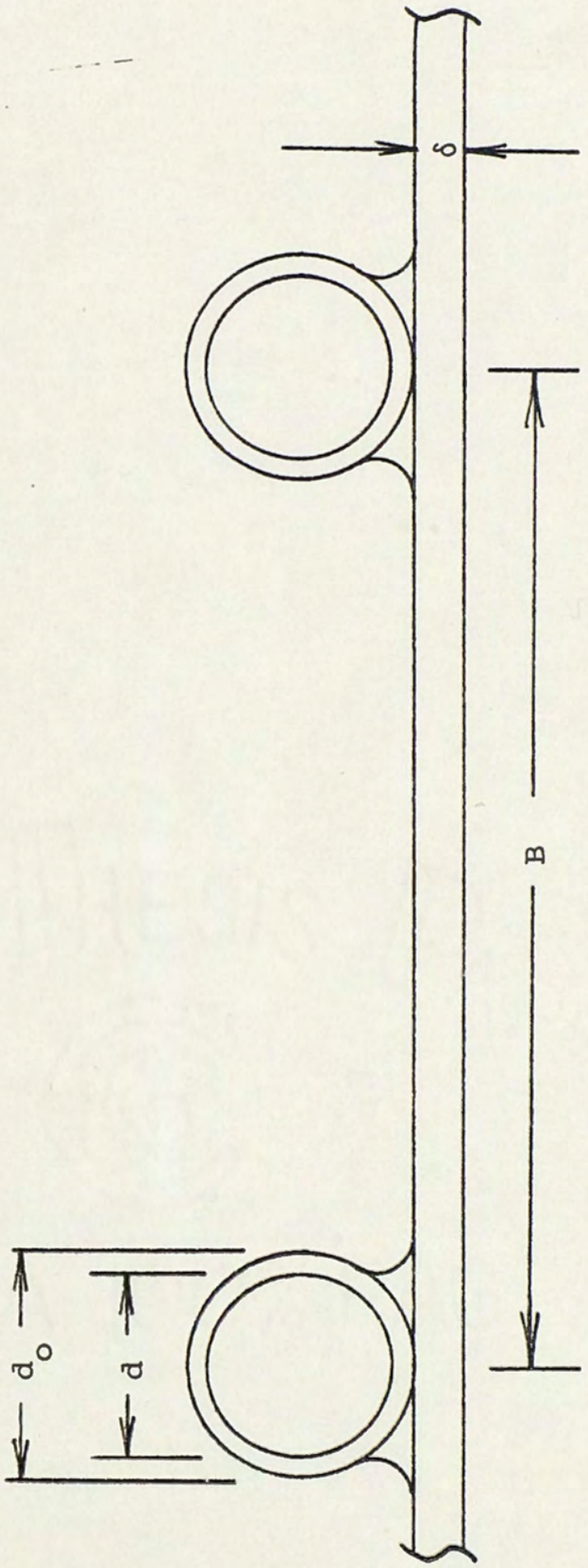

Figure 8. Tube and Sheet Dimensions

It should be noted that this efficiency factor is based on a collector having parallel tubes with unidirectional flow. In this report, the collector is assumed to have a single tube of the sinusoidal or serpentine type. Abdel-Khalik[15] has investigated heat removal factors for serpentine tube collectors. The heat removal factor, F_R, is a quantity relating actual useful energy gain of a collector to the useful gain if the whole collector were at the fluid inlet temperature. Although Abdel-Khalik does not deal with the collector efficiency factor, F', it can be related to F_R with much difficulty. However, for this report, it is assumed that the collector efficiency factor for the parallel tube collector is equal to that for the serpentine collector.

Equation III.2 can be rewritten as

$$\text{III.5} \qquad a\frac{\partial T}{\partial t} + b\frac{\partial T}{\partial x} + cT = g$$

where $a = WC_a$

$b = \dot{m}c_p$

$c = F'WU_L$

$g = F'WS + F'WU_L T_a$

Equation III.5 is a first order non-homogeneous partial differential equation with constant coefficients. The general solution of equation III.5, as developed in Appendix A, is

III.6 $$T(x,t) = e^{-\frac{c}{a}t} \phi(ax - bt) + \frac{g}{c}$$

To determine the arbitrary function ϕ, an initial or boundary condition must be specified. A reasonable initial condition is

$$T(x,t = 0) = T_{old}(x)$$

where $T(x,t = 0)$ = the temperature distribution for the beginning of the next time interval

$T_{old}(x)$ = the temperature distribution at the end of the previous time interval

Substitution of this condition into equation III.6 (refer to Appendix A) yields

III.7 $$T(x,t) = e^{-\frac{c}{a}t}\left[T_{old}(x - \frac{b}{a}t) - \frac{g}{c}\right] + \frac{g}{c}$$

for $0 \leq t \leq \Delta\tau$

Replacing the constants with the appropriate physical parameters gives

III.8 $$T(x,t) = e^{-\frac{F'U_L}{C_a}t}\left[T_{old}(x - \frac{\dot{m}c_p}{WC_a}t) - \frac{S}{U_L} - T_a\right] + \frac{S}{U_L} + T_a$$

for $0 \leq t \leq \Delta\tau$

This solution assumes constant coefficients. For a given collector, W, C_a, and c_p, will be constant. However, over an extended period of time, a real thermosyphon system collector would experience variations in ambient temperature (T_a), absorbed radiation (S), loss coefficient (U_L), collector efficiency (F'), and mass flow rate ($\dot{m}$). This being the case, equation III.8 can be considered valid only over a relatively short time period $\Delta\tau$ during which these coefficients may be treated as constants. At the end of that time period, new values of the coefficients are applied and the solution proceeds in a stepwise fashion. The new values required for T_a and S come from input data. The mass flow rate is determined from the overall system model (see Chapter V). This leaves the calculation of loss coefficient and collector efficiency factor. To obtain these two quantities in a manner consistent with the transient collector temperature distribution solution, a transient four node collector model is developed in the following paragraphs. The model yields a set of differential equations which can be solved for the various node temperatures. These temperatures lead to the loss coefficient which, in turn, leads to the collector efficiency factor.

The thermal capacitance of a single cover flat plate collector is assumed to be lumped into four nodes as shown in Figure 6. An energy balance can be written for each node. For the cover plate (node 1) an energy balance yields (refer to Figure 9)

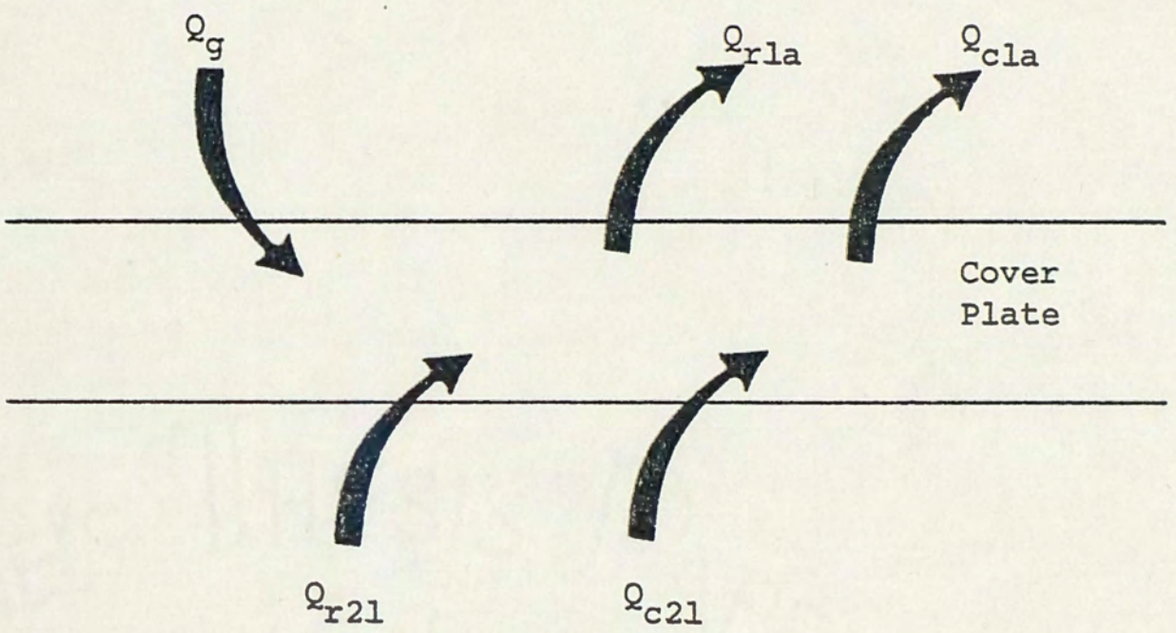

Figure 9. Energy Balance on Cover Plate

III.9 $$Q_{s1} = Q_g + Q_{r21} + Q_{c21} - Q_{r1a} - Q_{c1a}$$

where Q_g = radiation absorbed by the cover plate

Q_{r21} = net radiated energy from absorber plate to cover

Q_{c21} = convected energy from absorber plate to cover

Q_{r1a} = radiated energy from cover to ambient

Q_{c1a} = convected energy from cover to ambient

The radiation absorbed by the cover plate Q_g is

III.10 $$Q_g = A_1 S_g$$

where S_g = energy per unit area absorbed by cover plate from Chapter II

A_1 = surface area of node 1

From basic heat transfer considerations

III.11 $$Q_{r1a} = A_1 h_{r1a} (T_1 - T_a)$$

III.12 $$h_{r1a} = \varepsilon_1 \sigma (T_1^2 + T_a^2)(T_1 + T_a)$$

where ε_1 = emissivity of node 1

σ = Boltzmans constant

T_1 = temperature of node 1

T_a = ambient temperature

Similarly,

III.13 $$Q_{r21} = A_2 h_{r21} (T_2 - T_1)$$

III.14 $$h_{r21} = \frac{\sigma F_{2-1} (T_2^2 + T_1^2)(T_2 + T_1)}{(\frac{1}{\varepsilon_2} + \frac{1}{\varepsilon_1} - 1)}$$

where ε_2 = emissivity of node 2

T_2 = temperature of node 2

F_{2-1} = configuration factor from node 2 to node 1

If it is assumed that the cover plate and absorber plate are infinite planes, the configuration factor is one. Otherwise, F_{2-1} can be calculated from reference 16.

The convection term can be written as

III.15 $$Q_{c1a} = A_1 h_w (T_1 - T_a)$$

where the wind convection coefficient h_w is given by[17]

III.16 $$h_w = 1.0 + .3 \times (\text{windspeed in mph})$$

Similarly,

III.17 $$Q_{c21} = A_1 h_{c21} (T_2 - T_1)$$

where the convection coefficient h_{c21} between node 2 and node 1 is[18]

III.18 $$h_{c21} = C(T_2 - T_1)^{1/4}$$

where C = coefficient dependent on slope of collector

The energy stored in node 1 is

III.19 $$Q_{s1} = (mc)_1 \frac{dT_1}{dt}$$

where $(mc)_1$ = capacitance of node 1

Rewriting equation III.9

III.20 $$(mc)_1 \frac{dT_1}{dt} = A_1 S_g + A_2 h_{r21}(T_2 - T_1) + A_1 h_{c21}(T_2 - T_1) - A_1 h_{r1a}(T_1 - T_a) - A_1 h_w (T_1 - T_a)$$

Assuming all nodes will have a nominal common surface area A_c, equation III.20 can be written as

III.21 $$\frac{dT_1}{dt} = -\frac{A_c}{(mc)_1}(h_{r21} + h_{c21} + h_{r1a} + h_w)T_1 + \frac{A_c}{(mc)_1}(h_{r21} + h_{c21})T_2 + \frac{A_c}{(mc)_1}(S_g + h_{r1a}T_a + h_w T_a)$$

Similar analyses which can be carried out on the remaining three nodes are presented in detail in Appendix B. For convenience, only the results are presented here. For node 2 (absorber plate, tubes and fluid),

III.22 $$\frac{dT_2}{dt} = \frac{A_c}{(mc)_2}(h_{c21} + h_{r2})T_1 - \frac{A_c}{(mc)_2}(h_{c21} + h_{r2} + \frac{2K_3}{\Delta x_3})T_2$$

$$+ \frac{A_c}{(mc)_2}\left(\frac{2K_3}{\Delta x_3}\right) T_3 + \frac{A_c}{(mc)_2}\left(S + \frac{\dot{m}c_p}{A_c} T_{in} - \frac{\dot{m}c_p}{A_c} T_{out}\right)$$

where $h_{r2} = \frac{h_{r21}}{F_{2-1}}$ (refer to equation III.14)

$(mc)_2$ = capacitance of node 2

K_3 = conductivity of node 3 (back insulation)

Δx_3 = thickness of node 3

T_3 = temperature of node 3

$\dot{m}$ = mass flow

c_p = specific heat of fluid

T_{in} = collector inlet temperature

T_{out} = collector outlet temperature

S = absorbed solar energy (refer to Chapter II)

For node 3, the back insulation,

III.23 $$\frac{dT_3}{dt} = \frac{A_c}{(mc)_3}\left(\frac{2K_3}{\Delta x_3}\right) T_2 - \frac{A_c}{(mc)_3}\left(\frac{4K_3}{\Delta x_3}\right) T_3 + \frac{A_c}{(mc)_3}\left(\frac{2K_3}{\Delta x_3}\right) T_4$$

where T_4 = temperature of node 4

$(mc)_3$ = capacitance of node 3

For node 4, the pan or container,

III.24 $$\frac{dT_4}{dt} = \frac{2A_cK_3}{\Delta x_3 (mc)_4} T_3 - \frac{A_c}{(mc)_4}\left(\frac{2K_3}{\Delta x_3} + h_{r4a} + h_w\right) T_4 +$$

$$\frac{A_c}{(mc)_4} (h_{r4a} + h_w) T_a$$

where the radiation coefficient h_{r4a} is

III.25 $$h_{r4a} = \varepsilon_4 \sigma (T_4^2 + T_a^2)(T_4 + T_a)$$

Equations III.21, III.22, III.23 and III.24 constitute a set of differential equations. Rewriting them as a condensed set of equations:

$$\frac{dT_1}{dt} = a_{11}T_1 + a_{12}T_2 + b_1$$

$$\frac{dT_2}{dt} = a_{21}T_1 + a_{22}T_2 + a_{23}T_3 + b_2$$

$$\frac{dT_3}{dt} = a_{32}T_2 + a_{33}T_3 + a_{34}T_4$$

$$\frac{dT_4}{dt} = a_{43}T_3 + a_{44}T_4 + b_4$$

In matrix form

III.26 $$\begin{bmatrix} \dot{T}_1 \\ \dot{T}_2 \\ \dot{T}_3 \\ \dot{T}_4 \end{bmatrix} = \begin{bmatrix} a_{11} & a_{12} & 0 & 0 \\ a_{21} & a_{22} & a_{23} & 0 \\ 0 & a_{32} & a_{33} & a_{54} \\ 0 & 0 & a_{43} & a_{44} \end{bmatrix} \cdot \begin{bmatrix} T_1 \\ T_2 \\ T_3 \\ T_4 \end{bmatrix} + \begin{bmatrix} b_1 \\ b_2 \\ 0 \\ b_4 \end{bmatrix}$$

If these equations can be solved for the node temperatures, the energy lost from the absorber plate can be calculated and thus

a value for the collector loss coefficient, U_L, can be assigned. There are several solution methods available. For these particular equations, stability can be a problem if an explicit solution is used. Therefore, an implicit solution such as the Crank-Nicholson technique is suggested. If more accuracy in the solution is desired and computer time is not a major concern, a matrix solution can be used. Both of the above solution techniques are presented in Appendix C.

Having these node temperatures in hand for a given time interval, a corresponding loss coefficient may be developed. Consider the energy leaving the absorber plate. The total loss consists of losses through the top, edge and back:

$$\text{III.27} \qquad Q_{LOSS} = Q_{TOP} + Q_{EDGE} + Q_{BACK}$$

The top loss consists of radiative and convective terms which have been developed previously.

$$\text{III.28} \qquad Q_{TOP} = A_c h_{c12} (T_2 - T_1) + A_c h_{r2} (T_2 - T_1)$$

The only back loss term is a conductive one:

$$\text{III.29} \qquad Q_{BACK} = \frac{K_3 A_c}{\left(\frac{\Delta x_3}{2}\right)} (T_2 - T_3)$$

The following empirical relation for edge loss can be employed:[19]

III.30 $$Q_{EDGE} = (.08)\ (\text{perimeter})\,(\text{depth})\,(T_2 - T_a)$$

The loss coefficient used in equation III.2 may be expressed in terms of the heat losses as

III.31 $$U_L = \frac{Q_{TOP} + Q_{BACK} + Q_{EDGE}}{A_c (T_2 - T_a)}$$

Having the loss coefficient for one interval, the collector efficiency factor can be calculated from equation III.3. All quantities are now known for the evaluation of the local fluid temperature at any point in the collector (equation III.8).

In summary, the primary result to be obtained from this model is the temperature distribution through the collector. However, this model has also yielded other quantities which may be useful in future comparisons with data presented in the literature , such as:

1. a loss coefficient for the collector
2. mean temperature for the absorber plate (T_2)

IV

TANK MODEL

In addition to the solar collector, the storage tank constitutes a major portion of the thermosyphon system. In choosing a model to simulate tank performance, it must be recalled that the solution to the mass flow problem depends on the temperature distribution around the flow loop. Therefore, as was the case with the collector, a model yielding a temperature distribution through the storage tank is needed. In the following analysis, a capacitance model is developed to simulate tank performance. For generality, the model will allow for fluid drawoff.

If the storage tank is divided into a number of sections and the temperature of each section is determined, a suitable temperature distribution will have been obtained. In order to perform such an analysis, some simplifying assumptions will be made:

1. each section of the storage tank is well mixed
2. there are no heat exchangers or boosters in the tank
3. there are no controllers in the system to limit flow
4. fluid enters and leaves the tank as shown in Figure 10

Consider an arbitrary section of the stratified tank shown in Figure 11. The following energy balance can be written:

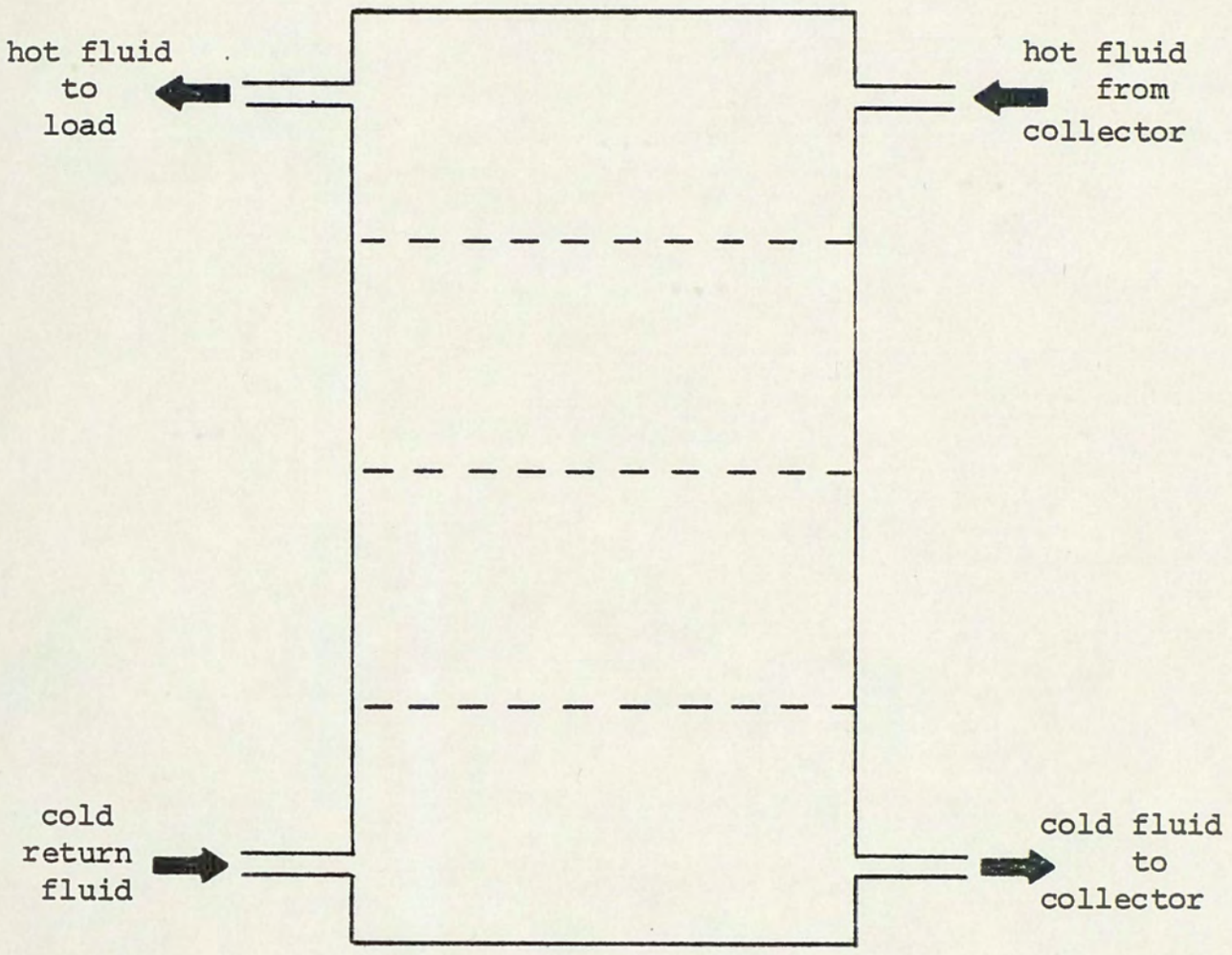

Figure 10. Stratified Storage Tank

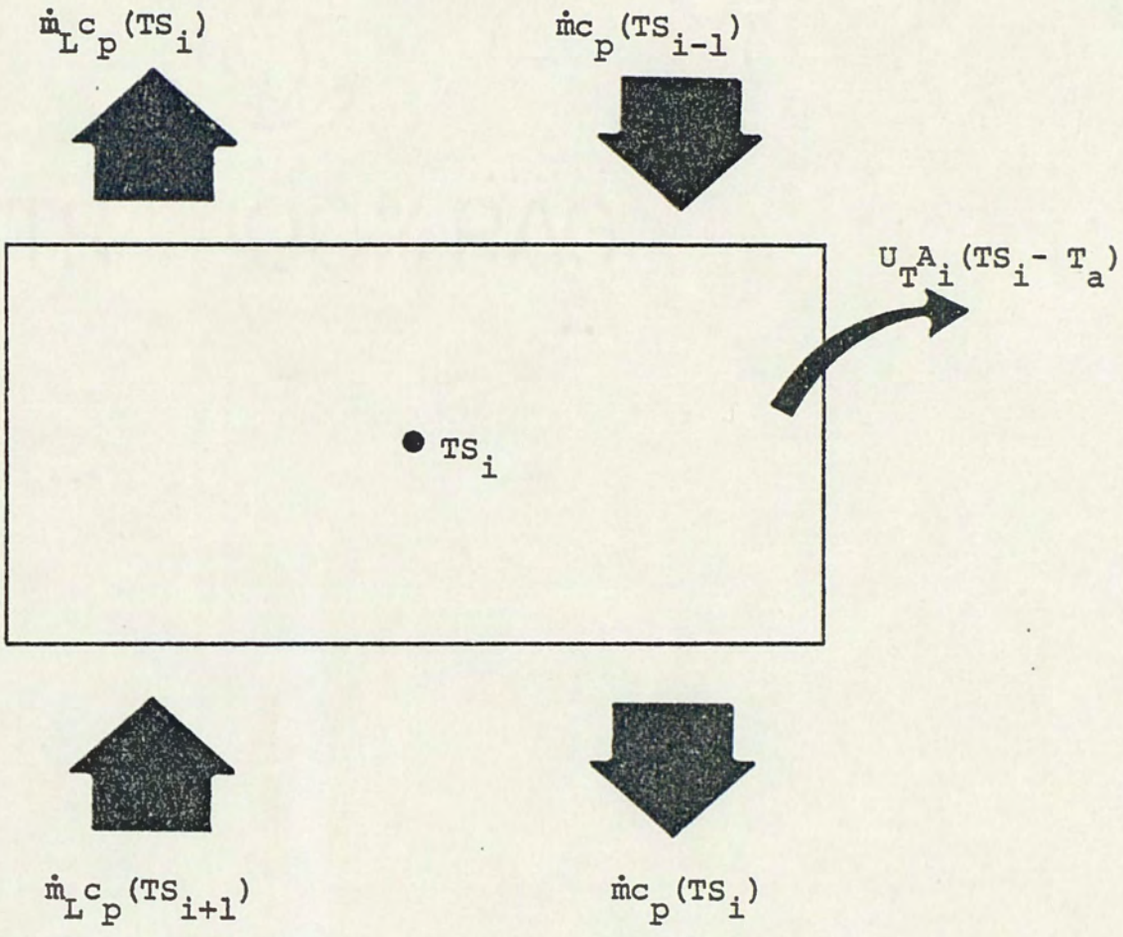

Figure 11. Energy Balance on i^{th} Section of Storage Tank

$$\text{IV.1} \qquad (mc)_i \frac{d}{dt}(TS_i) = \dot{m}c_p(TS_{i-1} - TS_i) - \dot{m}_L c_p(TS_i - TS_{i+1})$$

$$- U_T A_i (TS_i - T_a) \qquad i = 2, n-1$$

where t = time

TS_1 = temperature of section i of storage tank

$(mc)_i$ = capacitance of section i

$\dot{m}$ = flow rate of circulating fluid

c_p = specific heat of fluid

$\dot{m}_L$ = flow rate of fluid removed (drawoff)

U_T = tank loss coefficient

A_i = circumferential area of section i

T_a = ambient temperature

n = number of sections desired

For i equal to 1 (top section), equation IV.1 applies, but TS_{i-1} is replaced by the collector outlet temperature. For i equal to n (bottom section), equation IV.1 applies, but TS_{i+1} is replaced by the temperature of the makeup fluid.

To obtain a value for the tank loss coefficient, one can employ a steady state conduction analysis. By treating the tank as a simple insulated cylinder and neglecting the effect of convective films on the insulation,

$$\text{IV.2} \qquad U_T = \frac{K_t}{\ln\left[\frac{r_t + \Delta x}{r_t}\right]}$$

where K_t = conductivity of tank insulation

r_t = tank radius

Δx = thickness of insulation

After writing n equations, a set of differential equations similar in form to the collector node equations (chapter III) is obtained. Several methods of solving this set of equations are given in Appendix C. If a value for the flow rate, $\dot{m}$, can be assigned, these tank node temperatures can be found for any given time interval. In the following chapter, the problem of assigning a value for the flow rate will be addressed.

V

SYSTEM FLOW RATE

One of the problems in analyzing a thermosyphon system is the unknown flow rate of the circulating fluid. This problem will be addressed in this chapter.

Up to now, we have assumed the flow rate is known for a given time interval. Based on this assumed flow, expressions for a corresponding temperature distribution were determined for the storage tank and the collector. If some simplifying assumptions are made, one can use the results of Chapters III and IV to completely define the temperature around the flow loop. That is

1. the pipes connecting the collector and tank are well insulated
2. conduction effects along the pipe at the collector inlet and outlet are negligible
3. there is no back-syphoning or reverse flow

Under these assumptions, the temperature profile through the connecting pipes is a constant. Once flow has begun, the fluid temperature in the lower pipe (refer to Figure 1) becomes that of the tank bottom. Similarly, the fluid temperature in the upper pipe is that of the collector outlet. Now that the temperature

around the loop is specified, an analysis yielding the flow rate can be developed.

The temperature distribution around the flow loop has the general shape shown in Figure 12. Since density, in general, decreases with temperature, a corresponding density or specific gravity distribution would appear as shown in Figure 13. It is these density variations which induce thermosyphon flow or so called natural circulation. The pressure head which causes flow, herein referred to as the thermosyphon head, is proportional to the area inside the specific gravity versus position diagram. In particular,

$$V.1 \qquad H_T = \oint \gamma \, dy$$

where H_T = thermosyphon head

γ = specific gravity

y = vertical position in system

Expanding equation V.1 into sums, the integral becomes

$$V.2 \qquad H_T = \sum_{i=1}^{j} \gamma_i \, y_i \Big|_{TANK} + \sum_{i=1}^{k} \gamma_i \, y_i \Big|_{INLET} -$$

$$\sum_{i=1}^{l} \gamma_i \, y_i \Big|_{COLLECTOR} - \sum_{i=1}^{m} \gamma_i \, y_i \Big|_{OUTLET}$$

where γ_i = average specific gravity of i^{th} section

y_i = vertical distance of i^{th} section

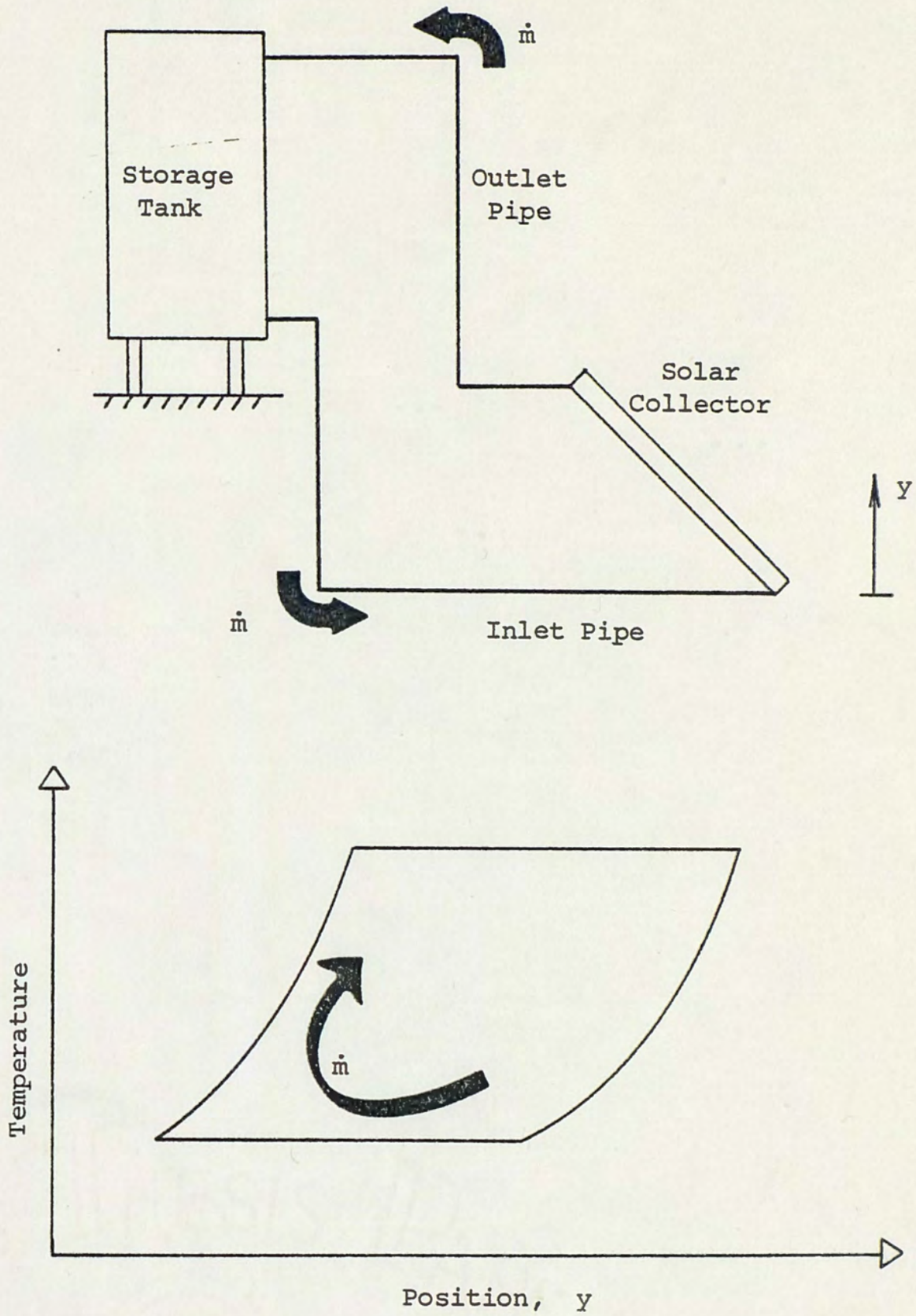

Figure 12. Temperature Distribution as a Function of Position in the System

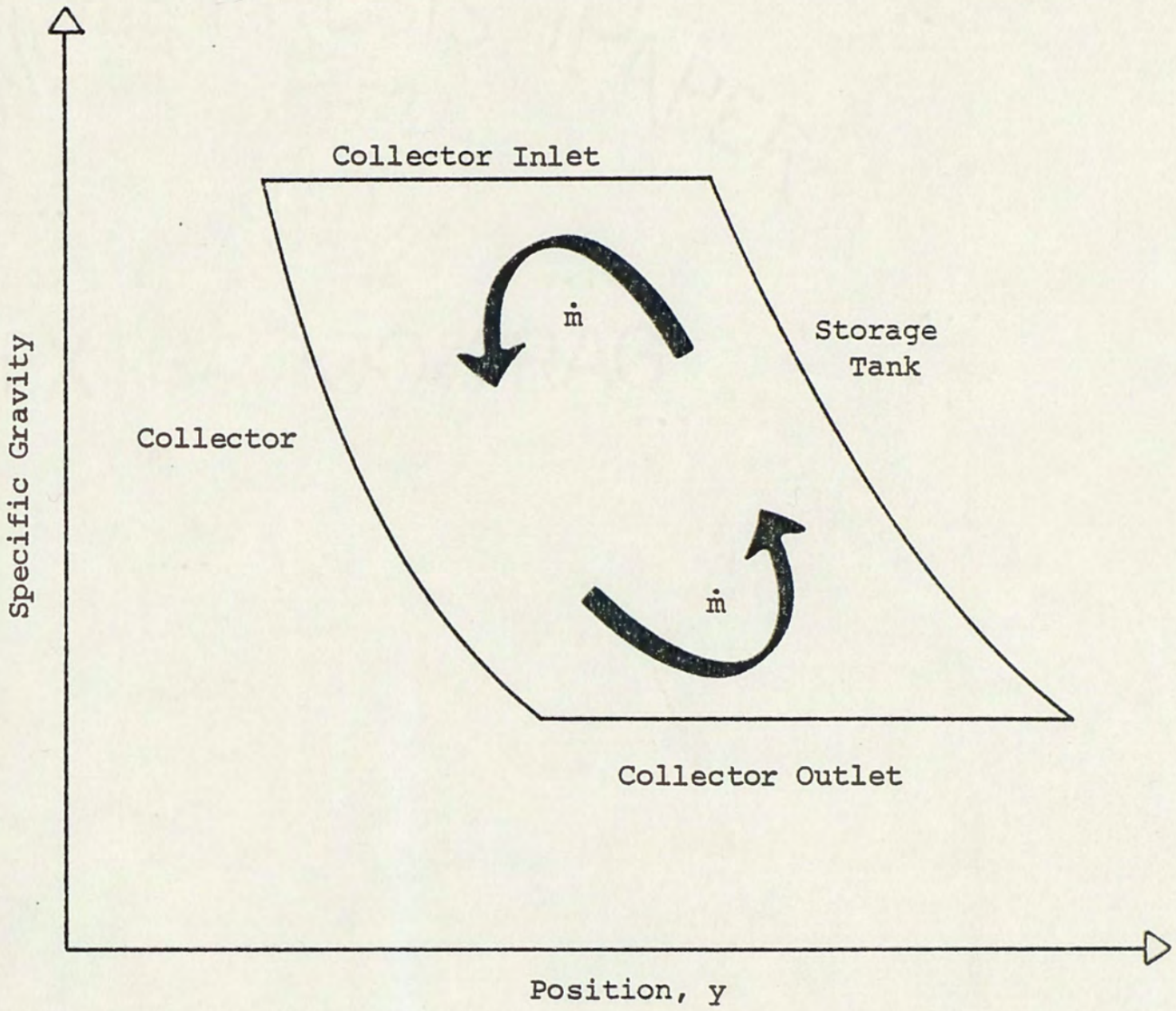

Figure 13. Specific Gravity as a Function of Position in the System

j,k,l,m = number of sections into which the tank, inlet, collector and outlet are divided respectively

Obviously, as j, k, l, and m approach infinity, equation V.2 becomes exactly equal to the thermosyphon head.

Since the temperature distribution in the pipes is assumed to be constant, it is not necessary to break them up into several sections. This is not the case for the storage tank and the collector where the temperature (and thus the specific gravity) is not a constant.

To evaluate equation V.2, the specific gravity is needed for each section around the flow loop. A temperature distribution has already been developed for the loop. Therefore, if the specific gravity is written as a function of temperature, the specific gravity at each section can be evaluated. An estimate of specific gravity is

V.3 $$\gamma = AT^n + BT^{n-1} + \ldots + Z$$

where A,B,C... = constants

For instance, if water is used as the circulating fluid, a second order polynomial representation yields

V.4 $$\gamma = AT^2 + BT + C$$

where $A = -1.116 \times 10^{-6}$

$B = 1.057 \times 10^{-3}$

$C = .7515$

T is in degrees Rankine

Substituting equation V.3 into V.2

$$V.5 \qquad H_T \cong \left[\sum_{i=1}^{i} (AT_i^n + BT_i^{n-1} + \ldots + Z)\Delta y_i\right]_{tank} +$$

$$(AT_{inlet}^n + BT_{inlet}^{n-1} + \ldots + Z) \cdot (\Delta y)_{inlet}$$

$$- \left[\sum_{i=1}^{1} (AT_i^n + BT_i^{n-1} + \ldots + Z)(\Delta y_i)\right]_{collector} -$$

$$(AT_{outlet}^n + BT_{outlet}^{n-1} + \ldots + Z)(\Delta y)_{outlet}$$

Assuming the flow rate to be quasi-steady, the thermosyphon head must equal the friction head which resists flow. That is,

$$V.6 \qquad H_T = H_f$$

where H_f = total friction head of flow loop

The total friction head is the sum of the individual friction heads in each section or length of pipe in the flow loop. Following Close[20], the Darcy Weisbach equation for the friction head in the i^{th} arbitrary section is

$$V.7 \qquad h_i = \frac{f_i l_i u_i^2}{2gd} + \frac{k_i u_i^2}{2g}$$

where f_i = friction factor in i^{th} section

l_i = length of i^{th} section

u_i = flow velocity in i^{th} section

g = gravitational constant

d = inside tube diameter

k_i = loss coefficient for bends, tees, etc., for i^{th} section

The term $\frac{k_i u_i^2}{2g}$ takes into account losses due to bends, tees, valves, and the like which are in the flow circuit. It is zero for straight sections.

Assuming thermosyphon flow is laminar, the friction factor is given as

V.8 $$f = \frac{64}{Re} = \frac{64v}{ud}$$

where Re = Reynolds number

v = kinematic viscosity

Substituting V.8 into V.7

V.9 $$h_i = \frac{32 v_i l_i u_i}{g d^2} + \frac{k_i u_i^2}{2g}$$

The flow rate is expressed as

V.10 $$\dot{m} = \rho_i A_i u_i$$

where ρ_i = density of fluid in i^{th} section

A_i = cross sectional area of pipe

u_i = velocity of fluid in i^{th} section

The cross sectional area of the pipe is just

$$A_i = \frac{\pi}{4} d_i^2 \qquad \text{V.11}$$

Equation V.11 becomes

$$\dot{m} = \frac{\rho_i u_i \pi d_i^2}{4} \qquad \text{V.12}$$

Solving for velocity u_i

$$u_i = \frac{4\dot{m}}{\rho_i \pi d_i^2} \qquad \text{V.13}$$

Substituting V.13 into V.9 yields

$$h_i = \frac{128 v_i l_i \dot{m}}{\rho_i \pi g d_i^4} + \frac{8 k_i \dot{m}^2}{\rho_i^2 \pi^2 g d_i^4} \qquad \text{V.14}$$

The total friction head of the flow circuit is then

$$H_f = \sum_{i=1}^{n} h_i = \sum_{i=1}^{n} \left\{ \frac{128 v_i l_i \dot{m}}{\rho_i \pi g d_i^4} + \frac{8 k_i \dot{m}^2}{\rho_i^2 \pi^2 g d_i^4} \right\} \qquad \text{V.15}$$

where n = total number of sections of pipe in the circuit

The summation does not include the tank sections because there is negligible friction head in the tank.

Assuming the pipe diameter remains a constant around the flow circuit, equation V.15 can be written as

$$H_f = \frac{128\dot{m}}{\pi g d^4} \left[\sum_{i=1}^{n} \frac{v_i l_i}{\rho_i} \right] + \frac{8\dot{m}^2}{\pi g d^4} \left[\sum_{i=1}^{n} \frac{k_i}{\rho_i^2} \right] \qquad \text{V.16}$$

Recall that the thermosyphon head, H_T, is equal to the friction head, H_f, so that

V.17
$$\frac{8\dot{m}^2}{\pi g d^4} \sum_{i=1}^{n} \frac{k_i}{\rho_i^2} + \frac{128\dot{m}}{\pi g d^4} \sum_{i=1}^{n} \frac{v_i l_i}{\rho_i} = H_T$$

This expression can be put in the form,

V.18
$$a\dot{m}^2 + b\dot{m} + c = 0$$

where
$$a = \frac{8}{\pi^2 g d^4} \sum_{i=1}^{n} \frac{k_i}{\rho_i^2}$$

$$b = \frac{128}{\pi g d^4} \sum_{i=1}^{n} \frac{v_i l_i}{\rho_i}$$

$$c = -H_T$$

The constants a and b contain the density ρ_i for each section. This can be converted to specific gravity for each section γ_i by

V.19
$$\rho_i = \gamma_i \rho_s$$

where ρ_s = standard value of density

so that
$$a = \frac{8}{\pi^2 g d^4 \rho_s^2} \sum_{i=1}^{n} \frac{k_i}{\gamma_i^2}$$

$$b = \frac{128}{\pi g d^4 \rho_s} \sum_{i=1}^{n} \frac{v_i l_i}{\gamma_i}$$

The b term contains a viscosity term for each section. Since temperature is known for each section, it is most convenient to express viscosity as a function of temperature just as was done previously with specific gravity. For example, if water is the circulating fluid, the following representation yields accurate values for the temperature ranges of interest:[21]

$$v = .000672 \cdot 10^{x} \qquad \frac{lbm}{ft\text{-}sec}$$

where $$x = \frac{1301}{998.333 + 8.1855(T-20) + 0.00585(T-20)^2} - 3.30233$$

$$\text{for } 0^{\circ} \leq T \leq 20^{\circ}C$$

and $$v = (.000672)(1.002)10^{y} \qquad \frac{lbm}{ft\text{-}sec}$$

where $$y = \frac{1.3272(20-T) - 0.001053(T-20)^2}{T + 105}$$

$$\text{for } 20^{\circ} \leq T \leq 100^{\circ}C$$

Solving equation V.18 for the flow rate,

$$\text{V.22} \qquad \dot{m} = \frac{-b \pm \sqrt{b^2 - 4ac}}{2a}$$

It should be noted that a and b are always positive and c is negative (assuming no reverse flow). Therefore, the quantity under the radical is positive. The two solutions for $\dot{m}$ are both real

with one positive and the other negative. The positive solution is chosen to be the desired mass flow rate. Thus,

$$\text{V.23} \qquad \dot{m} = \frac{-b + \sqrt{b^2 - 4ac}}{2a}$$

It is difficult to give the negative solution a physical interpretation. It does not represent an existing reverse flow condition because the thermosyphon head, H_T, is positive. If the thermosyphon head was negative, a reverse flow could theoretically exist. However, as this is not the case, no interpretation is given the negative solution.

To summarize, the flow rate is dependent on the temperature distribution around the flow circuit. One can relate the specific gravity to this distribution and integrate this specific gravity around the flow loop to obtain the thermosyphon head. Then, using the Darcy Weisbach relation, the friction head is related to the flow rate. Setting the friction head equal to the thermosyphon head, a solution for the flow rate is obtained. Obviously, this must be done in an iterative fashion since neither the flow rate nor the temperature distribution is known initially.

VI

COMPUTER MODEL

The constituents of a thermosyphon system are the solar collector, the storage tank and the connecting piping. The behavior of each component has been described in terms of a set of equations in Chapters III through V. As a result of the complexity and interdependence of these equations, an iterative solution technique using the digital computer is necessary to determine numerical results.

As discussed in previous chapters, the circulating fluid flow rate must be known before calculating the temperature distribution through the system. This distribution, on the other hand, determines the flow rate. After estimating a flow rate, a distribution can be generated. This leads to a better estimate of the flow rate and the process can be repeated. This is the procedure incorporated by the computer model, the TSP.

Functionally, the TSP may be broken down into three basic components. The first of these, calculation of the absorbed solar energy, is independent of the others. The other two components, namely the system temperature distribution and flow rate, are calculated iteratively as discussed earlier. A simplified flow chart

of the TSP is given in Figure 14.

The TSP requires an extensive list of input variables describing the system and the environmental operating conditions. One such input is the experimental radiation values for the tilted collector surface. Under the assumptions set forth in Chapter II, this form of incident energy input eliminates the need for calculating incident angles associated with obtaining incident beam energy normal to the collector. Having the normal radiation data, the energy absorbed by the cover plate and the absorber plate can be calculated directly.

To establish the temperature distribution through the system at the end of some time interval ($t = n\Delta\tau$), the initial ($t=0$) temperature distribution and the mean flow rate for the interval must be known. By using this previous flow rate as an estimate for the new flow rate, a final temperature distribution can be generated. This distribution is used to calculate a new flow rate value which, in turn, generates a new distribution. This continues until convergence when the calculated flow rate changes little from one solution to the next.

The determination of a temperature distribution through the system can be broken down into three basic parts, the calculation of the distribution through the collector, storage tank, and piping. The behavior of the collector is described as a set of four ordinary differential equations and a partial differential equa-

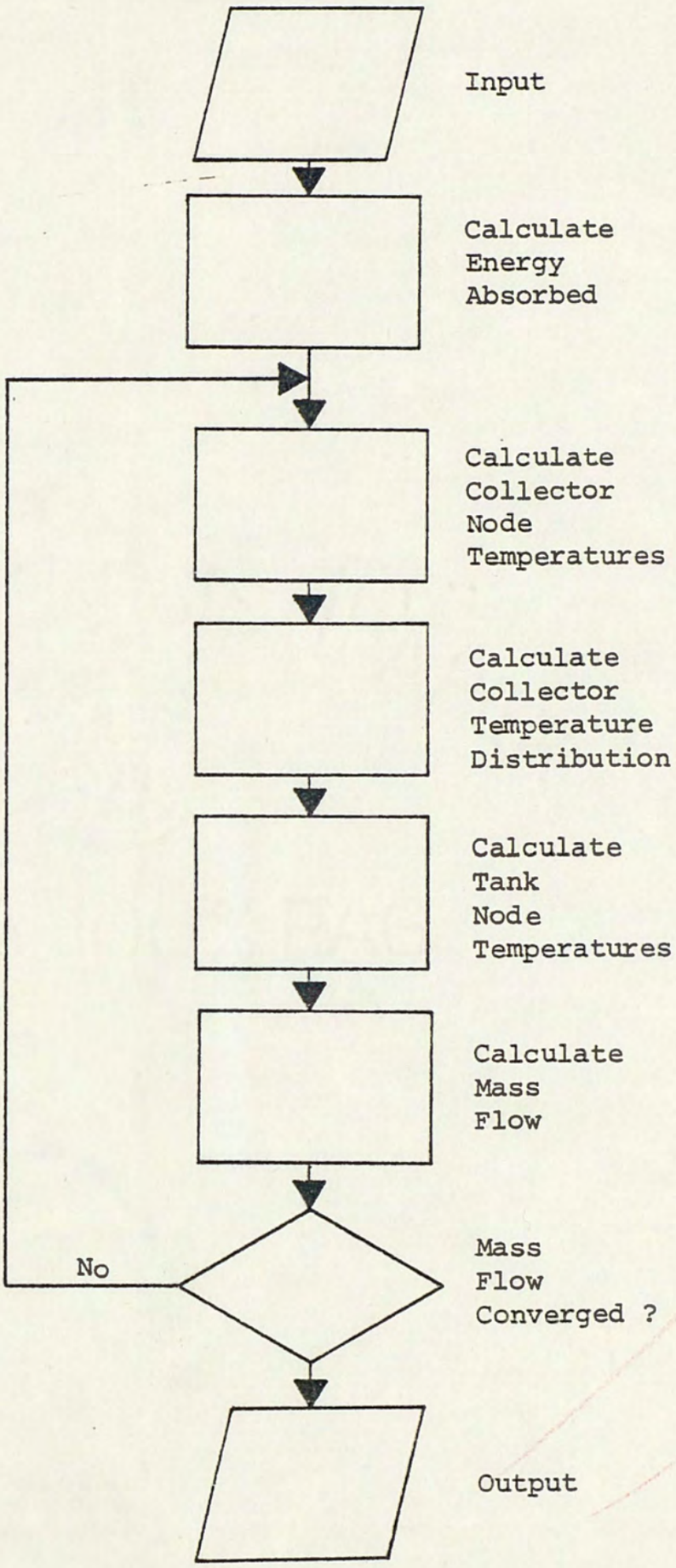

Figure 14. Simplified Flowchart of TSP

tion. The partial differential equation requires values for collector efficiency and loss coefficient which can only be assigned after solving the four ordinary differential equations.

Appendix C describes methods for solving the set of differential equations. To simplify the solution, the TSP approximates the coefficients in the set of ordinary differential equations as constants for any one time interval. From experience, it was found that the simpler predictor-corrector, an explicit numerical solution, was not stable for the collector node equations. However, the Crank-Nicholson technique, an implicit solution, was found to be in agreement with the exact solution. Although the exact solution requires several times the computation time needed by the Crank-Nicholson method, both are available in the TSP. The exact solution is composed of an infinite sum as described in Appendix C. This infinite sum must be truncated for use on a digital computer and this truncation is specified by the TSP user. It should be noted, however, that larger time steps require more terms in the sum to quarantee convergence to the correct solution.

Having solved the set of ordinary differential equations, the partial differential equation can be solved directly to yield the temperature distribution through the collector. The solution to this partial differential equation is described in Appendix A.

The behavior of the storage tank has been described as a set of n ordinary differential equations in Chapter IV. For ease of programming as well as solution accuracy, the tank was chosen to

have four sections (n = 4). The total capacitance associated with each of these equations is usually much larger than that associated with the collector's differential equations. As a result, the tank equations are much less affected by sudden changes such as load drawoff allowing the predictor-corrector method to remain stable. Therefore, in an effort to save computation time, the Adams-Moulton predictor-corrector technique is used to obtain a solution. The solution to the tank equations yields directly a temperature distribution through the storage tank.

In its present configuration, the TSP neglects pipe losses. Therefore, the temperature distribution in the piping is considered to be a constant. That is, the inlet pipe contains fluid at the tank bottom temperature, and the outlet pipe contains fluid at the collector outlet temperature.

The determination of the circulating fluid flow rate is straightforward after obtaining a temperature distribution. A numerical integration of the specific gravity around the flow loop yields the thermosyphon head. Setting this head equal to the friction head through the loop results in a solution for the flow rate.

A more complete understanding of the computer program may be obtained from the detailed flowchart presented in Appendix E.

The thermosyphon predictor program is intended to estimate performance characteristics and aid in design procedures. For this purpose, the output of the TSP contains the following parameters for the end of each time step:

1. Time
2. Flow rate through the collector ($\dot{m}$)
3. Load flow removed from the storage tank ($\dot{m}_L$)
4. Inlet temperature to the collector
5. Outlet temperature from the collector
6. Storage tank temperatures
7. Mean tank temperature
8. Insolation on the collector surface (I_o)

In addition to the above, the output contains the following parameters averaged over each time step:

1. Temperature rise across the collector (ΔT_{avg})
2. Useful energy gain from the collector (Q_u)
3. Collector efficiency (η)

Daily totals for the insolation, useful energy gain, collector efficiency, η_{day}, and a daily system efficiency, η_s, is also given.

The useful energy gain from the collector is described as

VI.1 $$Q_u = \dot{m}_a c_p \Delta T_{avg} \Delta\tau$$

where $\dot{m}_a$ = flow rate through the collector averaged over the time interval

c_p = specific heat of fluid

ΔT_{avg} = average temperature rise across the collector

$\Delta\tau$ = time step

The collector efficiency, η, is simply the useful gain for the period, Q_u, divided by the insolation, I_o over the period.

$$\text{VI.2} \qquad \eta = \frac{Q_u}{I_o}$$

Daily totals for useful energy gain, $(Q_u)_{day}$, and insolation, $(I_o)_{day}$, can be obtained by summing the individual time interval totals. The daily collector efficiency is then

$$\text{VI.3} \qquad \eta_{day} = \frac{(Q_u)_{day}}{(I_o)_{day}}$$

A daily system efficiency is described as

$$\text{VI.4} \qquad \eta_s = \frac{\Delta E_{TANK} + E_{LOAD}}{(I_o)_{day}}$$

where ΔE_{TANK} = energy increase of the storage tank over the day

E_{LOAD} = energy supplied by the storage tank to the load

The energy increase of the storage tank, ΔE_{TANK}, is

$$\text{VI.5} \qquad \Delta E_{TANK} = M_T C_p \Delta T_{TANK}$$

where M_T = mass of fluid in the storage tank

C_p = specific heat of fluid

ΔT_{TANK} = rise in mean tank temperature for the day

The energy supplied to the load, E_{LOAD}, is

VI.6 $$E_{LOAD} = M_L C_p \Delta T_{LOAD}$$

where M_L = mass of fluid supplied to the load

ΔT_{LOAD} = temperature difference between hot fluid supplied to the load and cold fluid returned to the storage tank

The preceding parameters constitute the output of the TSP. The accuracy of these predicted values will be discussed in the following chapter.

VII

MODEL VALIDATION

The following discussion presents a validation of the thermosyphon model, the TSP. This is accomplished by

1. investigating the face validity of the model
2. comparing the TSP to a model presently accepted in the literature
3. comparing experimental and predicted results

The face validity of the model can be accomplished by establishing the TSP solutions to be reasonable, non-oscillatory, and stable. It was decided that the most direct method to approach this problem was to provide the TSP with hypothetical data and observe the output closely. This test consisted of simulating the experimental system described later in this chapter and in Appendix D. Briefly, the system was composed of an 80 gallon storage tank connected to a collector with approximately 48 square feet of absorber surface.

An ideal eight hour day was simulated. The incident radiation for this day was described by

$$R = 300 \sin\left(\frac{\pi t}{8}\right) \quad \frac{BTU}{hr\text{-}ft^2} \qquad t = 0\text{-}8 \text{ hr}$$

The ambient temperature was described by

VII.2 $$T_a = 75 + 15 \sin\left(\frac{\pi t}{8}\right) \ (^{o}F) \qquad t = 0\text{-}8 \text{ hr}$$

In addition, there was no fluid removed from the storage tank for this simulation.

Given these ideal conditions, the system operation should be continuous smooth functions. Also, the flow rate and collector outlet temperature could be expected to be sinusoidal in nature following the radiation.

Figures 15-19 present radiation, collector inlet and outlet temperatures, flow rate, collector efficiency, and storage tank temperatures versus time. As these figures indicate, the TSP prediction exhibits no oscillations or instabilities. In addition, the results appear reasonable when compared to the sinusoidal insolation input.

A non-ideal day with cloud cover and load flow is simulated later in this chapter. This simulation is validated by experimental data. However, it should be noted here for the purpose of face validity no instabilities or oscillations were exhibited in the TSP predictions.

A second method of verifying a model is comparing it to other previously verified models. A thermosyphon system model presented by D. J. Close[22] has become widely accepted. Close's model assumes the ideal cases of no drawoff from the tank and the sun is not obscured by cloud or haze. Briefly, the model consists of two differential equations. Employing analytical expressions for insola-

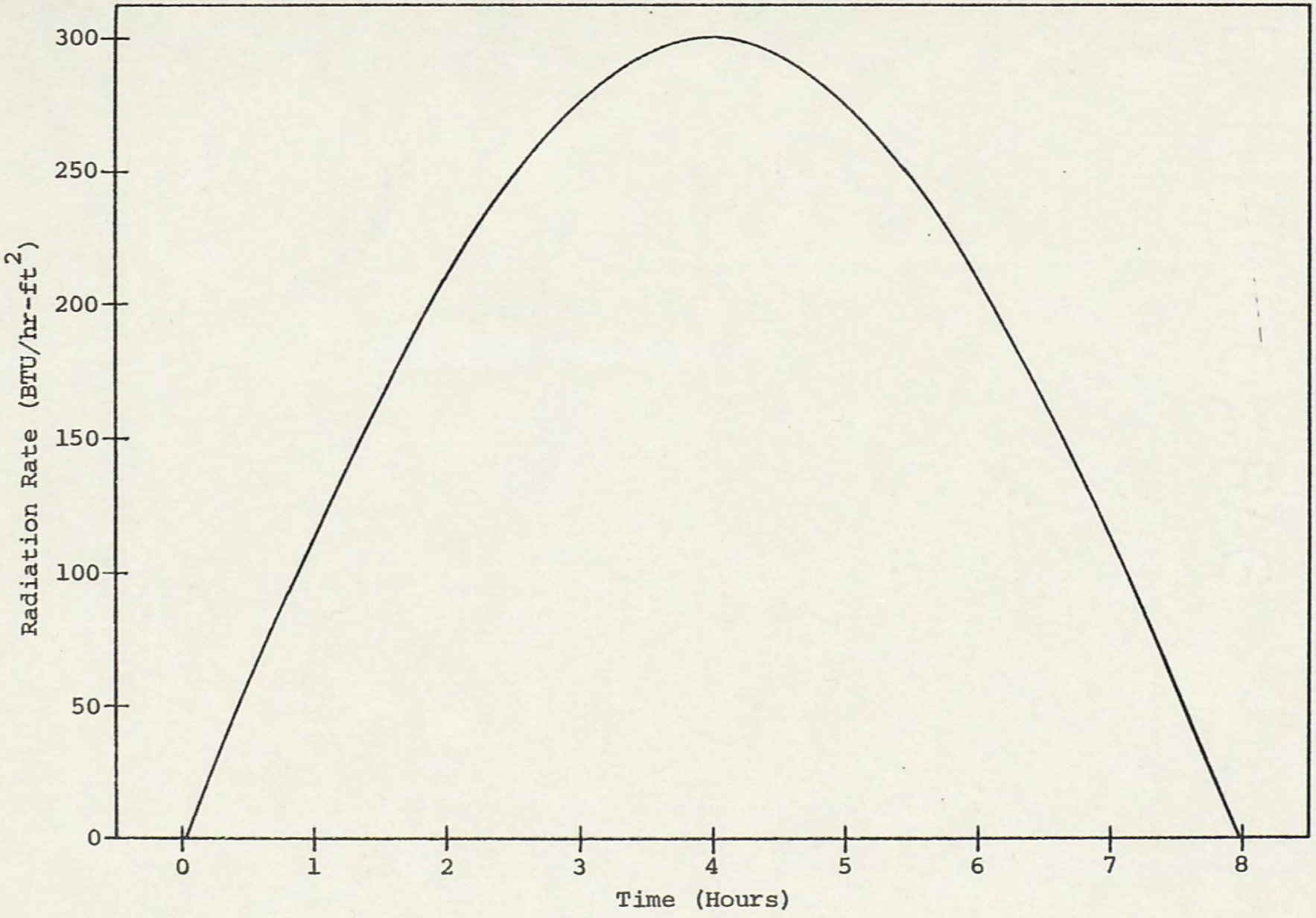

Figure 15. Radiation versus Time for Ideal Day

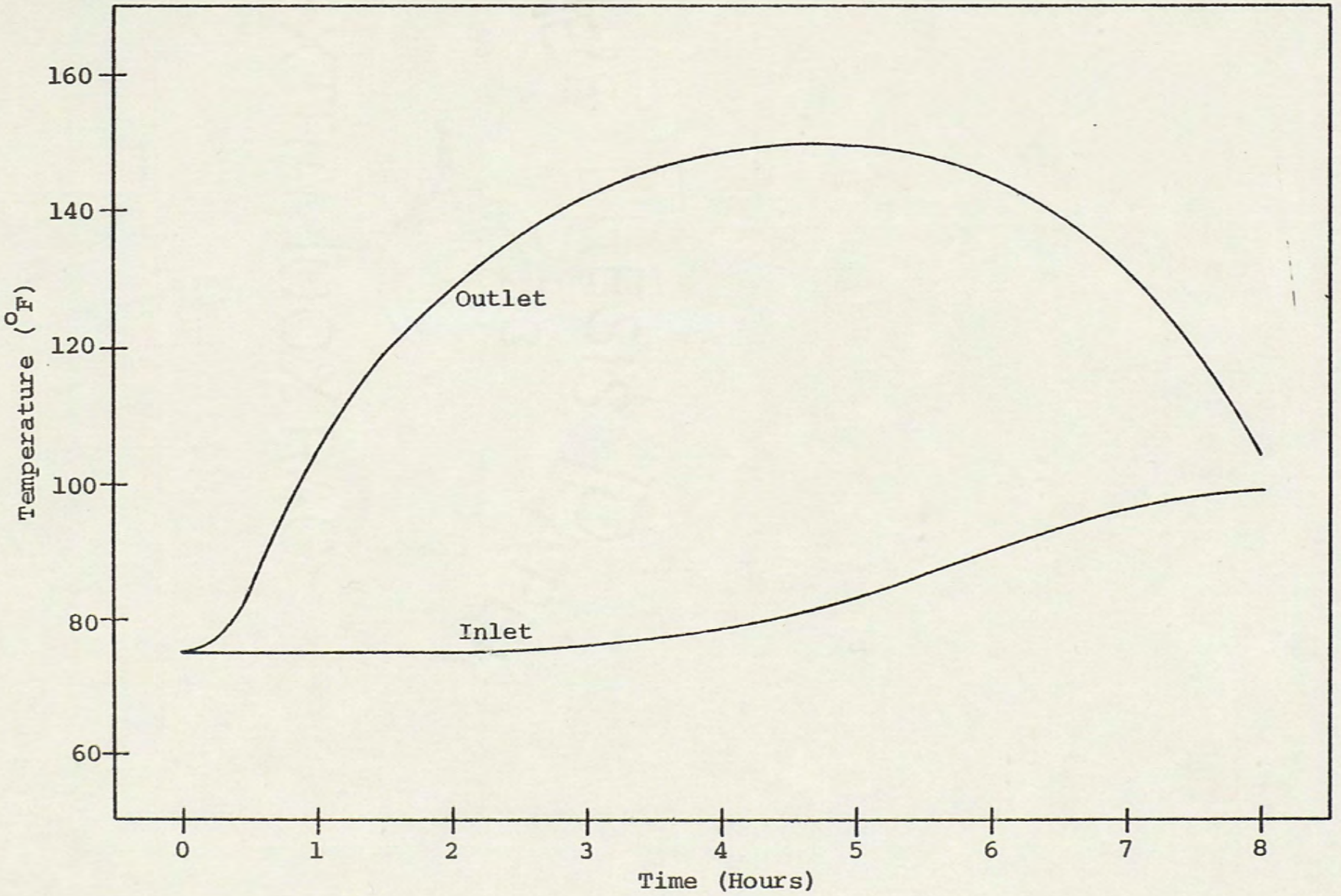

Figure 16. Collector Inlet and Outlet Temperatures versus Time for Ideal Day

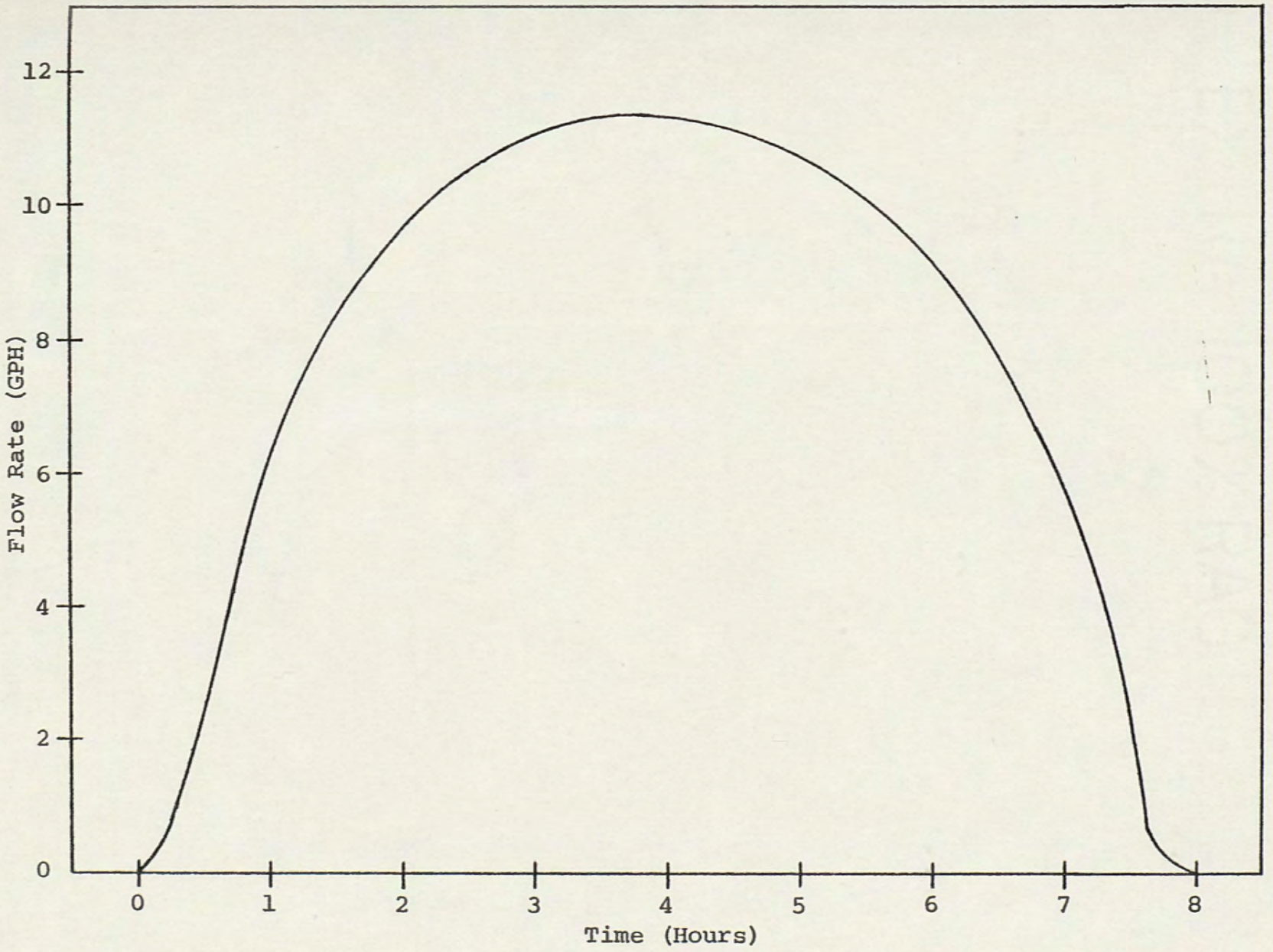

Figure 17. Collector Flow Rate versus Time for Ideal Day

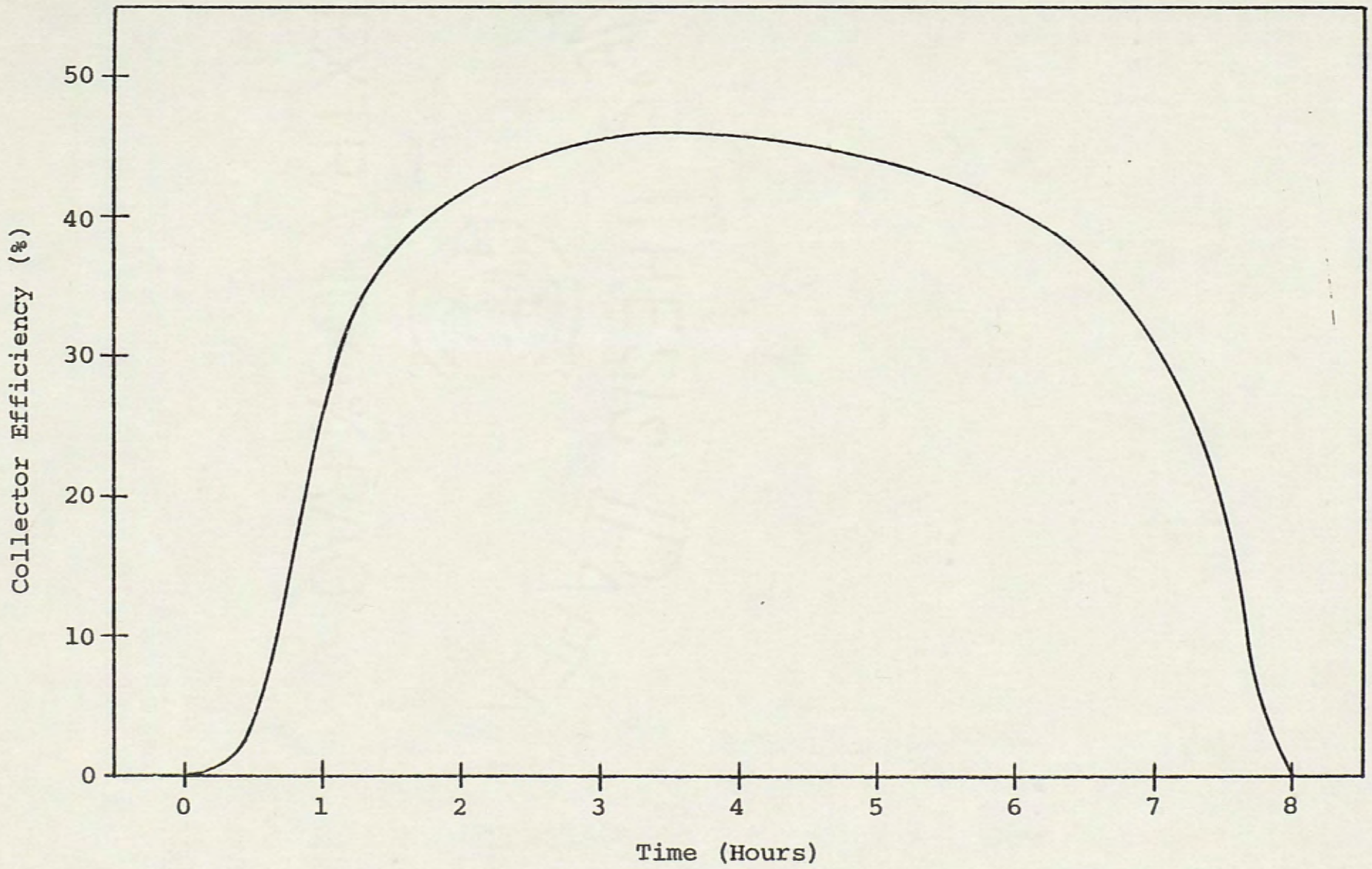

Figure 18. Collector Efficiency versus Time for Ideal Day

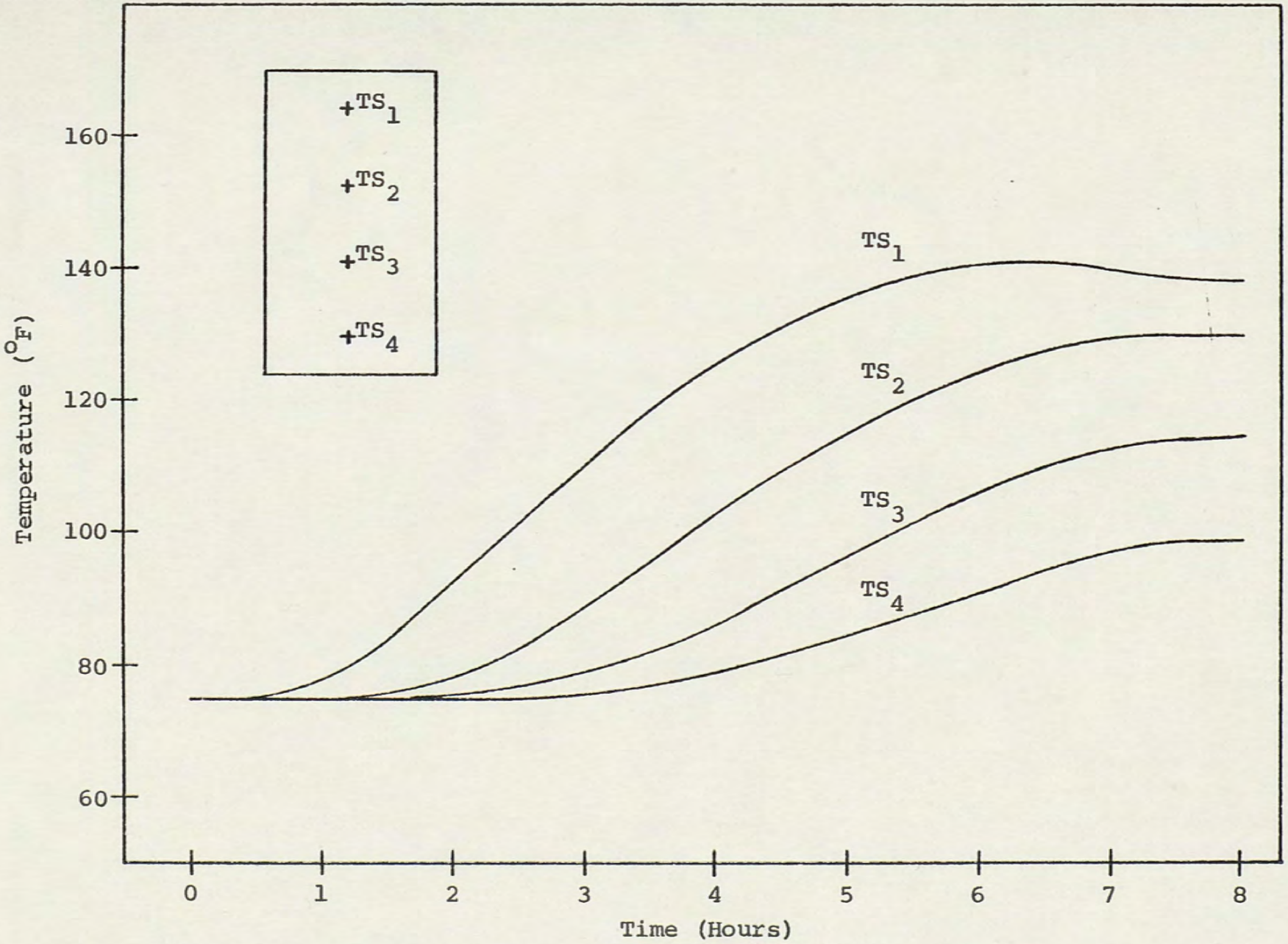

Figure 19. Storage Tank Temperatures versus Time for Ideal Day

tion and ambient temperature in energy balances for the absorber and tank, Close relates a mean system temperature and time in a single differential equation. The equation is solved to yield the mean system temperature as a function of time. The second differential equation, when solved, yields an expression for the flow rate and mean system temperature as a function of time. To obtain this equation, Close assumes a linear temperature distribution through the tank and absorber. Using a parabolic relationship between temperature and specific gravity, the thermosyphon head, H_T, can be expressed as a function of geometry and mean system temperature. An expression for the friction head, H_f, is derived from a direct application of the Darcy Weisbach equation. Equating the friction head and the thermosyphon head, an ordinary differential equation involving the flow rate is obtained.

The two differential equations, when solved, are sufficient to describe the absorber inlet and outlet temperatures and the flow rate. The solutions to these equations presented by Close are easily applied to the digital computer for a given thermosyphon system and operating conditions. Consequently, it was decided to use the Close model to simulate the previously described thermosyphon system (refer to Appendix D for detailed description) under the same ideal operation conditions. That is, the radiation is described by

$$\text{VII.3} \qquad R = 300 \sin\left(\frac{\pi t}{8}\right) \quad \frac{BTU}{hr\text{-}ft^2} \qquad t = 0\text{-}8 \text{ hr}$$

and the ambient temperature is described by

$$\text{VII.4} \qquad T_a = 75 + 15 \sin\left(\frac{\pi t}{8}\right) \quad (^{\circ}F) \qquad t = 0\text{-}8 \text{ hr}$$

The results of this simulation are compared to the TSP predictions in Figures 20 and 21. As indicated in Figure 20, the flow rate curves exhibit the same shape and are within 23% of one another at mid-day. The collector inlet and outlet temperatures as predicted by the TSP and the Close model are presented in Figure 21. Except for the initial dip in the inlet temperature present in the Close model, the shapes of the curves are the same. The initial dip is due to the nature of Close's solutions and does not reflect the actual case. In addition, the inlet temperature rises much more rapidly than that predicted by the TSP. This is a result of Close's assumption that the mean tank temperature and mean absorber temperature are equal. As the storage tank size and collector size increase, this assumption becomes less valid. It is believed that this caused the increasing difference between the inlet temperatures predicted by the two models. The outlet temperature predicted by the TSP agrees with the Close model. For the first seven hours, the models are within 20% of one another.

In conclusion, the TSP predicted a much slower rise in inlet temperature than the Close model. However, it is believed that the large storage tank and collector used in this simulation caused a violation of an assumption used in the Close model. This, in turn,

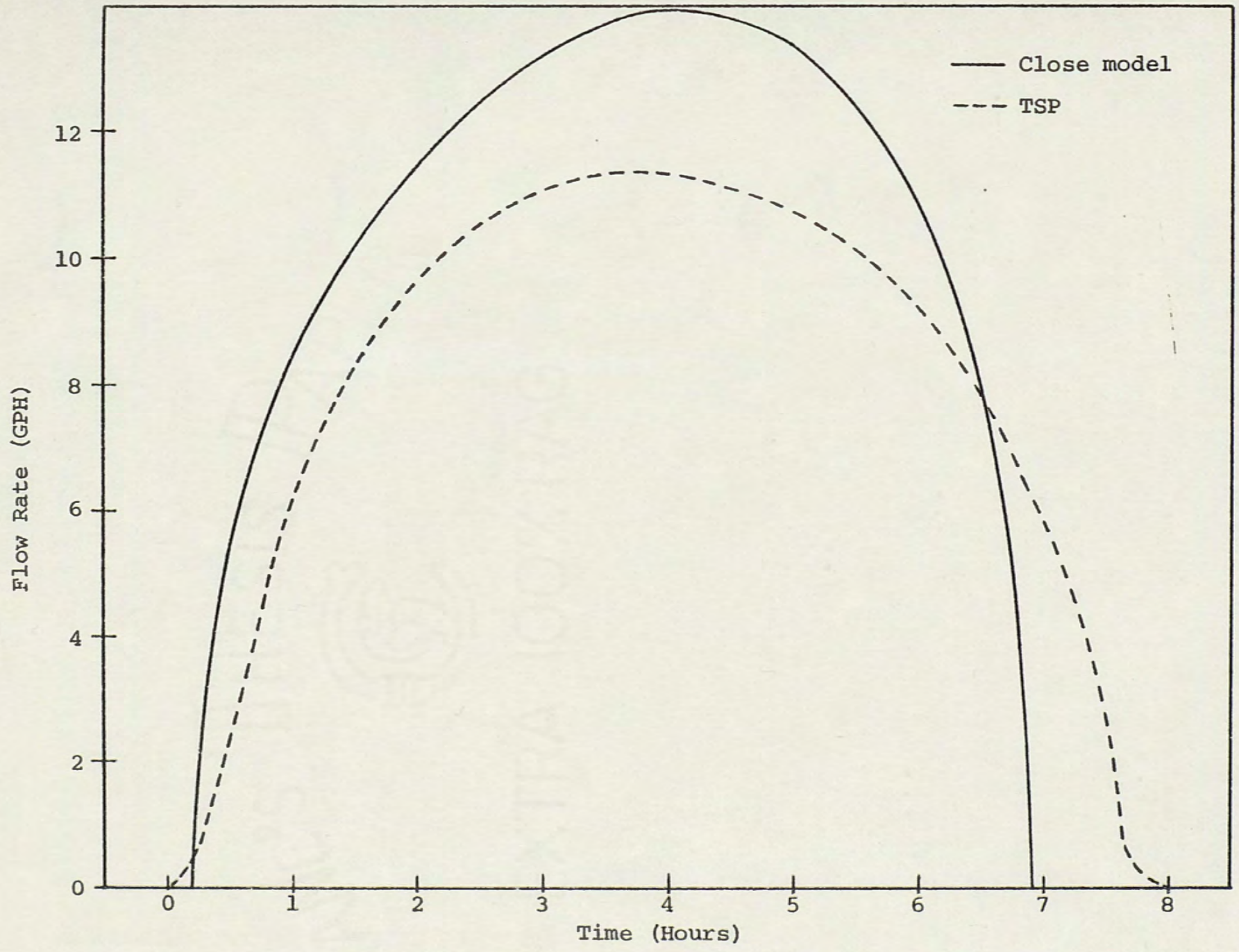

Figure 20. Flow Rate versus Time from TSP and Close model

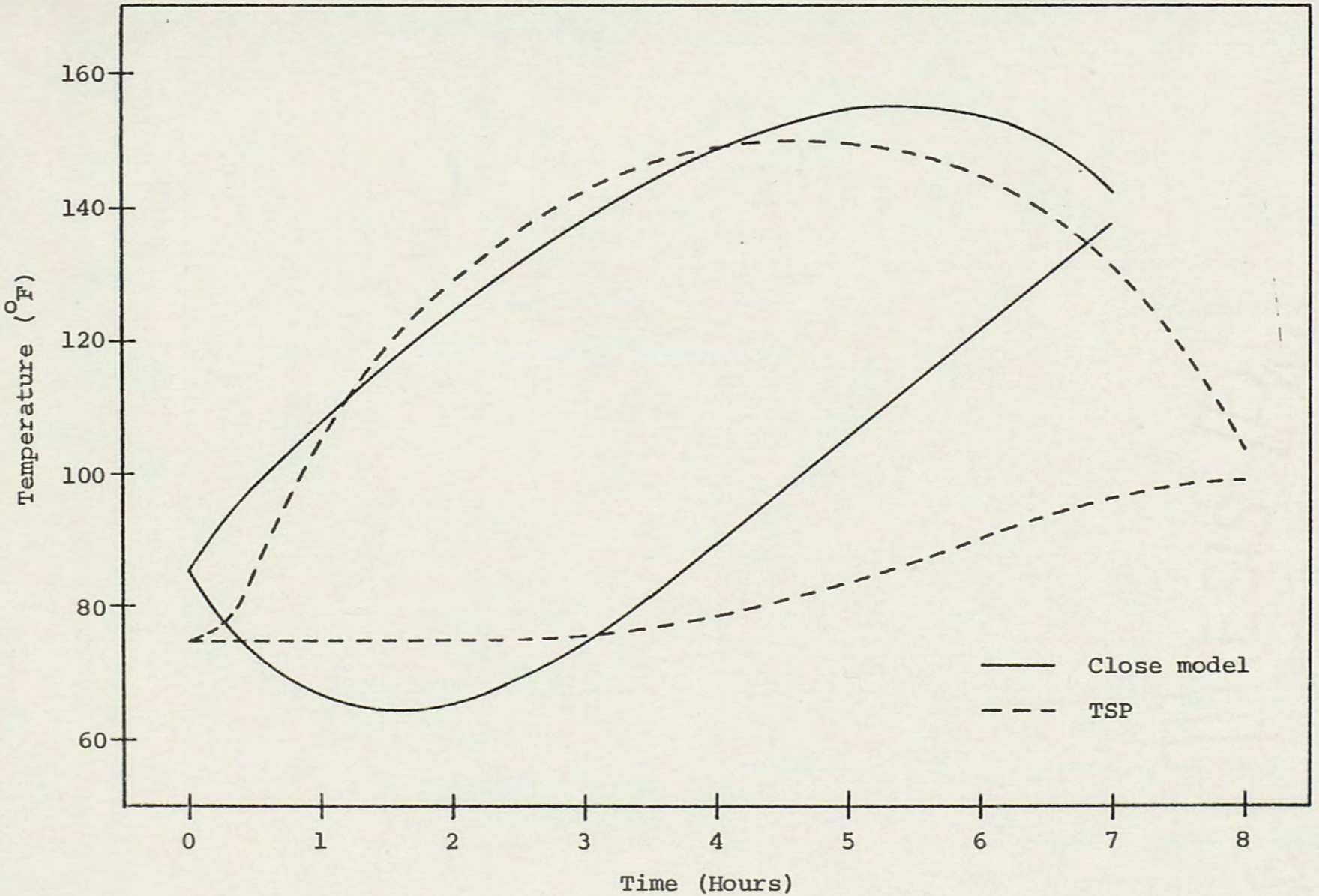

Figure 21. Collector Inlet and Outlet Temperatures versus Time from Close and TSP

resulted in the apparent overprediction of the inlet temperature. Nevertheless, the TSP predicted similar curves for the collector outlet temperature and the system flow rate.

The TSP model verification is finalized by a comparison of actual experimental data and predicted values. For this purpose, a thermosyphon unit located at Florida Technological University in Orlando, Florida, was tested under cloudy weather conditions. This test was taken with the mobile STAR (Solar Testing and Recording) unit developed at Florida Technological University under the direction of Bruce Nimmo. The STAR unit has been used to successfully monitor in situ domestic solar hot water systems.

Figure 22 shows the unit tested. Briefly, the unit consisted of an 80 gallon storage tank connected to a collector with an absorbing area of approximately 48 square feet. Further details on the thermosyphon system is presented in Appendix D.

The test setup is presented in Figure 23. Copper-Constantan thermocouples were equally spaced inside the storage tank. All thermocouple signals were referenced and amplified by an Omega Omni-Amp amplifier. The amplifier was calibrated such that the output voltage corresponded directly to the temperature in Centigrade. To determine the thermocouple's non-linearity, all thermocouples and accompanying amplifiers were previously calibrated. As a result of this calibration, the following fifth order temperature correction was derived.

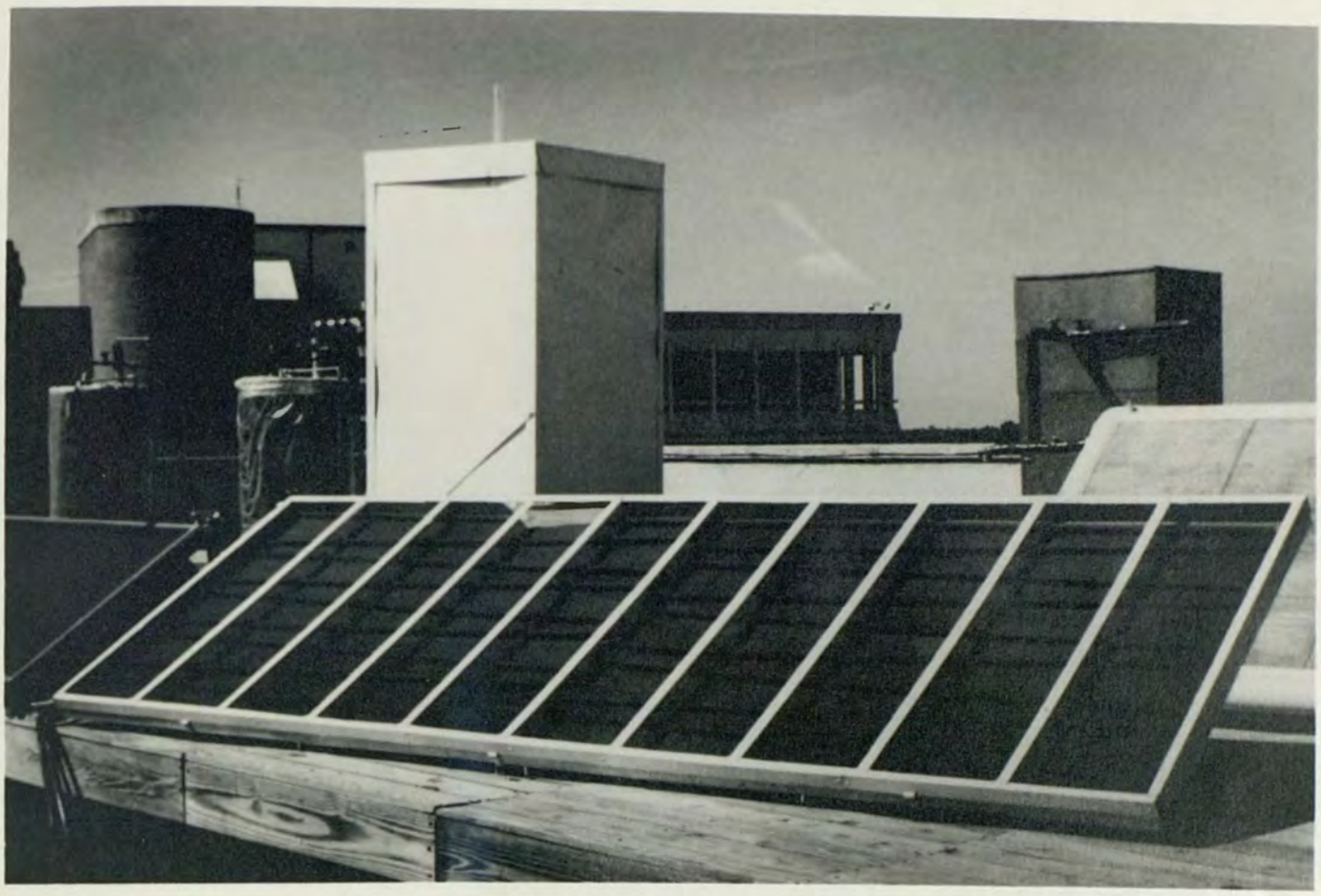

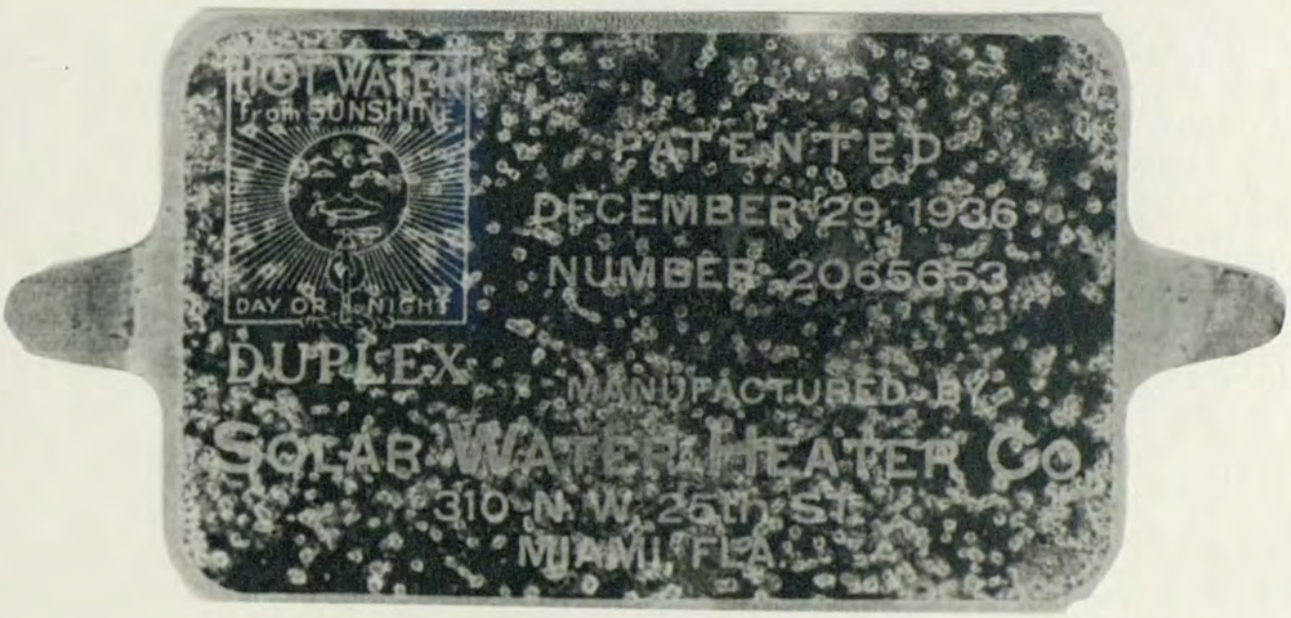

Figure 22. Thermosyphon Unit Tested

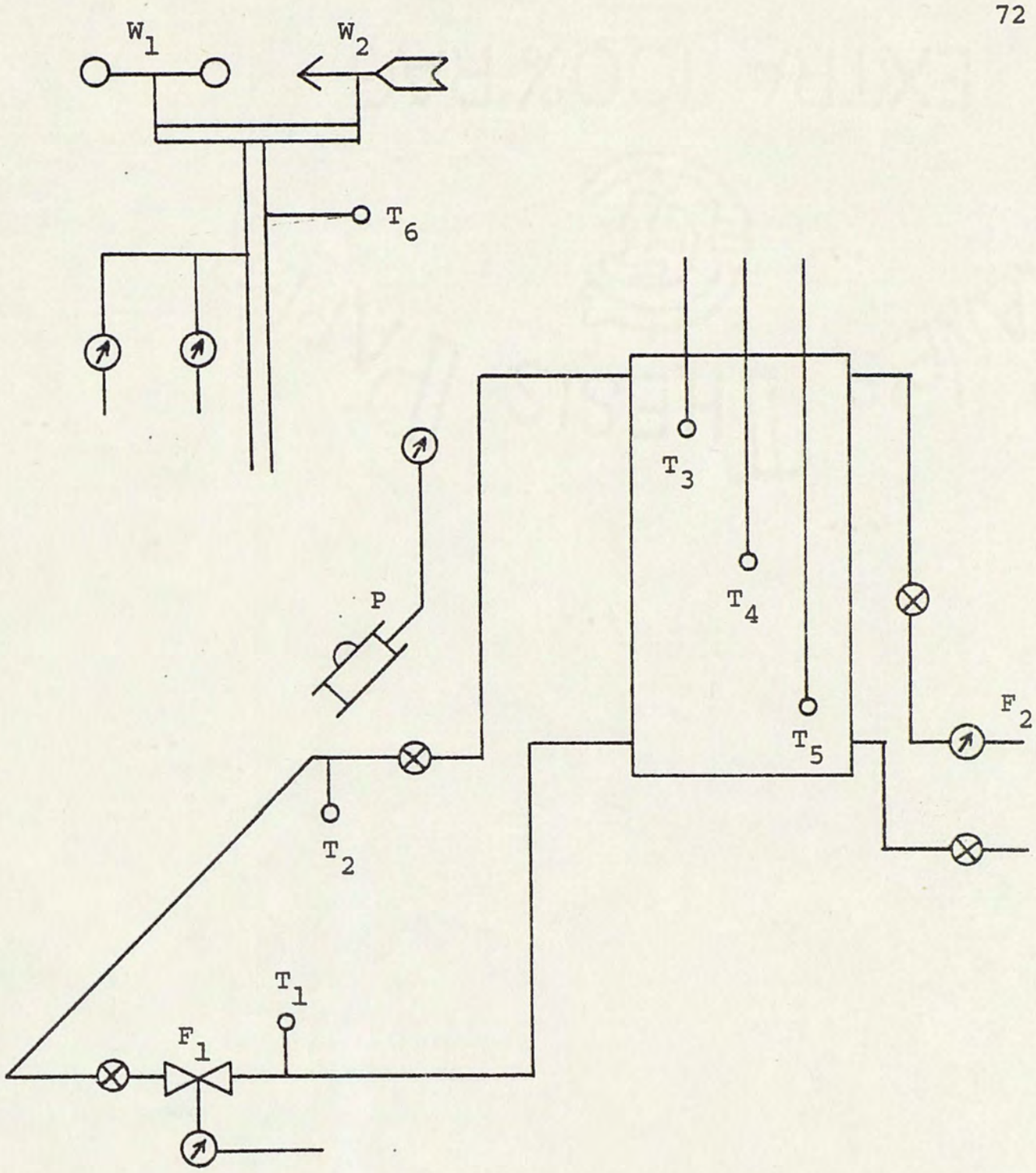

ⓘ	Indicates visual reading or recording
T_i	Thermocouple
$F_{1/2}$	Flowmeter (collector/drawoff)
P	Pyranometer
$W_{1/2}$	Wind indicator (speed/direction)

Figure 23. Test Setup

VII.5 $$T_c = AT^5 + BT^4 + CT^3 + DT^2 + ET + F$$

where T_c = corrected temperature (^oC)

T = measured temperature (^oC)

$A = 8.10586 \times 10^{-10}$

$B = -2.34205 \times 10^{-7}$

$C = 2.72754 \times 10^{-5}$

$D = -2.50217 \times 10^{-3}$

$E = 1.13378$

$F = -1.66236 \times 10^{-2}$

The uncorrected temperature readings were manually recorded.

Insolation was measured by an Epply pyranometer mounted at an angle of 34 degrees to the horizontal, that is, the same angle of inclination as the absorber. The pyranometer readings were continuously recorded with a Speedomax chart recorder.

One of the major difficulties of monitoring a thermosyphon unit is measuring the slow flow rates. For this test, the flow rate through the collector was obtained with a Barco 220 venturi flowmeter. Even for high thermosyphon flow rates, the pressure differential output from the venturi fell below the calibration curve provided by the manufacturer. Therefore, a calibration was performed for flow rates down to 1.5 gallons per hour.

The pressure differential across the venturi was measured with a Validyne pressure transducer with a one psi diaphragm. The

accompanying Validyne amplifier was adjusted so that a 0.5 psi differential corresponded to a full scale output of 5.0 volts. All voltage readings were recorded manually.

Two nine hour tests on the aforementioned thermosyphon unit were performed under the non-ideal condition of cloudy weather. The raw data for both days is contained in Appendix D. The temperature entries have not been corrected according to equation VII.5.

One of the two tests consisted of drawoff from the storage tank. In order to fully examine its capability, the TSP was used to simulate the thermosyphon system performance for this particular day. Tables 1 and 2 present the condensed data for this test. The temperatures have been corrected according to equation VII.5 and converted to degrees Farenheit. Insolation and load flow for the test are plotted as a function of time in Figures 24 and 25.

Figures 26-30 present measured and predicted values for the mass flow, absorber inlet and outlet temperatures, and mean tank temperature. Although the TSP yields temperatures of the tank at four equally spaced points and the experimental data is taken at three equally spaced points in the tank, both are plotted. This is done to compare trends and test the validity of the model.

As indicated from Figures 26 and 27, the tank is not as well mixed as the TSP predicts. That is, the TSP yields an approximately linear temperature distribution in the storage tank. However, the actual stratification exhibited an un-mixed condition. This

Table 1. Collector Data for September 29, 1976

Time	Mass Flow (GPH)	T_{inlet} (^{o}F)	T_{outlet} (^{o}F)	T_{amb} (^{o}F)
8:00	0.0	75.5	75.5	77.8
8:10	1.10	75.7	76.3	78.3
8:20	1.53	77.8	81.5	78.7
8:30	1.74	78.5	83.0	78.9
8:40	2.21	79.1	86.1	78.7
8:50	3.06	79.8	89.2	79.3
9:00	3.99	81.3	93.1	80.8
9:10	4.92	81.5	98.0	81.7
9:20	5.99	81.7	105.1	81.7
9:30	6.38	81.5	109.3	82.1
9:40	5.93	81.5	107.7	82.1
9:50	6.26	82.1	111.2	84.2
10:00	6.95	81.9	115.0	83.4
10:10	7.67	81.9	120.8	83.8
10:20	8.71	82.5	131.7	85.9
10:30	8.94	83.0	136.3	87.5
10:40	9.01	83.6	137.4	88.3
10:50	8.71	84.2	139.2	87.2
11:00	8.65	84.2	142.7	89.8
11:10	8.69	84.2	137.1	88.3
11:20	8.76	84.5	141.0	89.6

Table 1. (Continued)

Time	Mass Flow (GPH)	T_{inlet} (^{o}F)	T_{outlet} (^{o}F)	T_{amb} (^{o}F)
11:30	8.88	84.7	145.9	90.3
11:40	9.54	84.9	149.7	91.3
11:50	9.63	85.1	151.5	92.2
12:00	9.87	84.9	153.8	92.4
12:10	9.12	86.0	146.6	90.7
12:20	8.36	85.9	139.9	88.9
12:30	7.58	86.4	137.4	93.0
12:40	9.05	87.5	146.1	91.5
12:50	8.80	86.6	148.2	92.2
1:00	9.29	86.6	147.8	92.2
1:10	8.10	87.0	143.6	93.5
1:20	8.82	87.4	150.6	93.5
1:30	8.59	86.8	147.1	91.8
1:40	8.36	88.5	146.2	93.3
1:50	8.94	94.6	154.6	95.5
2:00	8.18	95.0	150.0	90.9
2:10	6.67	94.8	141.5	92.4
2:20	8.16	90.3	140.2	91.3
2:30	7.88	91.1	142.4	91.5
2:40	7.96	89.8	143.6	92.6
2:50	8.10	89.6	142.5	93.9

Table 1. (Continued)

Time	Mass Flow (GPH)	T_{inlet} (^{o}F)	T_{outlet} (^{o}F)	T_{amb} (^{o}F)
3:00	9.12	89.6	148.7	92.2
3:10	7.30	89.4	137.2	91.5
3:20	6.43	89.4	130.6	91.8
3:30	5.75	89.4	130.5	93.3
3:40	6.97	89.4	130.8	94.6
3:50	6.36	89.4	127.2	92.4
4:00	6.50	89.4	131.2	93.3
4:10	5.49	89.4	126.5	92.0
4:20	3.78	89.4	121.2	91.3
4:30	3.81	89.4	120.0	91.6
4:40	3.44	88.1	116.1	90.9
4:50	3.16	86.2	111.5	90.3
5:00	3.28	86.2	107.9	91.1

Table 2. Storage Tank Data for September 29, 1976

Time	Load Flow (Gal.)	$T_{TANK\ TOP}$ (^{o}F)	$T_{TANK\ MIDDLE}$ (^{o}F)	$T_{TANK\ BOTTOM}$ (^{o}F)	$T_{MEAN\ TANK}$ (^{o}F)
8:00	0.0	84.2	82.6	82.6	83.1
8:10	0.0	84.4	82.9	82.6	83.3
8:20	0.0	84.2	82.9	82.6	83.2
8:30	0.0	84.2	82.9	82.9	83.3
8:40	0.0	83.8	82.3	82.3	82.8
8:50	0.0	84.2	82.5	82.6	83.1
9:00	0.0	83.8	82.3	82.6	82.9
9:10	0.0	83.4	82.1	82.6	82.7
9:20	0.0	83.6	82.1	82.6	82.8
9:30	0.0	84.0	82.1	82.6	82.9
9:40	0.0	83.8	82.3	82.6	82.9
9:50	0.0	84.2	82.1	82.6	83.0
10:00	0.0	84.9	82.3	82.6	83.3
10:10	0.0	86.1	82.3	82.6	83.6
10:20	0.0	87.9	82.1	82.6	84.2
10:30	0.0	90.5	82.3	82.6	85.1
10:40	0.0	93.9	82.5	82.6	86.3
10:50	0.0	98.0	82.6	82.9	87.8
11:00	0.0	102.9	82.9	82.9	89.6
11:10	0.0	107.9	83.0	82.9	91.2

Table 2. (Continued)

Time	Load Flow – (Gal.)	$T_{TANK\ TOP}$ (^{o}F)	$T_{TANK\ MIDDLE}$ (^{o}F)	$T_{TANK\ BOTTOM}$ (^{o}F)	$T_{MEAN\ TANK}$ (^{o}F)
11:20	0.0	113.0	83.0	82.9	93.0
11:30	0.0	118.1	83.0	82.9	94.6
11:40	0.0	122.2	83.2	82.9	96.1
11:50	0.0	126.2	83.4	82.9	97.5
12:00	0.0	129.8	83.6	82.9	98.8
12:10	0.0	133.3	84.0	83.4	100.2
12:20	0.0	136.9	84.4	83.4	101.5
12:30	0.0	139.4	84.7	83.6	102.5
12:40	0.0	141.8	85.3	83.4	103.5
12:50	0.0	143.2	86.2	82.6	104.0
1:00	0.0	144.3	87.4	82.6	104.8
1:10	0.0	145.2	88.9	82.6	105.5
1:20	0.0	146.1	90.5	82.6	106.4
1:30	0.0	147.5	92.8	82.6	107.6
1:40	0.0	148.9	95.7	82.6	109.1
1:50	9.5	140.2	92.4	85.5	106.0
2:00	0.0	145.0	93.5	85.9	108.1
2:10	0.0	146.2	93.1	86.6	108.6
2:20	0.0	145.5	91.1	87.4	108.0
2:30	0.0	146.2	91.8	87.5	108.5

Table 2. (Continued)

Time	Load Flow (Gal.)	$T_{TANK\ TOP}$ (^{o}F)	$T_{TANK\ MIDDLE}$ (^{o}F)	$T_{TANK\ BOTTOM}$ (^{o}F)	$T_{MEAN\ TANK}$ (^{o}F)
2:40	0.0	146.8	93.7	87.5	109.3
2:50	11.2	131.9	91.1	87.4	103.5
3:00	0.0	133.6	90.2	87.2	103.6
3:10	0.0	138.6	89.4	87.4	105.1
3:20	0.0	141.6	89.6	87.4	106.2
3:30	0.0	141.0	90.2	87.4	106.2
3:40	0.0	139.9	90.7	87.4	106.0
3:50	0.0	140.0	91.6	87.4	106.3
4:00	0.0	139.9	92.6	87.4	106.6
4:10	0.0	139.5	93.7	87.5	106.9
4:20	0.0	139.2	95.0	87.7	107.3
4:30	12.0	123.8	90.5	86.2	100.2
4:40	0.0	123.1	87.9	86.2	99.1
4:50	0.0	122.4	87.7	86.0	98.7
5:00	0.0	121.5	87.9	86.1	98.5

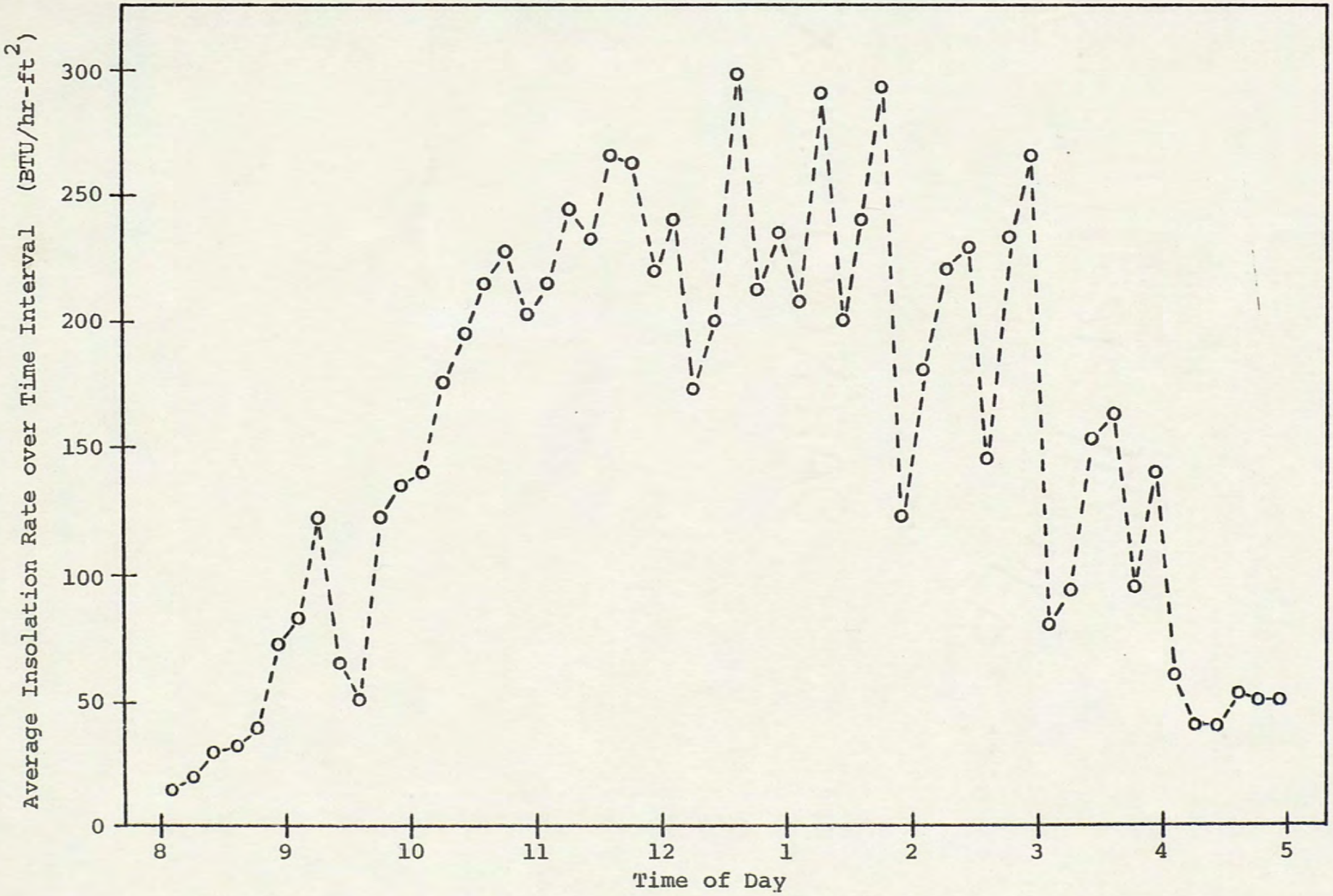

Figure 24. Average Insolation Rate versus Time of Day for 9/29/76

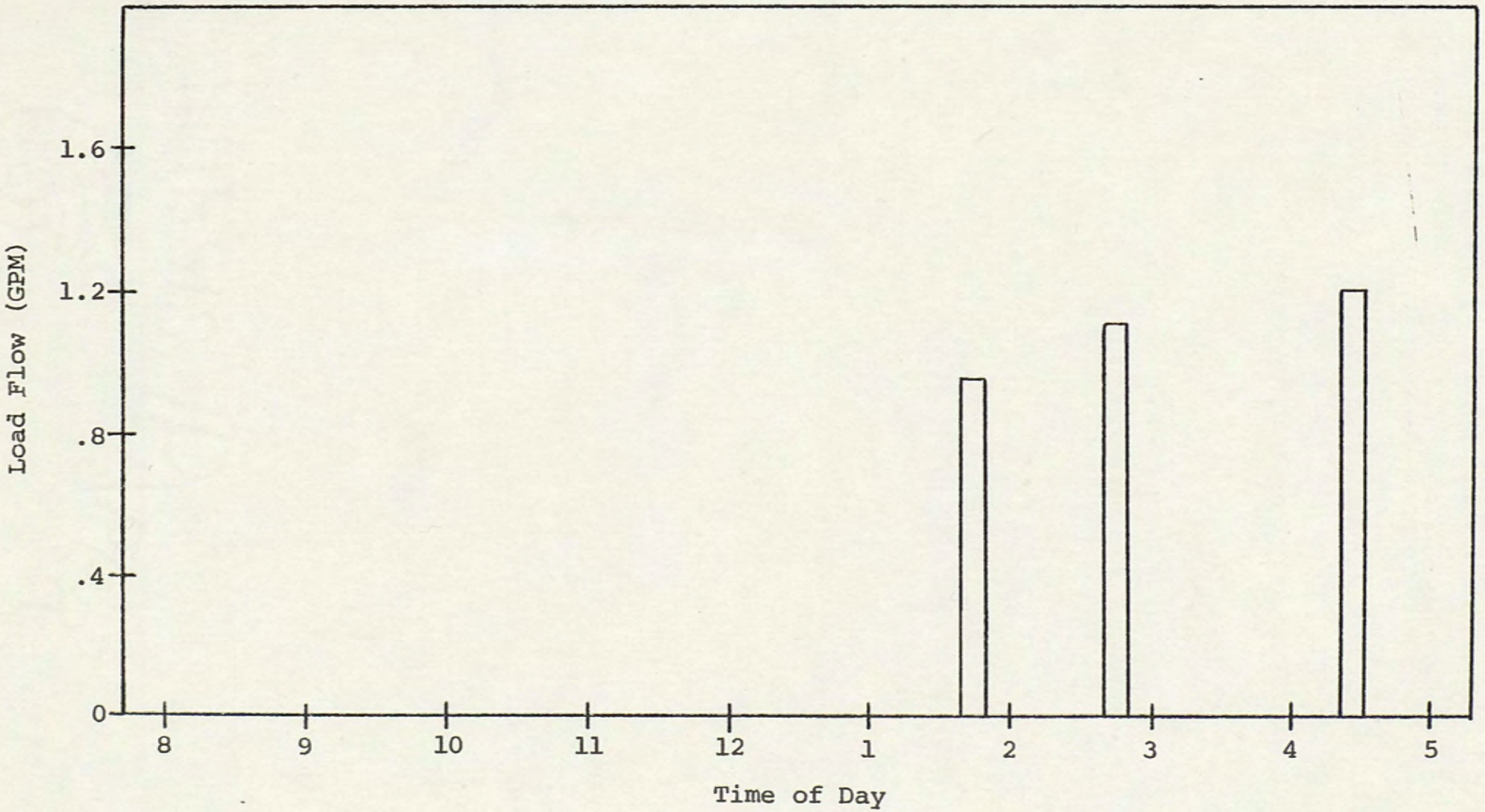

Figure 25. Load Flow versus Time of Day for 9/29/76

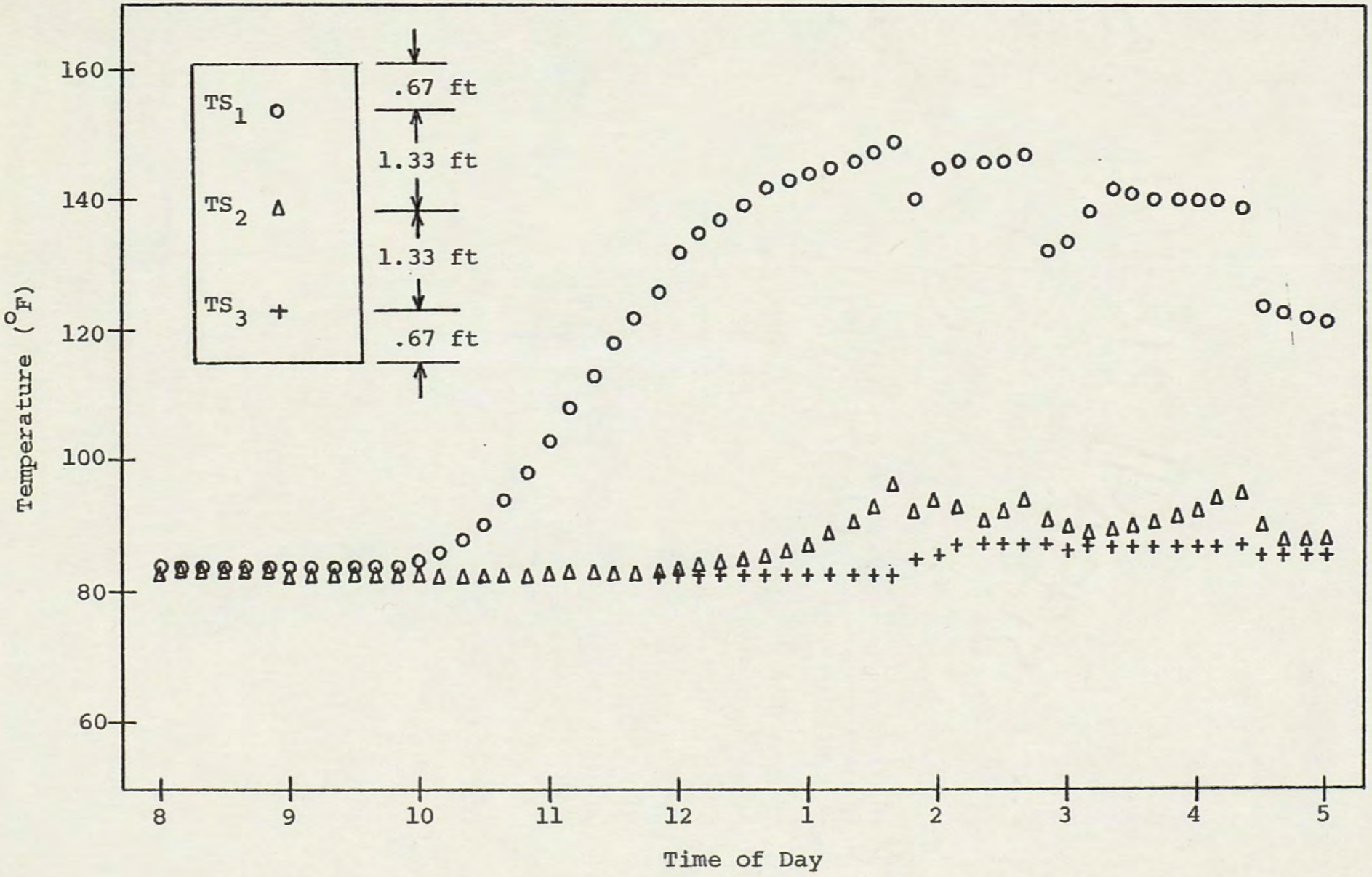

Figure 26. Measured Storage Tank Temperatures versus Time of Day for 9/29/76

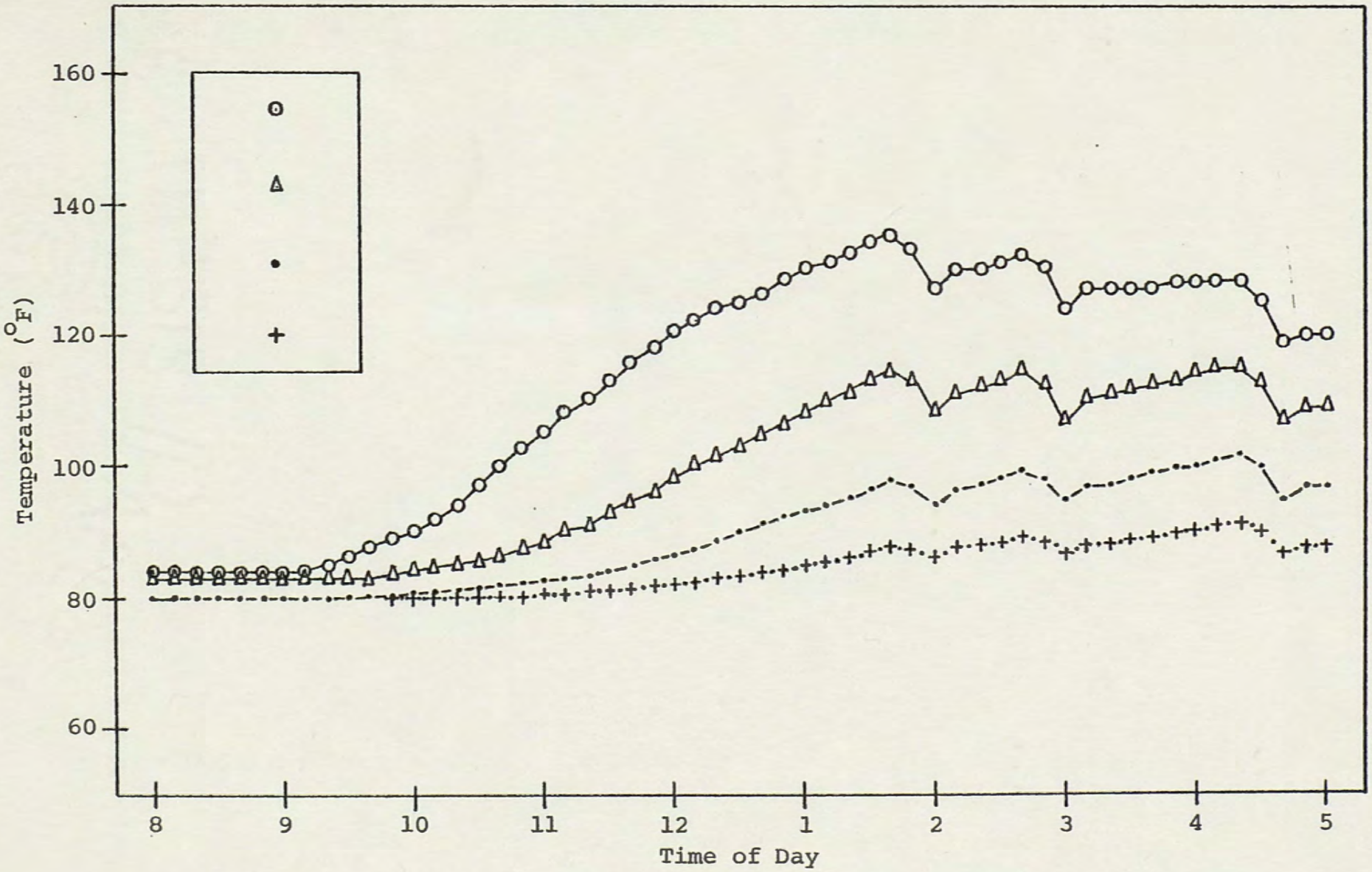

Figure 27. Predicted Storage Tank Temperatures versus Time for 9/29/76

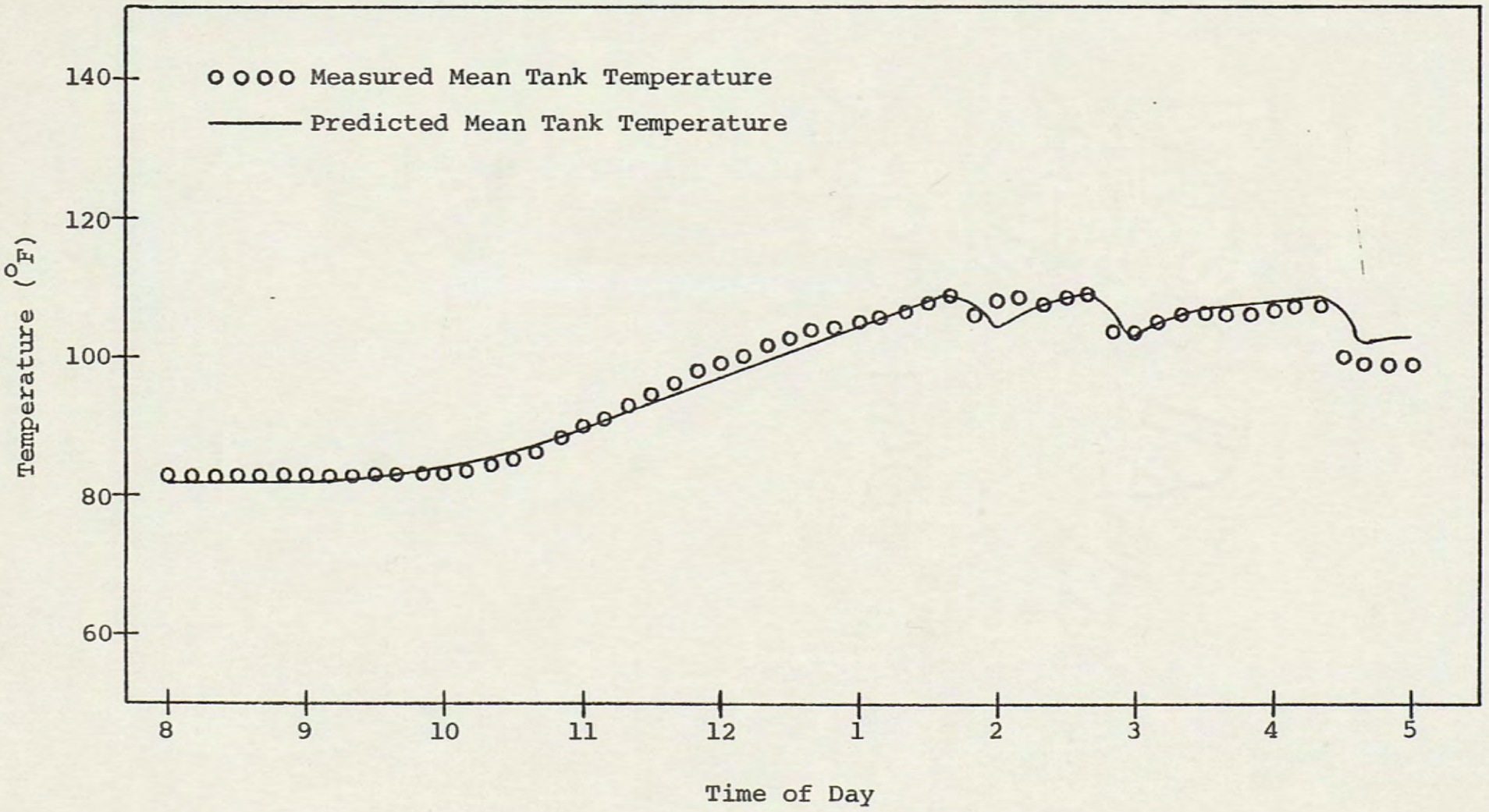

Figure 28. Mean Tank Temperature versus Time of Day for 9/29/76

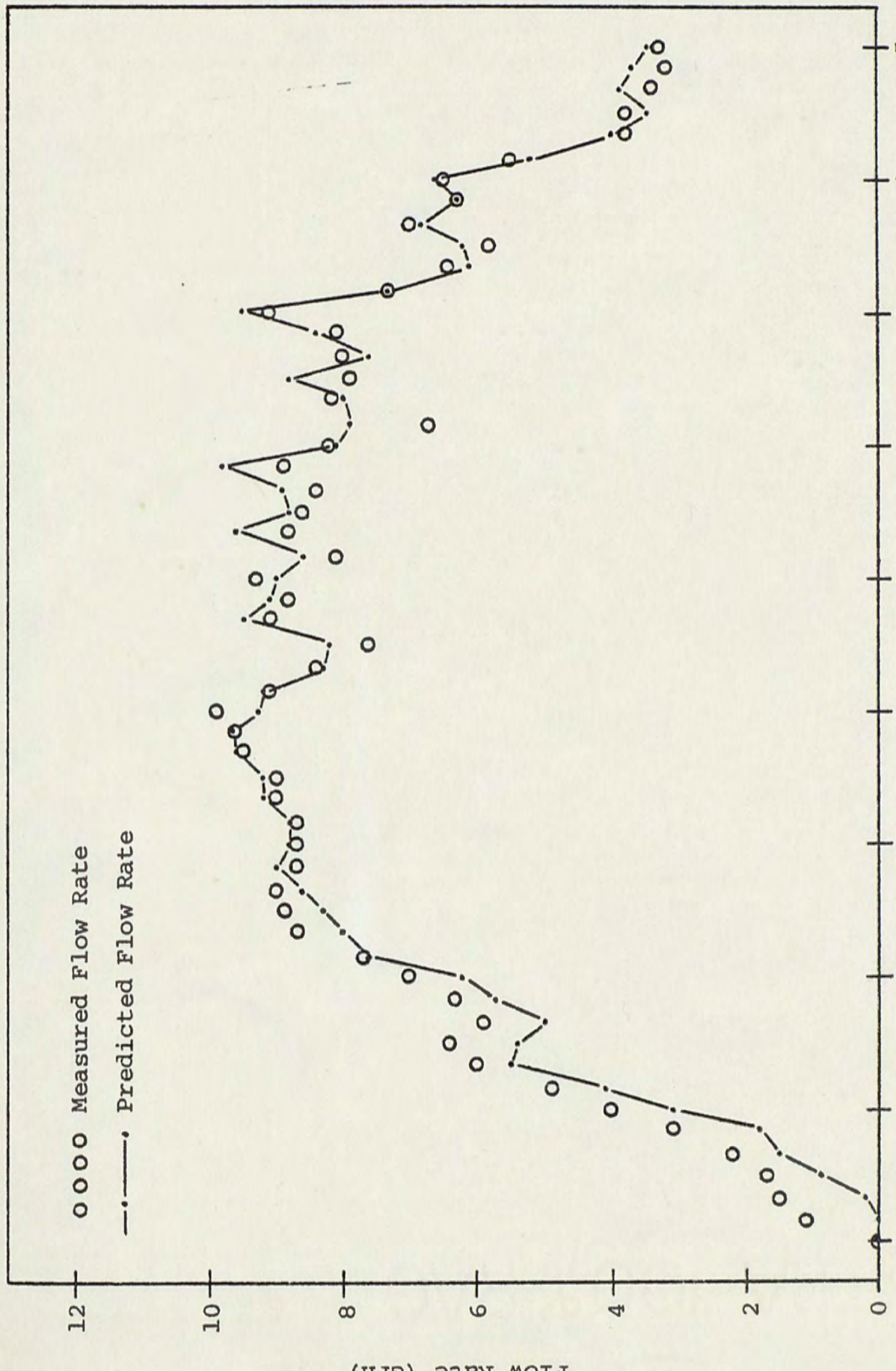

Figure 29. Collector Flow Rate versus Time of Day for 9/29/76

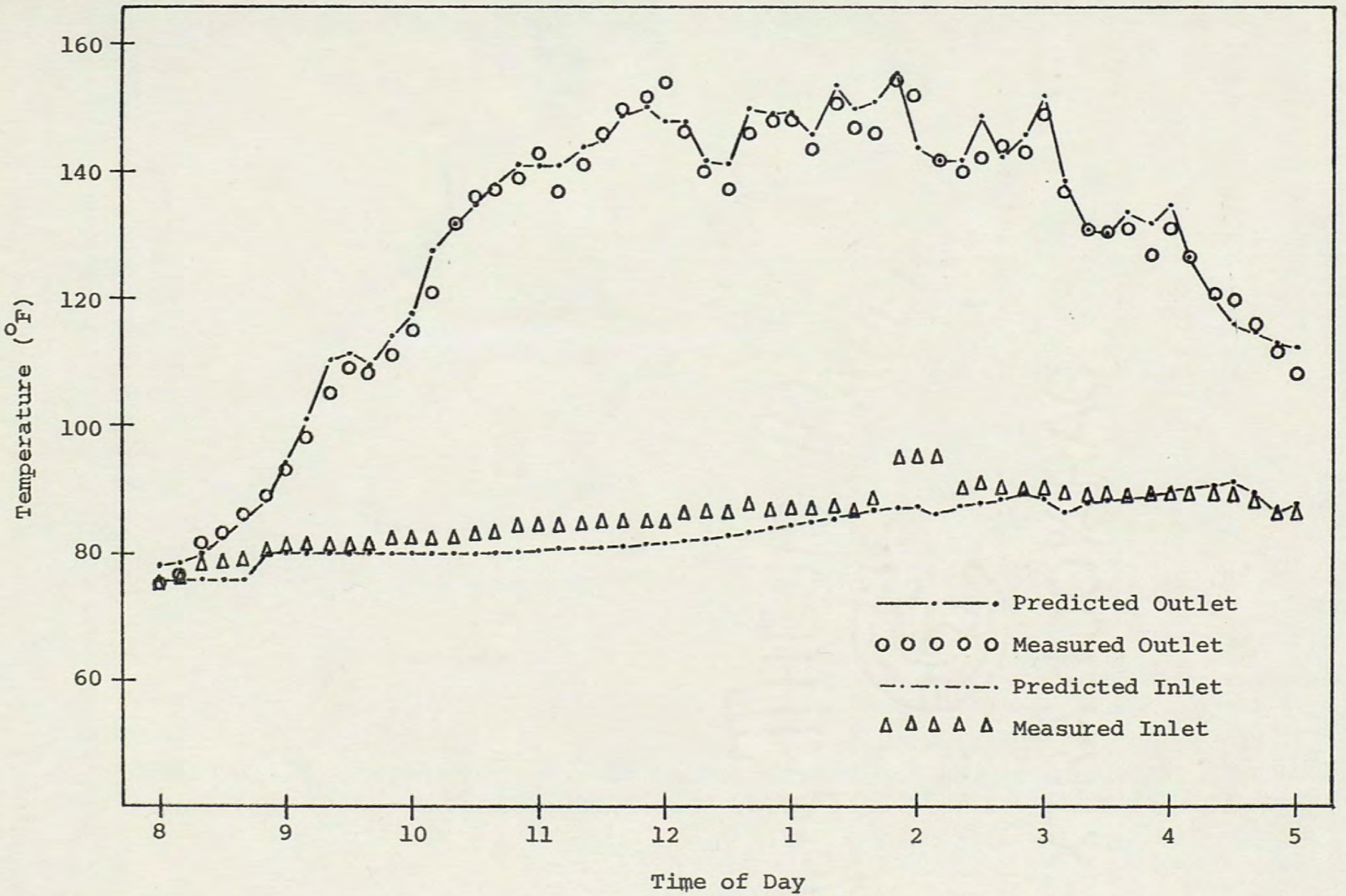

Figure 30. Collector Inlet and Outlet Temperatures versus Time of Day for 9/29/76

indicates the fluid in the tank to move in "slugs" when not disturbed by load flow, etc. This idea can be supported by comparing information derived from Figures 26 and 29. Knowing the distance between the thermocouples, one can estimate the time it will take the warm fluid to reach each thermocouple by integrating under the flow rate curve. One can then compare this time to the time the thermocouple actually sensed the warmer fluid (refer to Figure 26). For example, the first thermocouple in the tank is located eight inches below the tank top. This distance represents 13 gallons of fluid. An integration under the flow rate curve (Figure 29) indicates that a total of 13 gallons had flowed through the system by 10:30 am. From Figure 26 this is about the same time the first thermocouple senses hot fluid.

The second thermocouple is located 16 inches below the first thermocouple. This distance corresponds to 26 gallons of fluid in the tank. Another integration under the flow rate curve indicates that an additional 26 gallons had passed through the system by 1:10 pm. Therefore, if the fluid did move in "slugs," the middle thermocouple should have sensed the first warm fluid at this time. Figure 26 shows this to be the case.

Under the assumption the fluid moved in slugs, the last thermocouple in the storage tank would not sense warmer fluid until the end of the test. However, Figure 26 indicates a temperature rise at approximately 1:40 pm. This is due to a load imposed on

the tank. This represents a disturbance to the system which would tend to mix the tank. In addition, the return fluid for this particular load removal was much warmer than the fluid in the bottom of the tank.

The TSP appears to predict minimum tank temperatures after each load removal one time interval later than the actual case. This is due solely to the nature of the predictor-corrector solution used to obtain the tank node temperatures.

Regardless of its poor prediction of the actual storage tank stratification, the TSP accurately predicts the mean tank temperature as shown in Figure 28. The average error of the TSP in this case is 1.5 percent. The maximum error (6.5 percent) occured after intervals involving load flow. Nevertheless, the TSP exhibited the correct shape for these load flow intervals.

Figure 29 presents a comparison between the predicted and measured flow rate. The TSP is in close agreement with the actual values. The error is greatest in the early morning when the flow is getting started. This is due, in part, by the error in the flow monitoring device (pressure transducer) at the extremely low flows of 1.5 gallons per hour and less. Between the hours of 9 am and 5 pm, the average error is 6.4 percent. This error is increased to 9.6 percent if the first hour is included.

The collector inlet and outlet temperatures are presented in Figure 30. As with the system flow rate, the TSP yielded accurate

values. The TSP underpredicted the inlet temperature somewhat. This is attributed, in part, to insufficient insulation of the inlet pipe. A small portion of the pipe was subject to direct radiation and higher ambient temperatures. The largest error (9 percent) occurs after the first load flow test when the actual inlet temperature rose unexpectedly. It was later determined that the return water line had been exposed to direct radiation causing a portion of the return fluid to be at a significantly higher temperature than the tank bottom. Since this return fluid entered the tank well below the lowest thermocouple, the thermocouple on the collector inlet saw a much larger rise in temperature than did the one located in the tank. Nonetheless, the average error between predicted and measured inlet temperature is 3 percent.

The predicted outlet temperatures followed the measured values within 9 percent for the nine hour test. The average error in the TSP prediction is 2 percent. This close agreement is attributed to the rather sophisticated collector model. J. B. Pearce[23] has also successfully employed this model in a simulation of pumped solar hot water systems. He also found the collector model to be accurate for non-ideal days.

In conclusion, the TSP accurately predicted collector inlet and outlet temperatures, system flow rate, and mean tank temperature for a test involving cloudy weather and drawoff from the storage tank. It did not exhibit instability in the solutions and presented a somewhat more realistic simulation than the Close

model. Therefore, the TSP can be considered valid for normal weather conditions if the need for the storage tank temperature stratification is not essential to the user.

VIII

CONCLUSIONS AND RECOMMENDATIONS

The computer model presented in the preceeding chapters met its intended goal. That is, it represents an accurate model of a thermosyphon system subject to fluid drawn from the tank and cloudy weather conditions. The model is able to predict the system performance within 10 percent.

Although the mean tank temperature is accurately predictable, the tank stratification is not. Therefore, it is recommended that this be more closely investigated. If possible, a tank model which utilizes a continuous non-linear temperature distribution should be investigated.

The model can be used to evaluate design alternatives for thermosyphon units. The effects of collector geometry (tube size, tube spacing, tube configuration, etc.) can easily be determined as a guide to obtaining maximum performance.

This model can be used to investigate the effectiveness of adding a pump to the system. Obviously, a pumped system is more efficient than a similar thermosyphon system since the latter usually operates at a much higher temperature and thus has a greater energy loss to the environment. However, a pumped system

generally requires power, a controller, and more maintenance. It should be possible with this model and the pumped system model (referred to as PSP) developed by Pearce to determine the cost effectiveness of adding a pump to a solar hot water system.

Appendix A

SOLUTION TO THE FIRST ORDER PARTIAL DIFFERENTIAL EQUATION

The solution to

A.1 $$a\frac{\partial T}{\partial t} + b\frac{\partial T}{\partial x} + cT = g$$

where a, b, c, and g are arbitrary constants ($\neq 0$) is the sum of of the particular solution and the complimentary solution. The complimentary solution is obtained by solving equation A.1 with g set equal to zero:

A.2 $$a\frac{\partial T}{\partial t} + b\frac{\partial T}{\partial x} + cT = 0$$

Lagrange solved the more general case of the homogenous first order partial differential equation

A.3 $$f(x,t,T)\frac{\partial T}{\partial t} + g(x,t,T)\frac{\partial T}{\partial x} + h(x,t,T) = 0$$

by reducing the problem to an equivalent set of ordinary differential equations (the Lagrange system) of the form[24]

A.4 $$\frac{dt}{f(x,t,T)} = \frac{dt}{g(x,t,T)} = \frac{dt}{-h(x,t,T)}$$

For the case at hand, equation A.2 will have the Lagrange system

$$\text{A.5} \qquad \frac{dt}{a} = \frac{dx}{b} = -\frac{1}{c}\frac{dT}{T}$$

From equation A.5,

$$\text{A.6} \qquad \frac{dt}{a} = \frac{dx}{b}$$

$$\text{A.7} \qquad \int_0^x a\,dx = \int_0^t b\,dt + K_1$$

which yields,

$$\text{A.8} \qquad K_1 = ax - bt$$

Again from equation A.5,

$$\text{A.9} \qquad \frac{dt}{a} = -\frac{1}{c}\frac{dT}{T}$$

$$\text{A.10} \qquad -\frac{c}{a}\int_0^t dt + K_2 = \int_0^t \frac{dT}{T}$$

yielding

$$\text{A.11} \qquad -\frac{c}{a}t + \ln(K_2) = \ln(T)$$

which simplifies to

$$\text{A.12} \qquad T = K_3 e^{-\frac{c}{a}t}$$

Equations A.8 and A.12 are combined to give the general solution to A.2 as

$$A.13 \qquad T = e^{-\frac{c}{a}t} \left[\phi (ax - bt) \right]$$

where the function $\phi(ax - bt)$ is to be determined from initial conditions or boundary conditions. Equation A.13 constitutes the complimentary solution to A.1.

The particular solution can be had rather easily by noting that g is a constant. Therefore, assuming the particular solution to be a constant K_4, the total solution becomes

$$A.14 \qquad T(x,t) = e^{-\frac{c}{a}t} \left[\phi (ax - bt) \right] + K_4$$

Substituting this back into A.1 yields K_4

$$A.15 \qquad K_4 = \frac{g}{c}$$

so that the total solution to A.1 becomes

$$A.16 \qquad T(x,t) = e^{-\frac{c}{a}t} \left[\phi (ax - bt) \right] + \frac{g}{c}$$

If this equation is to be solved for various time intervals, it would be desirable to choose an initial condition which allows for time continuity of the solution. Such a condition would be

$$T_{new} \ (x, t = 0) = T_{old} \ (x, t = \Delta\tau)$$

where

T_{new} $(x, t = 0)$ = the temperature distribution for the beginning of the next time interval

T_{old} $(x, t = \Delta\tau)$ = the temperature distribution at the end of the last time interval

Substituting this condition into equation A.16 yields

A.17 $$T_{old}(x) = \phi(ax) + \frac{g}{c}$$

Solving for the unknown function ϕ

A.18 $$\phi(ax) = T_{old}(x) - \frac{g}{c}$$

Let $z = ax$. Then

A.19 $$\phi(z) = T_{old}\left(\frac{z}{a}\right) - \frac{g}{c}$$

Therefore,

A.20 $$\phi(ax - bt) = T_{old}\left(\frac{ax - bt}{a}\right) - \frac{g}{c}$$

Then the total solution becomes

A.20 $$T = e^{-\frac{c}{a}t}\left[T_{old}\left(x - \frac{b}{a}t\right) - \frac{g}{c}\right] + \frac{g}{c}$$

$$0 \leq t \leq \Delta\tau$$

Appendix B

COLLECTOR NODE EQUATIONS

The collector model used in this paper consists of four nodes, the cover plate, the absorber and fluid, the back insulation, and the container (refer to Figure 31). An energy balance written on each node will yield a set of differential equations describing mean temperatures of these nodes.

Consider the cover plate, node one, as shown in Figure 32. An energy balance yields

B.1 $$Q_{s1} = Q_g + Q_{r21} + Q_{c21} - Q_{r1a} - Q_{c1a}$$

where
Q_{s1} = energy stored in cover plate
Q_g = radiation absorbed by cover plate
Q_{r21} = radiated energy from absorber to cover
Q_{c21} = convected energy from absorber to cover
Q_{r1a} = radiated energy from cover to ambient
Q_{c1a} = convected energy from cover to ambient

The radiation absorbed by the cover plate Q_g is

B.2 $$Q_g = A_1 S_g$$

where
S_g = energy per unit area absorbed by cover plate (refer to Chapter II)

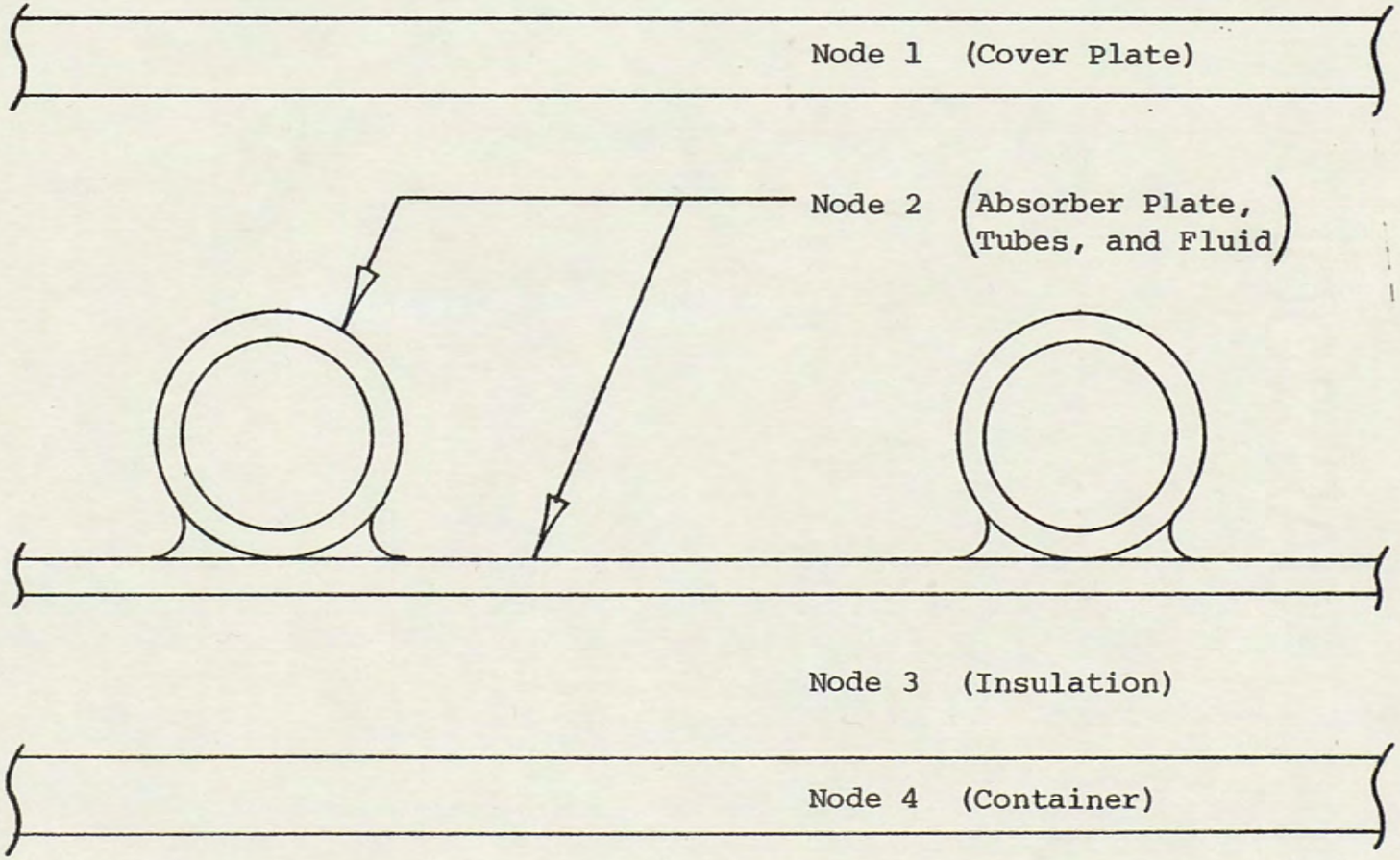

Figure 31. Four Node Collector Model

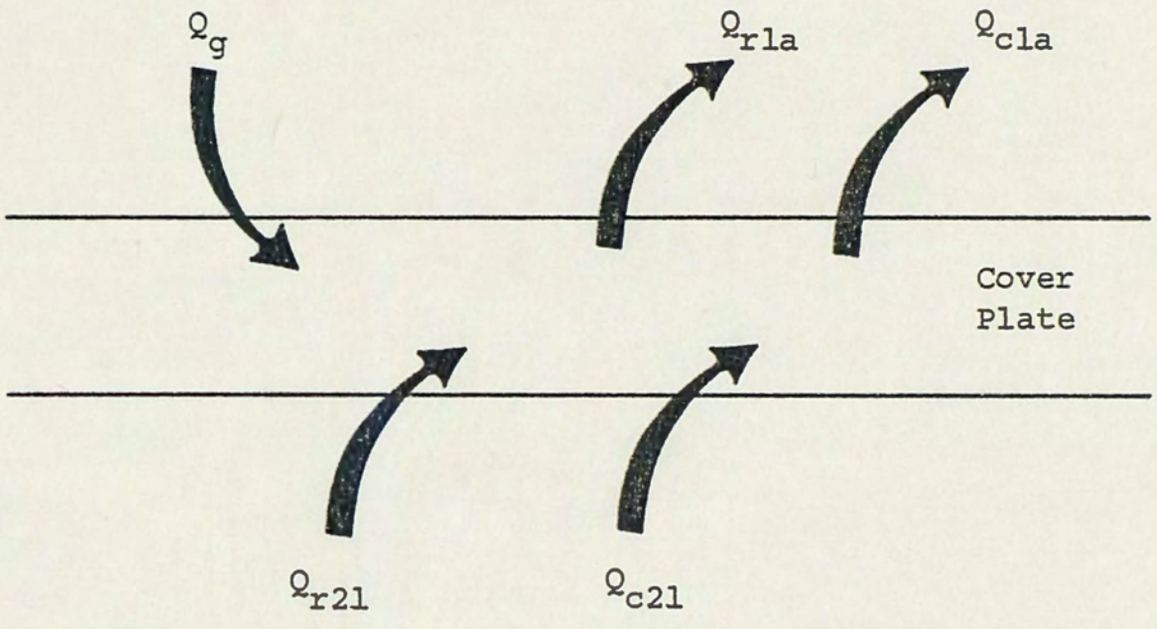

Figure 32. Energy Balance on Cover Plate

A_1 = area of node 1

From basic heat transfer considerations,

B.3 $$Q_{r1a} = A_1 h_{r1a} (T_1 - T_a)$$

where $$h_{r1a} = \varepsilon_1 \sigma (T_1^2 + T_a^2) (T_1 + T_a)$$

ε_1 = emissivity of node 1

σ = Boltzman's constant

A_1 = area of node 1

T_1 = temperature of node 1

T_a = ambient temperature

Similarly,

B.4 $$Q_{r21} = A_2 h_{r21} (T_2 - T_1)$$

where $$h_{r21} = \frac{\sigma F_{2-1} (T_2^2 + T_1^2) (T_2 + T_1)}{\frac{1}{\varepsilon_2} + \frac{1}{\varepsilon_1} - 1}$$

ε_2 = emissivity of node 2

T_2 = temperature of node 2

F_{2-1} = configuration from node 2 to node 1

If it is assumed that the cover plate and absorber plate are infinite planes, the configuration factor is one. Otherwise,

F_{2-1} can be calculated from reference 16.

The convection terms can be written as

B.5 $$Q_{c1a} = A_1 h_w (T_1 - T_a)$$

where the wind convection coefficient h_w is given by [25]

B.6 $$h_w = 1.0 + .3 \times (\text{windspeed in mph})$$

Similarly,

B.7 $$Q_{c21} = A_1 h_{c21} (T_2 - T_1)$$

where the convection coefficient h_{c21} between node 2 and node 1 is given by[26]

B.8 $$h_{c21} = C \cdot (T_2 - T_1)^{\frac{1}{4}}$$

where C = coefficient dependent on slope of collector

The energy stored in node 1 is

B.9 $$Q_{s1} = (mc)_1 \frac{dT_1}{dt}$$

where $(mc)_1$ = capacitance of node 1

Rewriting equation B.1,

B.10 $$(mc)_1 \frac{dT_1}{dt} = A_1 S_g + A_2 h_{r21} (T_2 - T_1) + A_1 h_{c21} \cdot$$

$$(T_2 - T_1) - A_1 h_{r1a} (T_1 - T_a) -$$

$$A_1 h_w (T_1 - T_a)$$

Assuming all nodes will have a nominal common surface area A_c, equation B.10 can be written as

B.11 $$\frac{dT_1}{dt} = - \frac{A_c}{(mc)_1} (h_{r21} + h_{c21} + h_{r1a} + h_w) T_1 +$$

$$\frac{A_c}{(mc)_1} (h_{r21} + h_{c21}) T_2 + \frac{A_c}{(mc)_1} (S_g + h_{r1a} T_a$$

$$+ h_w T_a)$$

The second node is the absorber plate, tubes and fluid as shown in Figure 33. An energy balance yields

B.12 $$Q_{s2} = Q_p - Q_{c21} - Q_r - Q_{K23} - Q_{REMOVED}$$

where

Q_{s2} = energy stored in node 2

Q_p = absorbed solar energy

Q_{c21} = energy convected from absorber to cover

Q_r = net energy radiated from absorber

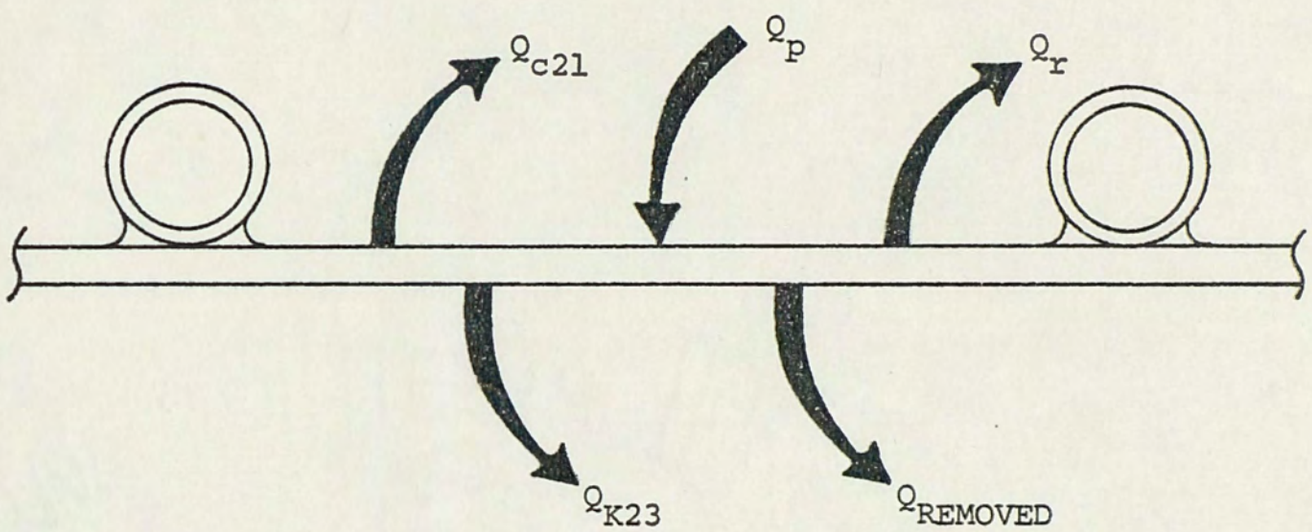

Figure 33. Energy Balance on Absorber Plate, Tubes, and Fluid

Q_{K23} = energy conducted from absorber through insulation

$Q_{REMOVED}$ = energy removed via moving fluid

From equation B.7,

B.13 $$Q_{c21} = A_c h_{c21} (T_2 - T_1)$$

Assuming the absorber radiates primarily to the cover, basic heat transfer considerations yield

B.14 $$Q_r = A_c h_{r2} (T_2 - T_1)$$

where the radiation coefficient is

$$h_{r2} = \frac{\sigma (T_2^2 + T_1^2)(T_2 + T_1)}{\frac{1}{\varepsilon_2} + \frac{1}{\varepsilon_1} - 1}$$

For a linear temperature drop through the insulation the energy conducted from the absorber through the insulation is

B.15 $$Q_{K23} = \frac{K_3 A_c}{\left(\frac{\Delta x_3}{2}\right)} (T_2 - T_3)$$

where K_3 = conductivity of insulation

Δx_3 = thickness of insulation

The energy removed from the absorber via the circulating

fluid is

B.16 $$Q_{REMOVED} = \dot{m} c_p (T_{OUT} - T_{IN})$$

where $\dot{m}$ = flow rate

c_p = constant specific heat

T_{OUT} = outlet temperature of collector

T_{IN} = inlet temperature of collector

The absorbed solar radiation is given in Chapter II as

B.17 $$Q_p = A_c S$$

The energy stored in the absorber plate is

B.18 $$Q_{s2} = (mc)_2 \frac{dT_2}{dt}$$

Substituting equations B.13 through B.18 into B.12

B.19 $$(mc)_2 \frac{dT_2}{dt} = A_c S - A_c h_{c21}(T_2 - T_1) - A_c h_{r2}(T_2 - T_1) - \frac{K_3 A_c}{\left(\frac{\Delta x_3}{2}\right)} (T_2 - T_3) - \dot{m} c_p (T_{out} - T_{in})$$

This can be condensed to

B.20 $$\frac{dT_2}{dt} = \frac{A_c}{(mc)_2} (h_{c21} + h_{r2}) T_1 - \frac{A_c}{(mc)_2} (h_{c21} + h_{r2} +$$

$$\left(\frac{2K_3}{\Delta x_3}\right) T_2 + \frac{A_c}{(mc)_2} \left(\frac{2K_3}{\Delta x_3}\right) T_3 + \frac{A_c}{(mc)_2} (S + \frac{\dot{m}c_p}{A_2} T_{IN} - \frac{\dot{m}c_p}{A_2} T_{OUT})$$

The back insulation is the third node. An energy balance on node 3 (refer to Figure 34) yields

B.21 $$Q_{s3} = Q_{K23} - Q_{K34}$$

where Q_{s3} = energy stored in insulation

Q_{K23} = energy conducted into node 3 from absorber

Q_{K34} = energy conducted out of node 3 to the container

From equation B.15

B.22 $$Q_{K23} = \frac{K_3 A_c}{\left(\frac{\Delta x_3}{2}\right)} (T_2 - T_3)$$

The energy conducted to the container is

B.23 $$Q_{K34} = \frac{K_3 A_c}{\left(\frac{\Delta x_3}{2}\right)} (T_3 - T_4)$$

The stored energy is

B.24 $$Q_{s3} = (mc)_3 \frac{dT_3}{dt}$$

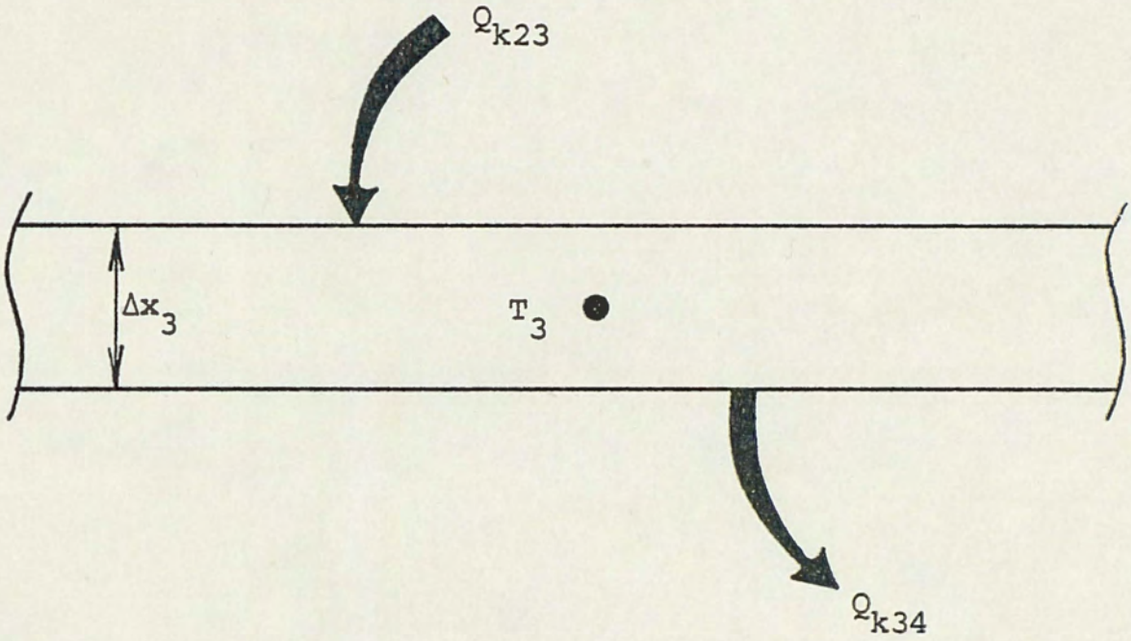

Figure 34. Energy Balance on Back Insulation

Combining equations B.22, 23, 24

B.25 $$(mc)_3 \frac{dT_3}{dt} = \frac{K_3 A_c}{\left(\frac{\Delta x_3}{2}\right)} (T_2 - T_3) - \frac{K_3 A_c}{\left(\frac{\Delta x_3}{2}\right)} (T_3 - T_4)$$

which can be condensed to

B.26 $$\frac{dT_3}{dt} = \frac{A_c}{(mc)_3}\left(\frac{2K_3}{\Delta x_3}\right) T_2 - \frac{A_c}{(mc)_3}\left(\frac{4K_3}{\Delta x_3}\right) T_3 +$$

$$\frac{A_c}{(mc)_3}\left(\frac{2K_3}{\Delta x_3}\right) T_4$$

The last node to consider is the container or pan. An energy balance on this fourth node (refer to Figure 35)

B.27 $$Q_{s4} = Q_{K34} - Q_{c4a} - Q_{r4a}$$

where Q_{s4} = energy stored in node 4

Q_{K34} = energy conducted from node 3 to 4

Q_{r4a} = energy radiated from node 4 to ambient

From equation B.23

B.28 $$Q_{K34} = \frac{K_3 A_c}{\left(\frac{\Delta x_3}{2}\right)} (T_3 - T_4)$$

The energy radiated from node 4 is

B.29 $$Q_{r41} = A_c h_{r4a} (T_4 - T_a)$$

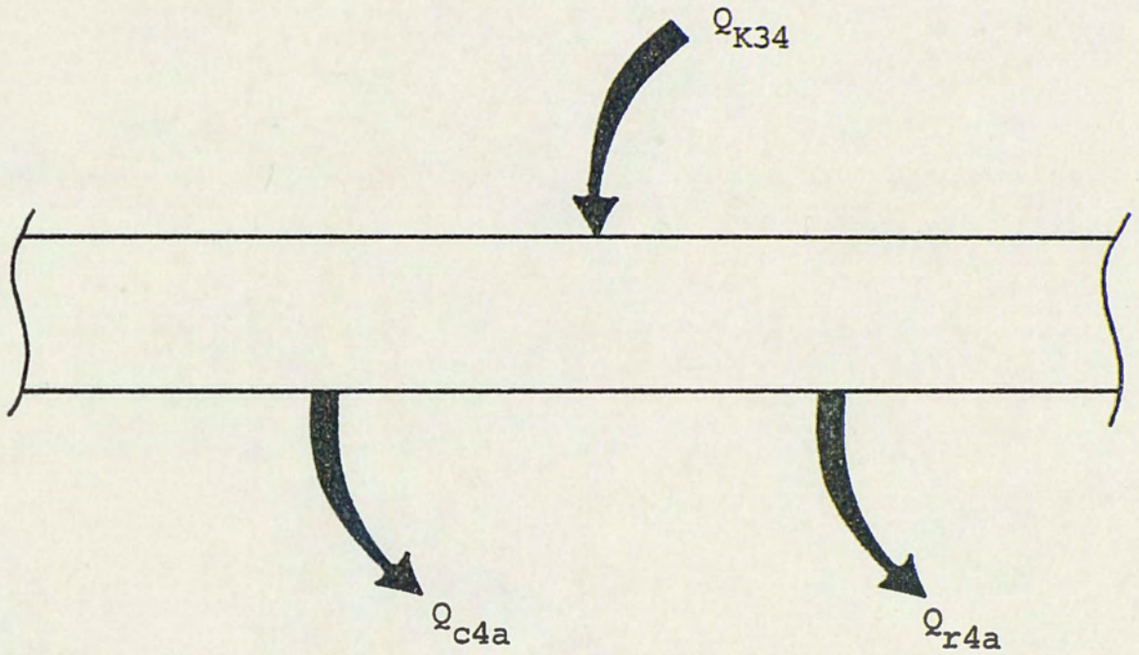

Figure 35. Energy Balance on Container

where the radiation coefficient is just

$$h_{r4a} = \sigma \varepsilon_4 (T_4^2 + T_a^2)(T_4 + T_a)$$

The energy convected from node 4 is

B.30 $$Q_{c4a} = A_c h_w (T_4 - T_a)$$

The energy stored in node 4 is

B.31 $$Q_{s4} = (mc)_4 \frac{dT_4}{dt}$$

Substituting equations B.28 - B.31 into B.27

B.32 $$(mc)_4 \frac{dT_4}{dt} = \frac{K_3 A_c}{\left(\frac{\Delta x_3}{2}\right)}(T_3 - T_4) - A_c h_w (T_4 - T_a) -$$

$$A_c h_{r4a} (T_4 - T_a)$$

This can be condensed to

B.33 $$\frac{dT_4}{dt} = \frac{A_c}{(mc)_4}\left(\frac{2K_3}{\Delta x_3}\right)T_3 - \frac{A_c}{(mc)_4}\left(\frac{2K_3}{\Delta x_3}\right) + h_w + h_{r4a}$$

$$\cdot T_4 + \frac{A_c}{(mc)_4} h_w T_a + h_{r4a} T_a)$$

Equations B.11, B.20, B.26 and B.33 constitute a set of linear differential equations describing the mean temperatures of the collector's four nodes.

Appendix C

SOLUTION OF A SET OF FOUR ORDINARY DIFFERENTIAL EQUATIONS

The general set of four simultaneous ordinary linear differential equations which occurs in this paper has the matrix form

C.1
$$\begin{bmatrix} \dot{T}_1 \\ \dot{T}_2 \\ \dot{T}_3 \\ \dot{T}_4 \end{bmatrix} = \begin{bmatrix} a_{11} & a_{12} & a_{13} & a_{14} \\ a_{21} & a_{22} & a_{23} & a_{24} \\ a_{31} & a_{32} & a_{33} & a_{34} \\ a_{41} & a_{42} & a_{43} & a_{44} \end{bmatrix} \cdot \begin{bmatrix} T_1 \\ T_2 \\ T_3 \\ T_4 \end{bmatrix} + \begin{bmatrix} b_1 \\ b_2 \\ b_3 \\ b_4 \end{bmatrix}$$

or in condensed form

C.2
$$\left[\dot{T}(t)\right] = \left[A\right]\left[T(t)\right] + \left[B\right]$$

The initial conditions are at $t = t_o$

C.3
$$\begin{bmatrix} T_1(t_o) \\ T_2(t_o) \\ T_3(t_o) \\ T_4(t_o) \end{bmatrix} = \begin{bmatrix} C_1 \\ C_2 \\ C_3 \\ C_4 \end{bmatrix}$$

or

C.4
$$\left[T_o\right] = \left[C\right]$$

To simplify the solution of equation C.1, it is assumed that a_{ij} and b_i are constants for the time interval under consideration.

An exact solution to this set of coupled differential equations is possible using the method of Laplace transforms. In theory, this approach can be employed successfully if the initial conditions are known. In practice, however, the initial transformation, the ensuing matrix manipulation and the inverse Laplace transformations become overwhelming for this system size. Alternatively, the equations can be uncoupled using the method of determinants[27] and solved independently. However, the resulting equations are no less difficult to solve than the original coupled set.

Bronson[28] develops a matrix approach to the solution of the initial value problem

$$\text{C.5} \qquad \left[\dot{T}(t)\right] = \left[A\right]\left[T(t)\right] + \left[f(t)\right]$$

$$\text{with} \qquad \left[T(t_o)\right] = \left[C\right]$$

where the matrix $\left[A\right]$ is a constant coefficient matrix and $\left[C\right]$ is the initial condition matrix. Equation C.5 is identical to C.2 if $\left[f(t)\right]$ is just a constant matrix.

The result of Bronson's analysis yields the exact solution

$$\text{C.6} \qquad \left[T(t)\right] = e^{[A](t-t_o)}\left[C\right] + e^{[A]t}\int_{t_o}^{t}\left\{e^{-[A]s}\left[f(s)\right]\right\}ds$$

If the time axis is adjusted so that the initial condition of any time interval occurs at time t equal to zero then equation C.6 becomes

C.7 $$\left[T(t)\right] = e^{[A]t} \cdot \left[C\right] + e^{[A]t} \int_0^t \left\{e^{-[A]s} \cdot \left[f(s)\right]\right\} ds$$

The matrix $e^{[A]t}\left[C\right]$ constitutes the transient portion while the integrated term constitutes the steady state solution. Equation C.7 now allows the calculation of the four node temperatures, T_i, at the end of some time interval ($t = n\Delta\tau$) when the matrix $\left[A\right]$ can be considered constant for the interval.

To employ equation C.7, the calculation of the matrix $e^{[A]t}$ is required. This term may be expressed as[29]

C.8 $$e^{[A]t} = \alpha_3\left\{\left[A\right]t\right\}^3 + \alpha_2\left\{\left[A\right]t\right\}^2 + \alpha_1\left\{\left[A\right]t\right\} + \alpha_o\left[I\right]$$

where $\left[I\right]$ = identity matrix

and α_i is found by solving the equations

$$e^{\lambda 1} = \alpha_3\lambda_1^3 + \alpha_2\lambda_1^2 + \alpha_1\lambda_1 + \alpha_o$$

C.9 $$e^{\lambda 2} = \alpha_3\lambda_2^3 + \alpha_2\lambda_2^2 + \alpha_1\lambda_2 + \alpha_o$$

$$e^{\lambda 3} = \alpha_3 \lambda_3^{\,3} + \alpha_2 \lambda_3^{\,2} + \alpha_1 \lambda_3 + \alpha_o$$

$$e^{\lambda 4} = \alpha_3 \lambda_4^{\,3} + \alpha_2 \lambda_4^{\,2} + \alpha_1 \lambda_4 + \alpha_o$$

where λ_i = eigenvalues of the matrix $[At]$

It becomes apparent that the calculations to obtain $e^{[A]t}$ are time consuming. This is due mainly to the problem of obtaining the eigenvalues for the four by four matrix $[A]$.

An alternate method for obtaining the matrix $e^{[A]t}$ is use of the definition

C.10 $$e^{[A]t} = \sum_{K=0}^{\infty} \frac{([A]t)^K}{K!} = [I] + \frac{[A]t}{1!} + \frac{([A]t)^2}{2!} + \ldots$$

where $[I]$ is the identity matrix. The error of taking a finite sum is at the most the size of the first neglected term. Therefore, the number of terms needed for a desired accuracy depends largely on the time step ($t = \Delta\tau$) chosen.

Using the results of equations C.8 or C.10, the exact solution to the set of coupled differential equations can be calculated from equation C.7. It should be recalled that the solution is for a constant $[A]$ matrix. If $[A]$ is not constant but is a function of the dependent variables T_i, a first guess at $[A]$ can be made. Using this matrix, a solution for $[T]$ can be found. Then using $[T]$, a new $[A]$ matrix can be calculated which leads to a new solution for the $[T]$ matrix. This technique can be carried out until there

is little change in the $[T]$ matrix.

In many cases with differential equations, exact solutions become prohibitive with respect to the time required for a solution. The alternative is a numerical approach. Perhaps the easiest numerical solution technique which could be used to solve equation C.1 is the common predictor-corrector method. There are several different routines[30,31], many of which have higher order predictors and correctors. For purposes of illustration, the Adams-Moulton predictor-corrector of order 3 is described here. The predictor is

$$T_{n+1}^{p} = T_n + \frac{\Delta\tau}{24}\left[55\dot{T}_n - 59\dot{T}_{n-1} + 37\dot{T}_{n-2} - 9\dot{T}_{n-3}\right] \tag{C.11}$$

where n = present time

p = predicted value

$\Delta\tau$ = time step

T = dependent variable to be predicted

$\dot{T}$ = time derivative of dependent variable

For the system of four equations, there will be four predicted values. The next step is to calculate the $(n + 1)$ time derivatives of the dependent variables using the predicted values. That is,

$$\dot{T}_{n+1} = f\,(T_n^{p} + 1) \tag{C.12}$$

where f is the differential equation.

Now the corrector is

$$C.13 \qquad T^{c}_{n+1} = T_n + \frac{\Delta\tau}{24}\left[9\dot{T}_{n+1} + 19\dot{T}_n - 5\dot{T}_{n-1} + \dot{T}_{n-2}\right]$$

where the superscript c denotes the corrected value. One can accept this corrected value or use it to go through the routine again until some convergence occurs between the predicted and corrected values.

For a set of coupled differential equations, it is difficult to determine stability and error criteria by other than a trial basis. However, for a single first-order equation, Gerald[32] gives the convergence criteria as

$$\Delta\tau < \frac{24/9}{|\dot{T}|}$$

$$D \cdot 10^{N} < \frac{24/9}{\Delta\tau|\dot{T}|}$$

and the accuracy criteria as

$$D \cdot 10^{N} < 14$$

where D = difference between corrected and predicted value

N = N^{th} decimal place

$\dot{T}$ = value of derivative

The error of this method is on the order of $(\Delta\tau)^5$.

Although the predictor-corrector can be readily applied, it is an explicit method and is subject to oscillations which can

easily cause instability. The alternative is an implicit method which is not subject to instability. The Crank-Nicholson technique is such a method. This technique predicts the new values by using the averages of the time derivatives at the old time, t, and the new time, $t + \Delta\tau$.[33] That is,

C.14 $$[T]^{(V+1)} = [T]^{(V)} + \frac{1}{2}\left\{[\dot{T}]^{(V)} + [\dot{T}]^{(V+1)}\right\}\Delta\tau$$

where $[T]$ = dependent variable matrix (equation C.2)

$[\dot{T}]$ = time derivative of

$\Delta\tau$ = time step

V = V^{th} time period

From the differential equations describing the system (equation C.1)

C.15 $$[\dot{T}]^{(V)} = [A]^{(V)}[T]^{(V)} + [B]^{(V)}$$

C.16 $$[\dot{T}]^{(V+1)} = [A]^{(V+1)}[T]^{(V+1)} + [B]^{(V+1)}$$

Substitution of these two equations into equation C.14 yields after suitable manipulation

C.17 $$\left\{[I] - \frac{1}{2}[A]^{(V+1)}\Delta\tau\right\}[T]^{(V+1)} = [T]^{(V)} + \frac{1}{2}\left\{[A]^{(V)} \cdot [T]^{(V)}\right\}\Delta\tau + \frac{1}{2}\left\{[B]^{(V)} + [B]^{(V+1)}\right\}\Delta\tau$$

An iterative process can be used to obtain $[T]^{(V+1)}$. That is, assume $[A]^{(V+1)}$ and $[B]^{(v+1)}$ are approximately equal to $[A]^{(V)}$ and

$[B]^{(V)}$ respectively, and solve equation C.17 for $[T]^{(V+1)}$. This process can be repeated until a convergence criteria is satisfied.

Appendix D

EXPERIMENTAL DATA

The following presents the raw data from the tests performed on the thermosyphon system described in Chapter VII (see Figure 22). Also included is specific information on the characteristics of the system.

Solar Collector Characteristics

collector slope	34^{o}
surface area	48 sq. ft.
glass cover thickness	.062 in.
glass emissivity	.88
glass to plate spacing	2.5 in.
absorber plate thickness	.012 in.
absorptance	.80
absorber emissivity	.9
tube to plate bond	continuous solder
tube configuration	2 parallel sinusoids (10 passes)
inside tube diameter	.785 in.
outside tube diameter	.875 in.
back insulation thickness	.5 in.

insulation conductivity	.03 BTU/hr-ft ^{o}F
collector container	galvanized steel
container emissivity	.1
collector perimeter	32 ft.
collector depth	3 in.

Storage Tank Characteristics

tank capacity	80 gal.
height	4 ft.
diameter	1.84 ft.
insulation thickness	.5 ft.
insulation conductivity	.028 BTU/hr-ft ^{o}F

More system geometry is given in Figure 36.

The following is the instrumentation used to obtain data recorded September 28, 1976, and September 29, 1976, on a thermosyphon system at Florida Technological University.

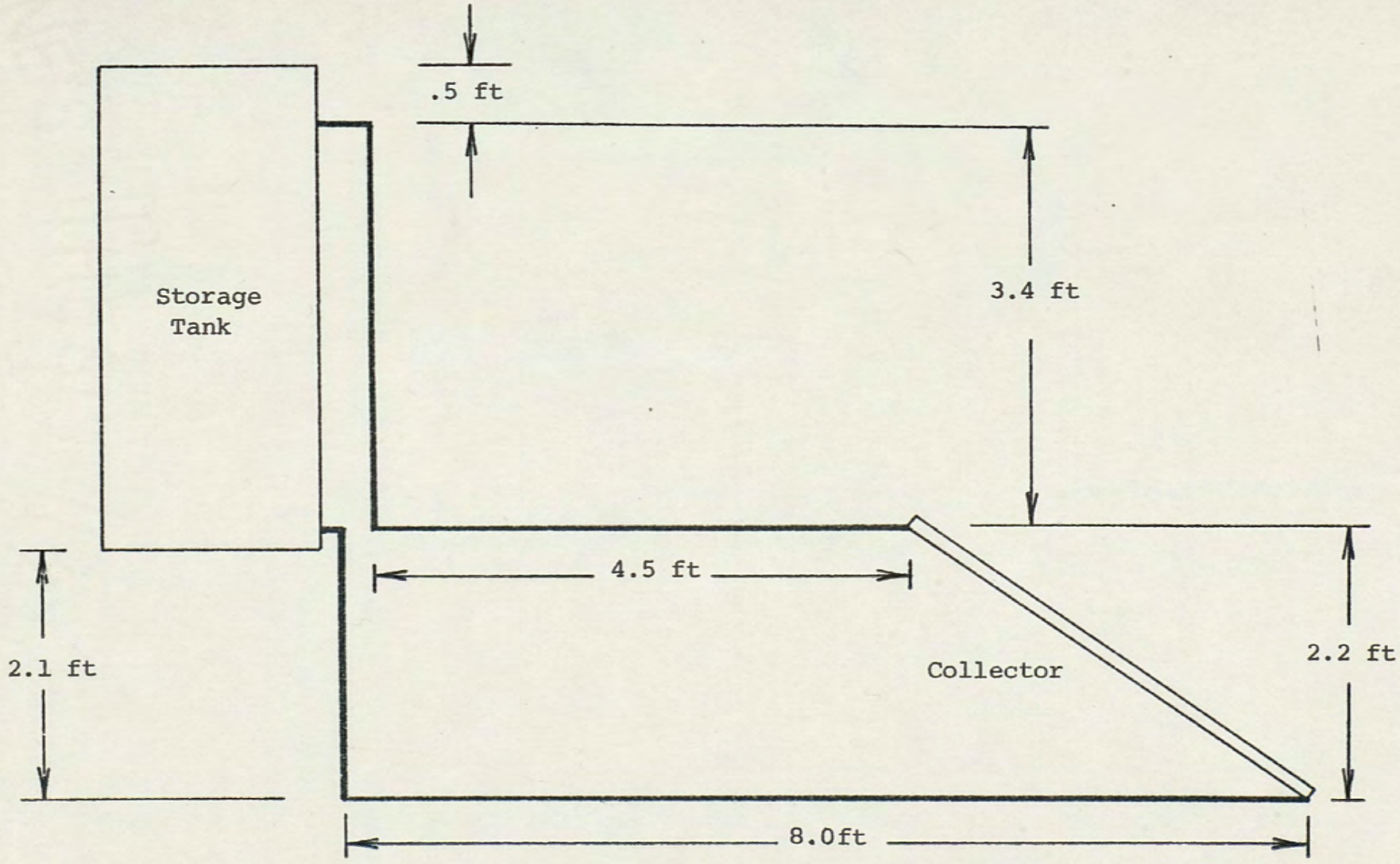

Figure 36. Geometry of System

Insolation	Eppley pyranometer with Leeds and Northrup Speedomax recorder
Flow Rate	Barco 220 venturi with Validyne pressure transducer/amplifier (flow is given by: $10.53 \times 10^{.56578\log(\Delta P)}$ in GPH $\Delta P = 2.77 \times$ voltage reading
Temperature (uncorrected)	Copper-Constantan thermocouples with Omega Omni-Amp millivolt amplifier/reference junction
Load Flow	Carlon Flow Detector
Wind Speed	Texas Electronics Wind Direction and Velocity Monitor and Recording System
Voltage Signals	Data Precision digital multimeter

TEST DATE : 9/28/76

TEST SITE : F. T. U. - Thermosyphon System

	Initials	Date
Prepared By	Pg.	1A
Approved By		

	(1) Time	(2) Mass flow	(3) Load flow	(4) T_{inlet}	(5) T_{outlet}	(6) $T_{TANK\ TOP}$	(7) $T_{TANK\ MIDDLE}$	(8) $T_{TANK\ BOTTOM}$
1								
2	7:30	-.005	0.0	19.7	24.0	26.5	25.4	25.4
3								
4	7:40	-.005	0.0	19.7	23.2	26.2	25.4	25.4
5								
6	7:50	-.004	0.0	19.6	22.4	26.0	25.3	25.4
7								
8	8:00	-.003	0.0	20.0	22.1	26.1	25.2	25.4
9								
10	8:10	.000	0.0	20.4	21.8	25.9	24.9	25.3
11								
12	8:20	.002	0.0	20.5	21.9	26.0	25.0	25.3
13								
14	8:30	.004	0.0	20.9	22.5	26.0	25.0	25.3
15								
16	8:40	.006	0.0	20.9	23.0	26.0	25.1	25.4
17								
18	8:50	.009	0.0	21.6	24.7	26.1	25.1	25.4
19								
20	9:00	.020	0.0	22.1	29.2	26.1	25.1	25.3
21								
22	9:10	.080	0.0	23.9	35.1	26.0	25.1	25.3
23								
24	9:20	.148	0.0	24.3	39.9	26.2	25.2	25.3
25								
26	9:30	.189	0.0	24.4	43.9	26.2	25.2	25.3
27								
28	9:40	.215	0.0	24.8	48.1	26.5	25.4	25.3
29								
30	9:50	.229	0.0	24.9	49.5	26.7	25.5	25.3
31								
32	10:00	.240	0.0	25.2	51.6	27.6	25.8	25.6
33								
34	10:10	.256	0.0	25.5	53.8	28.9	25.8	25.6
35								
36	10:20	.274	0.0	25.7	56.6	30.8	25.9	25.7
37								
38	10:30	.264	0.0	25.9	57.6	33.2	26.0	25.8
39								
40	10:40	.277	0.0	26.1	58.8	35.8	26.0	26.0

9/28/76

	Initials	Date
Prepared By	PG	1B
Approved By		

(1)	(2)	(3)	(4)	(5)	(6)	(7)	(8)
$T_{ambient}$			COMMENTS				
20.7							
20.8							
20.9							
20.9							
21.1			Rezeroed Mass flow transducer				
21.4			(no observable offset of flow				
21.9			readings)				
22.1							
23.1							
25.5							
26.9							
28.4							
26.2							
26.9							
26.5							
26.3							
27.4							
29.2							
			Rezeroed Mass flow transducer (10:25)				
30.6			(observed slight offset of flow readings)				
29.2							

9/28/76

	Initials	Date
Prepared By	Pg.	2A
Approved By		

	(1) Time	(2) Mass flow	(3) Load flow	(4) T_{inlet}	(5) T_{outlet}	(6) $T_{TANK\ TOP}$	(7) $T_{TANK\ MIDDLE}$	(8) $T_{TANK\ BOTTOM}$
1								
2	10:50	.286	0.0	26.2	61.2	38.6	26.1	26.1
3								
4	11:00	.295	0.0	26.4	60.3	41.4	26.2	26.1
5								
6	11:10	.302	0.0	26.6	63.4	44.2	26.3	26.1
7								
8	11:20	.278	0.0	26.4	63.1	46.9	26.5	26.1
9								
10	11:30	.284	0.0	26.5	62.4	49.3	26.5	26.1
11								
12	11:40	.300	0.0	27.2	62.0	51.4	26.5	26.2
13								
14	11:50	.244	0.0	27.2	58.9	53.5	26.7	26.2
15								
16	12:00	.190	0.0	27.3	53.8	54.8	26.8	26.3
17								
18	12:10	.207	0.0	27.6	55.5	56.1	26.9	26.3
19								
20	12:20	.244	0.0	27.5	57.6	56.9	27.2	26.3
21								
22	12:30	.235	0.0	27.8	59.1	57.5	27.5	26.3
23								
24	12:40	.316	0.0	28.6	65.9	58.0	27.9	26.3
25								
26	12:50	.368	0.0	28.7	69.5	58.5	28.6	26.3
27								
28	1:00	.292	0.0	28.8	64.9	59.2	29.6	26.4
29								
30	1:10	.216	0.0	27.9	58.0	59.9	30.6	26.4
31								
32	1:20	.135	0.0	28.3	51.7	60.3	31.5	26.5
33								
34	1:30	.178	0.0	29.4	54.2	59.5	32.5	26.5
35								
36	1:40	.256	0.0	29.1	59.3	59.7	33.8	26.6
37								
38	1:50	.314	0.0	29.3	67.0	60.1	35.4	26.7
39								
40	2:00	.354	0.0	29.6	72.2	60.9	37.3	26.8

	Initials	Date
Prepared By	Pg.	2B
Approved By		

	(1)	(2)	(3)	(4)	(5)	(6)	(7)	(8)
	$T_{ambient}$			COMMENTS				
1								
2	30.0							
3								
4	29.5							
5								
6	29.1							
7								
8	30.5							
9								
10	32.8							
11								
12	30.5							
13								
14	31.0							
15								
16	30.5							
17								
18	31.8							
19								
20	29.5							
21								
22	29.9							
23								
24	32.2							
25								
26	30.7							
27								
28	30.5							
29								
30	30.7							
31								
32	30.3							
33								
34	30.9							
35								
36	31.1							
37								
38	32.7							
39								
40	32.8							

9/28/76 (cont'd)

	Initials	Date
Prepared By	PG	3A
Approved By		

	(1) Time	(2) Mass flow	(3) Load flow	(4) T_{inlet}	(5) T_{outlet}	(6) $T_{TANK\ TOP}$	(7) $T_{TANK\ MIDDLE}$	(8) $T_{TANK\ BOTTOM}$
1								
2	2:10	.251	0.0	28.8	62.9	62.0	39.3	26.8
3								
4	2:20	.172	0.0	29.1	59.2	63.0	41.0	26.9
5								
6	2:30	.240	0.0	29.8	63.4	63.4	42.4	27.0
7								
8	2:40	.250	0.0	29.4	63.2	63.7	44.3	27.3
9								
10	2:50	.233	0.0	29.8	64.2	64.1	46.0	27.5
11								
12	3:00	.258	0.0	30.1	63.8	64.6	47.6	27.6
13								
14	3:10	.217	0.0	28.4	62.2	65.1	49.2	27.9
15								
16	3:20	.193	0.0	30.1	60.5	64.9	50.3	28.0
17								
18	3:30	.227	0.0	30.0	63.3	65.0	51.5	28.4
19								
20	3:40	.221	0.0	30.0	64.9	65.0	52.7	28.7
21								
22	3:50	.240	0.0	30.3	67.5	65.2	53.7	29.3
23								
24	4:00	.224	0.0	30.3	65.6	65.4	54.7	30.0
25								
26	4:10	.196	0.0	30.2	63.2	65.7	55.5	30.6
27								
28	4:20	.149	0.0	30.6	60.5	65.9	56.2	31.4
29								
30	4:30	.163	0.0	31.0	59.6	65.3	56.6	32.0
31								
32	4:40	.166	0.0	31.0	57.9	65.2	57.2	32.8
33								
34	4:50	.148	0.0	31.2	59.7	65.1	57.8	33.6
35								
36	5:00	.128	0.0	31.3	59.4	64.8	58.2	34.4
37								
38	5:10	.106	0.0	31.2	57.7	64.7	58.6	35.2
39								
40	5:20	.080	0.0	31.4	54.3	64.4	59.0	36.2

9/28/76

	Initials	Date
Prepared By	Pg	3B
Approved By	g	

	(1)	(2)	(3)	(4)	(5)	(6)	(7)	(8)
	$T_{ambient}$			COMMENTS				
1								
2	30.8							
3								
4	32.2							
5								
6	32.0							
7								
8	31.9							
9								
10	32.8							
11								
12	32.3							
13								
14	32.3							
15								
16	32.1							
17								
18	33.6							
19								
20	33.1							
21								
22	33.9							
23								
24	33.9							
25								
26	34.3							
27								
28	34.3							
29								
30	34.4							
31								
32	33.2							
33								
34	33.5							
35								
36	33.3							
37								
38	33.3							
39								
40	33.3							

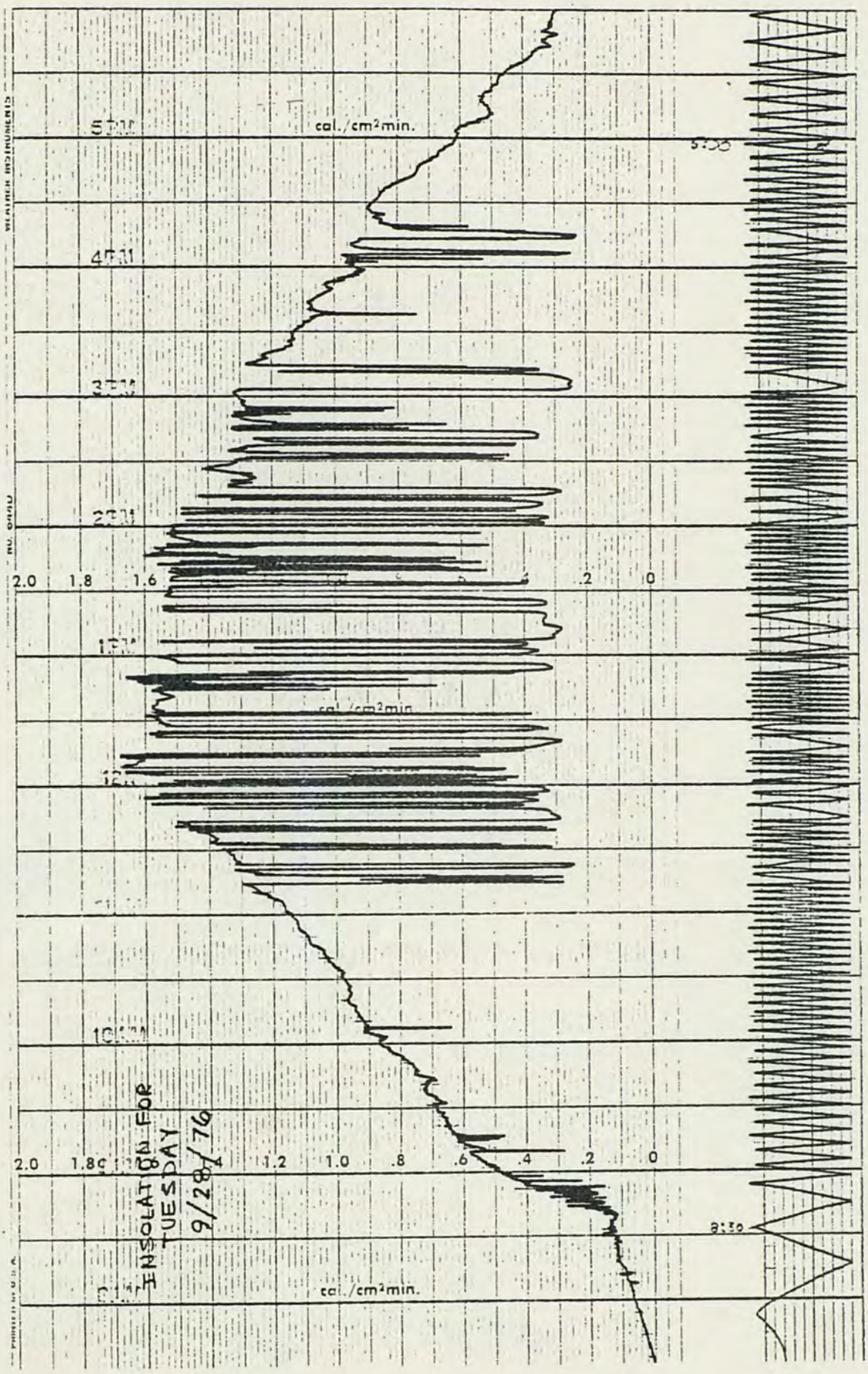
cal./cm²min.
2.0
1.8
1.6
.2
0
cal./cm²min.
2.0
1.2
1.0
.8
.6
.4
.2
0
cal./cm²min.
8:30
INSOLATION FOR
TUESDAY
9/28/76

TEST DATE 9/29/76

	Initials	Date
Prepared By	PJ	1A
Approved By		

TEST SITE : F. T. U. - THERMOSYPHON SYSTEM

	(1) Time	(2) Mass flow	(3) Load flow	(4) T_{inlet}	(5) T_{outlet}	(6) $T_{TANK\ TOP}$	(7) $T_{TANK\ MIDDLE}$	(8) $T_{TANK\ BOTTOM}$
1								
2	8:00	.000	0.0	22.2	22.2	26.8	26.0	26.0
3								
4	8:10	.007	0.0	22.3	22.6	26.9	26.1	26.0
5								
6	8:20	.0120	0.0	23.4	25.4	26.8	26.1	26.0
7								
8	8:30	.0150	0.0	23.8	26.2	26.8	26.1	26.1
9								
10	8:40	.0234	0.0	24.1	27.8	26.6	25.8	25.8
11								
12	8:50	.0406	0.0	24.5	29.5	26.8	25.9	26.0
13								
14	9:00	.0650	0.0	25.3	31.6	26.6	25.8	26.0
15								
16	9:10	.0940	0.0	25.4	34.2	26.4	25.7	26.0
17								
18	9:20	.133	0.0	25.5	38.1	26.5	25.7	26.0
19								
20	9:30	.149	0.0	25.4	40.4	26.7	25.7	26.0
21								
22	9:40	.131	0.0	25.4	39.5	26.6	25.8	26.0
23								
24	9:50	.144	0.0	25.7	41.4	26.8	25.7	26.0
25								
26	10:00	.173	0.0	25.6	43.5	27.2	25.8	26.0
27								
28	10:10	.206	0.0	25.6	46.7	27.8	25.8	26.0
29								
30	10:20	.258	0.0	25.9	52.8	28.8	25.7	26.0
31								
32	10:30	.270	0.0	26.2	55.4	30.2	25.8	26.0
33								
34	10:40	.274	0.0	26.5	56.0	32.0	25.9	26.0
35								
36	10:50	.258	0.0	26.8	57.0	34.2	26.0	26.1
37								
38	11:00	.255	0.0	26.8	59.0	36.9	26.1	26.1
39								
40	11:10	.257	0.0	26.8	55.8	39.6	26.2	26.1

9/29/76

	Initials	Date
Prepared By	Pg	1B
Approved By		

	(1)	(2)	(3)	(4)	(5)	(6)	(7)	(8)
	$T_{ambient}$			COMMENTS				
1								
2	23.4							
3								
4	23.7							
5								
6	23.9							
7								
8	24.0							
9								
10	23.9							
11								
12	24.2							
13								
14	25.0							
15								
16	25.5							
17								
18	25.5							
19								
20	25.7							
21								
22	25.7							
23								
24	26.8							
25								
26	26.4							
27								
28	26.6							
29								
30	27.7							
31								
32	28.6							
33								
34	29.0							
35								
36	28.4							
37								
38	29.8							
39								
40	29.0							

9/29/76 (cont'd)

	Initials	Date
Prepared By	PG	2A
Approved By		

(1)	(2)	(3)	(4)	(5)	(6)	(7)	(8)
Time	Mass flow	Load flow	T_{inlet}	T_{outlet}	$T_{TANK\ TOP}$	$T_{TANK\ MIDDLE}$	$T_{TANK\ BOTTOM}$
11:20	.261	0.0	27.0	58.0	42.4	26.2	26.1
11:30	.267	0.0	27.1	60.8	45.2	26.2	26.1
11:40	.303	0.0	27.2	63.0	47.5	26.3	26.1
11:50	.308	0.0	27.3	64.0	49.7	26.4	26.1
12:00	.322	0.0	27.2	65.3	51.7	26.5	26.1
12:10	.280	0.0	27.8	61.2	53.7	26.7	26.4
12:20	.240	0.0	27.7	57.4	55.7	26.9	26.4
12:30	.202	0.0	28.0	56.0	57.1	27.1	26.5
12:40	.276	0.0	28.6	60.9	58.5	27.4	26.4
12:50	.263	0.0	28.1	62.1	59.3	27.9	26.0
1:00	.289	0.0	28.1	61.9	59.9	28.5	26.0
1:10	.227	0.0	28.3	59.5	60.4	29.3	26.0
1:20	.264	0.0	28.5	63.5	60.9	30.2	26.0
1:30	.252	0.0	28.2	61.5	61.7	31.4	26.0
1:40	.240	0.0	29.1	61.0	62.5	33.0	26.0
1:50	.270	9.5	32.4	65.8	57.6	31.2	27.5
2:00	.231	0.0	32.6	63.2	60.3	31.8	27.7
2:10	.161	0.0	32.5	58.3	61.0	31.6	28.1
2:20	.230	0.0	30.1	57.6	60.6	30.5	28.5
2:30	.216	0.0	30.5	58.8	61.0	30.9	28.6

9/29/76

	Initials	Date
Prepared By	PG	2B
Approved By	g	

	(1)	(2)	(3)	(4)	(5)	(6)	(7)	(8)
	$T_{ambient}$			COMMENTS				
1								
2	29.7							
3								
4	30.1							
5								
6	30.6							
7								
8	31.1							
9								
10	31.2							
11								
12	30.3							
13								
14	29.3							
15								
16	31.5							
17								
18	30.7							
19								
20	31.1							
21								
22	31.1							
23								
24	31.8							
25								
26	31.8							
27								
28	30.9							
29								
30	31.7							
31								
32	32.9							
33								
34	30.4							
35								
36	31.2							
37								
38	30.6							
39								
40	30.7							

9/29/76

	Initials	Date
Prepared By	Pg	3A
Approved By	d	

	(1)	(2)	(3)	(4)	(5)	(6)	(7)	(8)
	Time	Mass flow	Load flow	T_{inlet}	T_{outlet}	$T_{TANK\ TOP}$	$T_{TANK\ MIDDLE}$	$T_{TANK\ BOTTOM}$
1								
2	2:40	.220	0.0	29.8	59.5	61.3	31.9	28.6
3								
4	2:50	.227	11.2	29.7	58.9	52.9	30.5	28.5
5								
6	3:00	.280	0.0	29.7	62.4	53.9	30.0	28.4
7								
8	3:10	.189	0.0	29.6	55.9	56.7	29.6	28.5
9								
10	3:20	.151	0.0	29.6	52.2	58.4	29.7	28.5
11								
12	3:30	.124	0.0	29.6	52.1	58.0	30.0	28.5
13								
14	3:40	.174	0.0	29.6	52.3	57.4	30.3	28.5
15								
16	3:50	.148	0.0	29.6	50.3	57.5	30.8	28.5
17								
18	4:00	.154	0.0	29.6	52.5	57.4	31.3	28.5
19								
20	4:10	.114	0.0	29.6	49.9	57.2	31.9	28.6
21								
22	4:20	.059	0.0	29.6	52.5	57.0	32.6	28.7
23								
24	4:30	.060	12.0	29.6	46.3	48.4	30.2	27.9
25								
26	4:40	.050	0.0	28.9	44.1	48.0	28.8	27.9
27								
28	4:50	.043	0.0	27.9	41.6	47.6	28.7	27.8
29								
30	5:00	.046	0.0	27.9	39.6	47.1	28.8	27.8
31								
32								
33								
34								
35								
36								
37								
38								
39								
40								

9/29/76

	Initials	Date
Prepared By	Pg	3B
Approved By		

	(1)	(2)	(3)	(4)	(5)	(6)	(7)	(8)
	Tambient			COMMENTS				
1								
2	31.3							
3								
4	32.0							
5								
6	31.1							
7								
8	30.7							
9								
10	30.9							
11								
12	31.7							
13								
14	32.4							
15								
16	31.2							
17								
18	31.7							
19								
20	31.0							
21								
22	30.6							
23								
24	30.8							
25								
26	30.4							
27								
28	30.1							
29								
30	30.5							
31								
32								
33				Return water temp. measured at 25.8				
34								
35								
36								
37								
38								
39								
40								

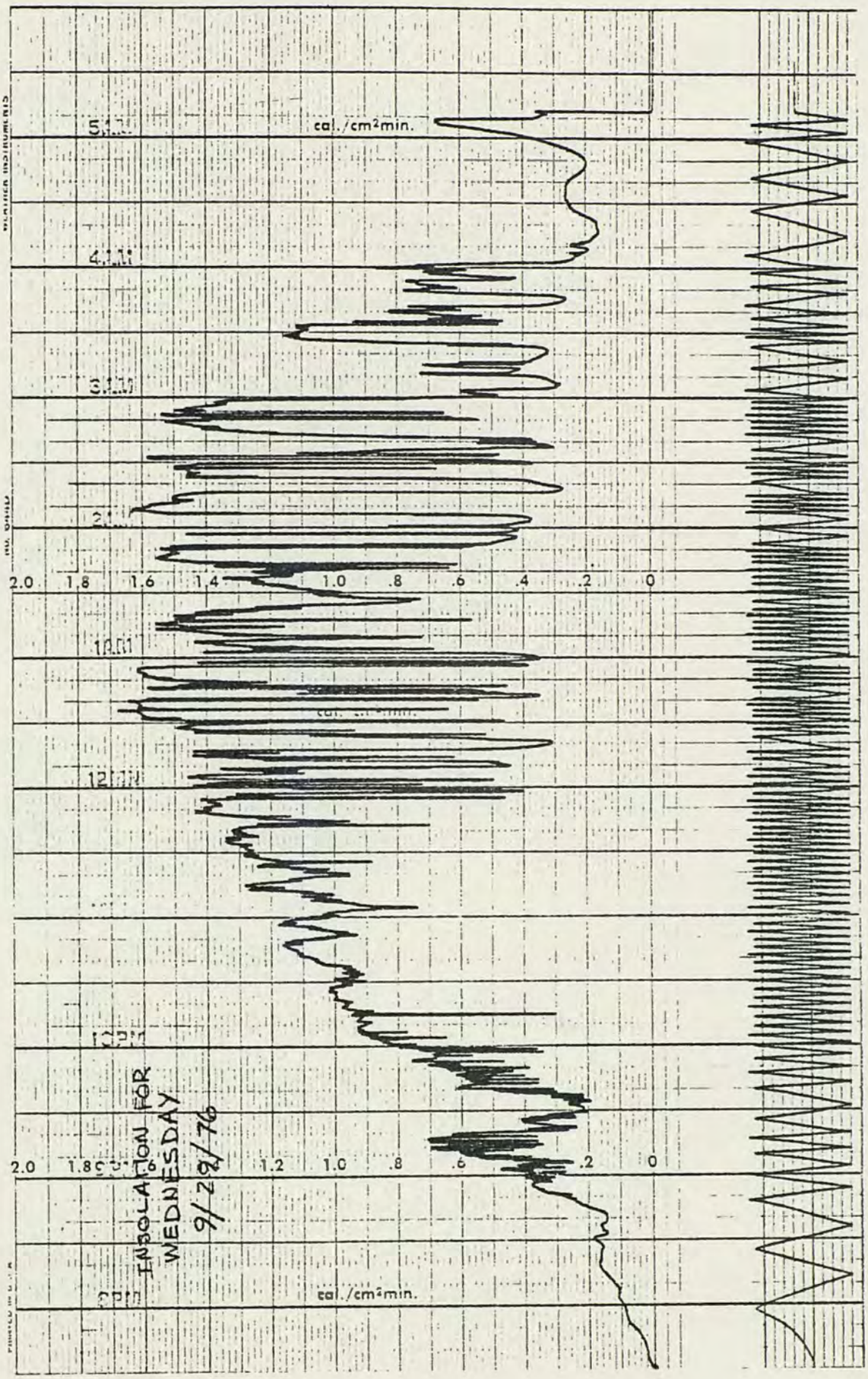
cal./cm²min.
2.0 1.8 1.6 1.4 1.0 .8 .6 .4 .2 0
cal./cm²min.
2.0 1.8 1.2 1.0 .8 .6 .2 0
INSOLATION FOR
WEDNESDAY
9/29/76

Appendix E

TSP FLOWCHART

The following represents a detailed flowchart for the TSP. Also included is a complete TSP listing and sample output.

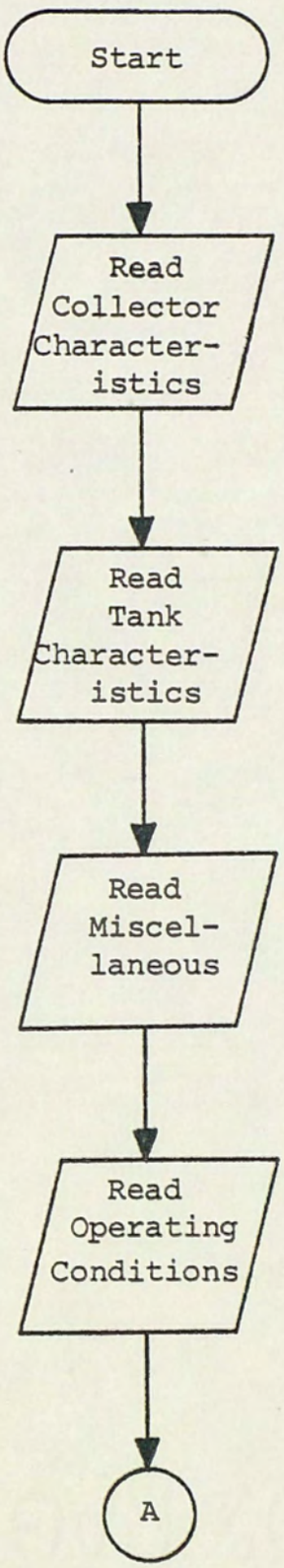
Start
Read Collector Character-istics
Read Tank Character-istics
Read Miscel-laneous
Read Operating Conditions
A

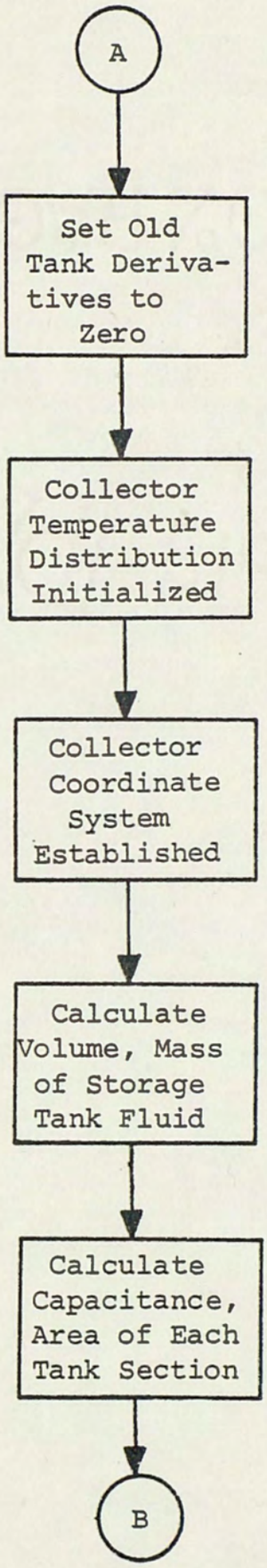
A
Set Old Tank Derivatives to Zero
Collector Temperature Distribution Initialized
Collector Coordinate System Established
Calculate Volume, Mass of Storage Tank Fluid
Calculate Capacitance, Area of Each Tank Section
B

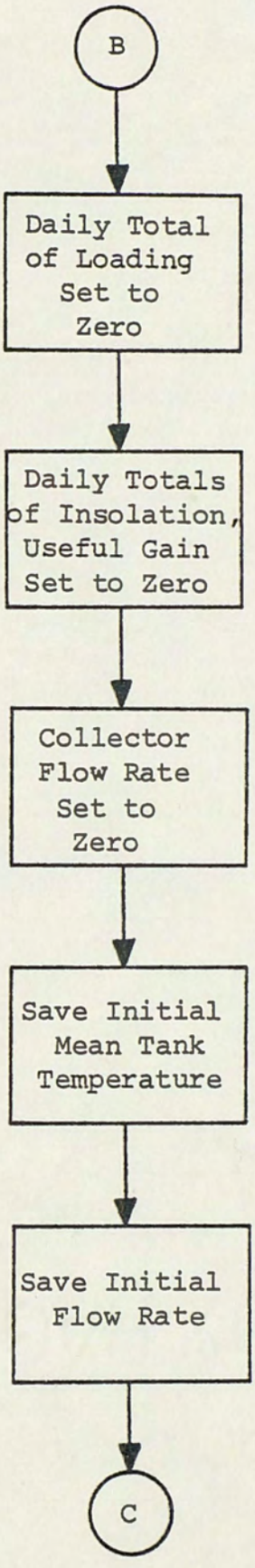
B
Daily Total of Loading Set to Zero
Daily Totals of Insolation, Useful Gain Set to Zero
Collector Flow Rate Set to Zero
Save Initial Mean Tank Temperature
Save Initial Flow Rate
C

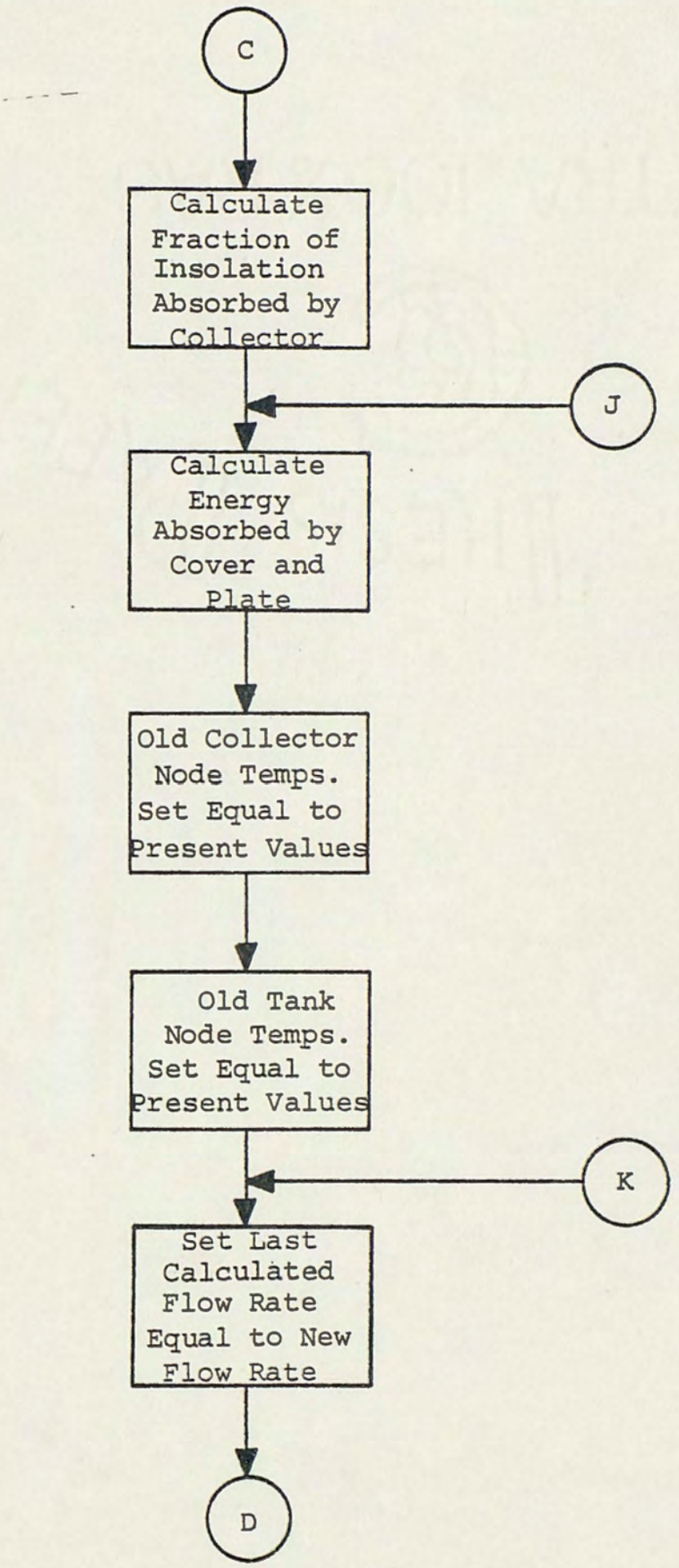
C
Calculate Fraction of Insolation Absorbed by Collector
J
Calculate Energy Absorbed by Cover and Plate
Old Collector Node Temps. Set Equal to Present Values
Old Tank Node Temps. Set Equal to Present Values
K
Set Last Calculated Flow Rate Equal to New Flow Rate
D

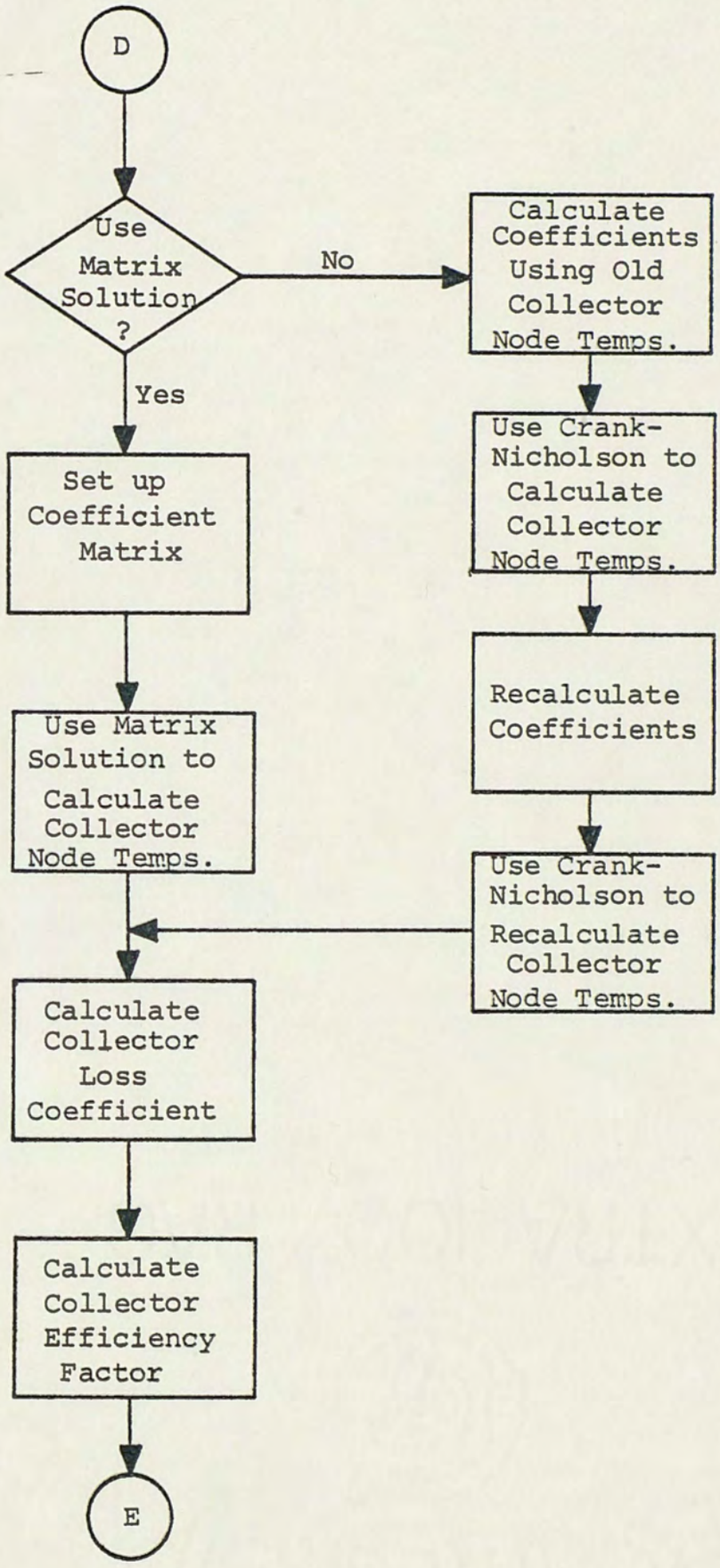
D
Use Matrix Solution ?
No
Yes
Calculate Coefficients Using Old Collector Node Temps.
Use Crank-Nicholson to Calculate Collector Node Temps.
Recalculate Coefficients
Use Crank-Nicholson to Recalculate Collector Node Temps.
Set up Coefficient Matrix
Use Matrix Solution to Calculate Collector Node Temps.
Calculate Collector Loss Coefficient
Calculate Collector Efficiency Factor
E

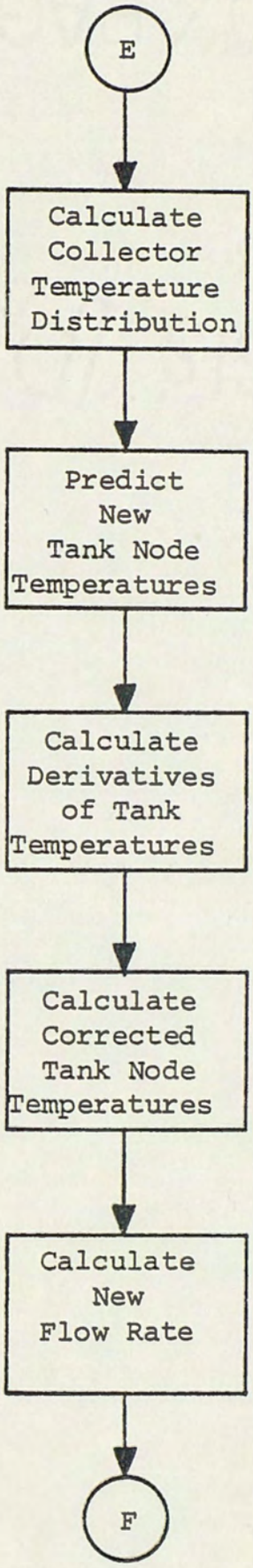
E
Calculate Collector Temperature Distribution
Predict New Tank Node Temperatures
Calculate Derivatives of Tank Temperatures
Calculate Corrected Tank Node Temperatures
Calculate New Flow Rate
F

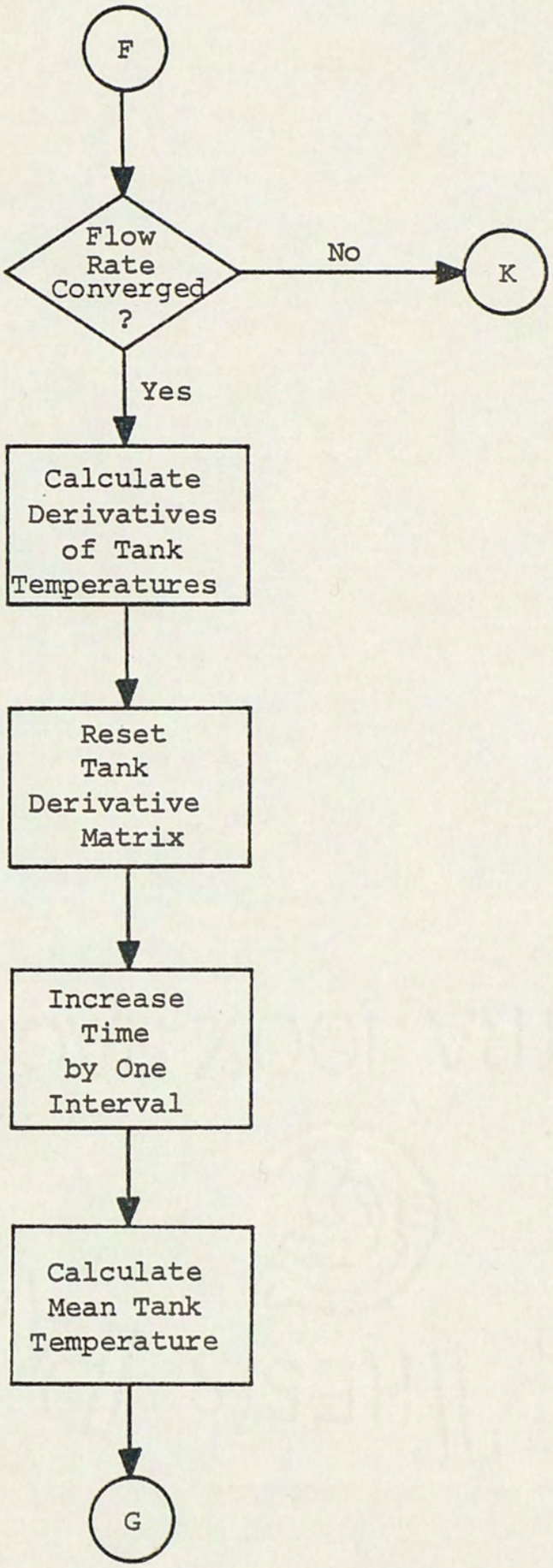
F
Flow Rate Converged ?
No
K
Yes
Calculate Derivatives of Tank Temperatures
Reset Tank Derivative Matrix
Increase Time by One Interval
Calculate Mean Tank Temperature
G

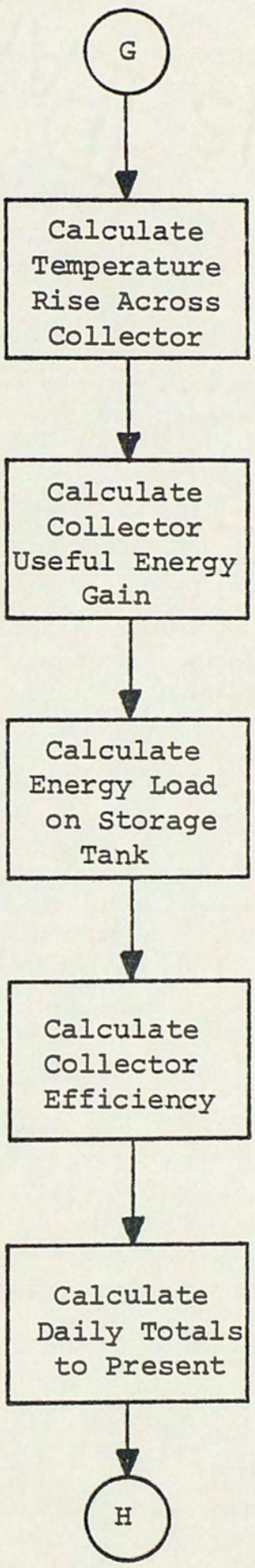
G
Calculate Temperature Rise Across Collector
Calculate Collector Useful Energy Gain
Calculate Energy Load on Storage Tank
Calculate Collector Efficiency
Calculate Daily Totals to Present
H

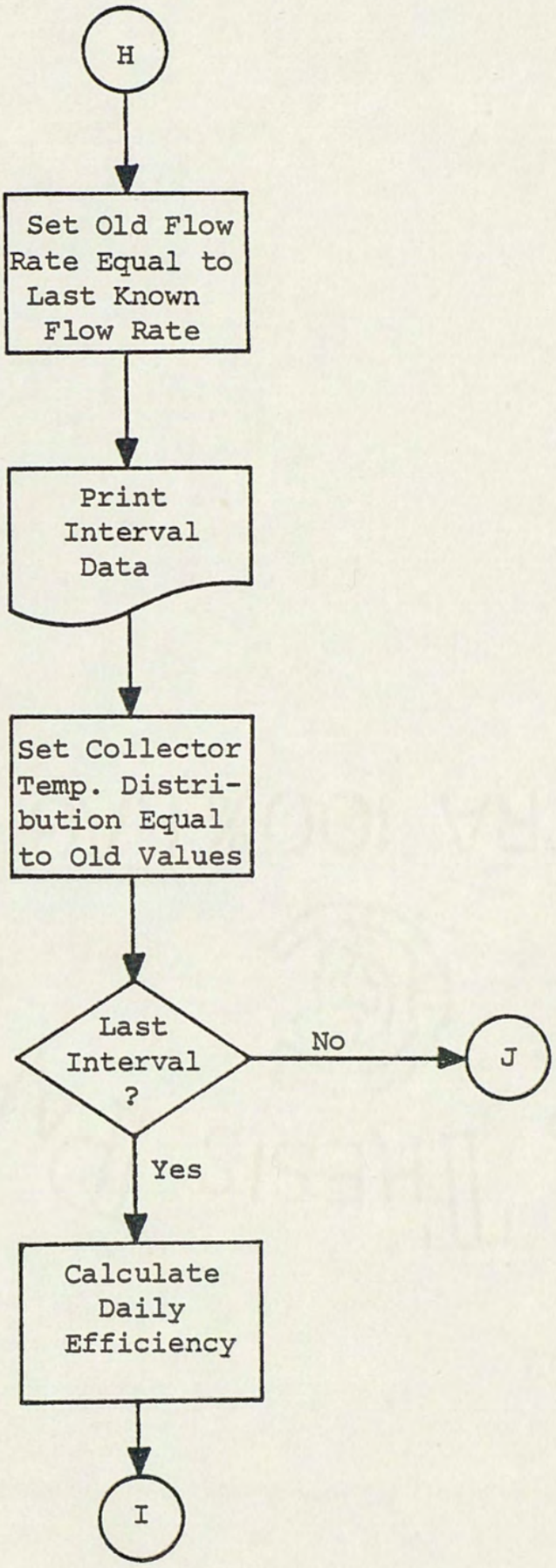
H
Set Old Flow Rate Equal to Last Known Flow Rate
Print Interval Data
Set Collector Temp. Distribution Equal to Old Values
Last Interval ?
No
J
Yes
Calculate Daily Efficiency
I

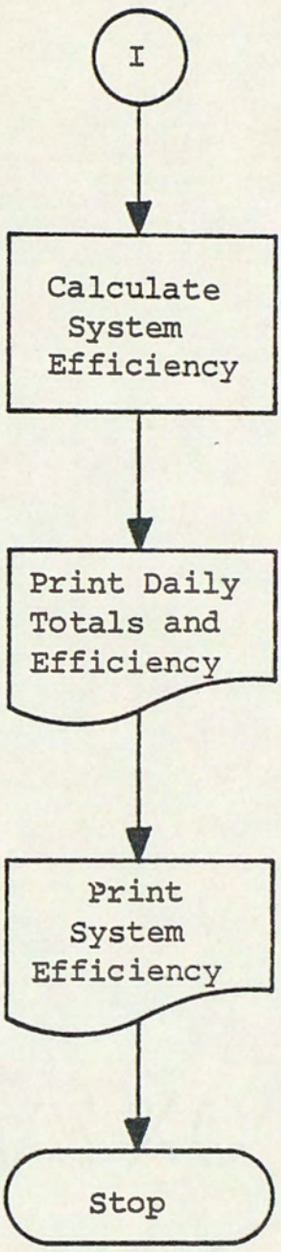
I
Calculate System Efficiency
Print Daily Totals and Efficiency
Print System Efficiency
Stop

```
$JOB            TSP,LINES=60
C
C
C
C
C       THIS PROGRAM IS A SIMULATION FOR A THERMOSYPHON SYSTEM.  IT
C   EMPLOYS TRANSIENT MODELS FOR THE COLLECTOR AND STORAGE TANK.  PIPE
C   LOSSES ARE NEGLECTED.  IT IS ASSUMED THAT THE SYSTEM IS CONTROLLED
C   ONLY TO THE EXTENT THAT REVERSE FLOW DOES NOT OCCUR.
C
C       IN ITS PRESENT CONFIGURATION, THIS PROGRAM REQUIRES THE COLLECTOR
C   TO BE A SINGLE COVER, FLAT PLATE TYPE WITH A TUBE OVER SHEET
C   CONFIGURATION.  THE TANK IS ASSUMED NOT TO CONTAIN AUXILLARY HEAT-
C   ING ELEMENTS OR HEAT EXCHANGERS.  THE PIPING IS ASSUMED TO BE SUCH
C   THAT THE TOP FOURTH OF THE TANK RECEIVES FLUID FROM THE COLLECTOR
C   AND DELIVERS FLUID TO THE LOAD.  THE BOTTOM FOURTH OF THE TANK
C   RECEIVES MAKEUP FLUID AND DELIVERS FLUID TO THE COLLECTOR.
C
C       THE PROGRAM MUST BE INITIALIZED AT SOME TIME EARLY IN THE DAY
C   WHEN IT CAN BE ASSUMED THAT THE COLLECTOR IS AT AMBIENT TEMPERATURE
C   AND THE TANK HAS BEEN IN STEADY STATE FOR FOUR PREVIOUS TIME STEPS.
C
C       ALL EQUATIONS INVOLVING VISCOSITY AND DENSITY OF THE WORKING
C   FLUID IS FOR WATER.  THEREFORE, THIS SIMULATION IS FOR A SYSTEM
C   UTILIZING ONLY WATER.
C
C       THE FOLLOWING INPUT VARIABLES ARE REQUIRED:
C
C   COLLECTOR CHARACTERISTICS
C
C   SLOPE  = COLLECTOR SLOPE (RADIANS)
C   T      = THICKNESS OF COVER PLATE ON COLLECTOR
C   EC     = EXTINCTION COEFFICIENT OF COVER PLATE
C   REFIDX = REFRACTIVE INDEX OF COVER PLATE
C   UC     = BOND CONDUCTANCE
C   W      = AVERAGE FIN WIDTH FOR COLLECTOR TUBE
C   B      = DISTANCE BETWEEN TUBE CENTERS
C   DI     = INSIDE TUBE DIAMETER
C   LP     = HALF THE DISTANCE BETWEEN BONDS
C   DE     = OUTSIDE TUBE DIAMETER
C   PER    = PERIMETER OF COLLECTOR
C   DEP    = DEPTH OF COLLECTOR
C   MCG    = THERMAL CAPACITANCE OF COVER PLATE
C   MCP    = THERMAL CAPACITANCE OF ABSORBER PLATE
C   MCINS  = THERMAL CAPACITANCE OF BACK INSULATION
C   MCPAN  = THERMAL CAPACITANCE OF CONTAINER
C   CA     = OVERALL COLLECTOR CAPACITANCE PER UNIT AREA
C   EMISP  = EMISSIVITY OF ABSORBER PLATE
C   EMISG  = EMISSIVITY OF COVER PLATE
C   EMISPN = EMISSIVITY OF CONTAINER
C   VF     = VIEW FACTOR FROM ABSORBER TO COVER PLATE
C   CP     = SPECIFIC HEAT OF WORKING FLUID
C   AC     = NOMINAL SURFACE AREA OF COLLECTOR
C   CV     = CONVECTION COEFFICIENT DEPENDENT ON SLOPE OF COLLECTOR
C   KINS   = THERMAL CONDUCTIVITY OF BACK INSULATION IN COLLECTOR
C   XINS   = THICKNESS OF BACK INSULATION
C   TUBLEN = TOTAL LENGTH OF TUBE IN COLLECTOR
C   DELTA  = THICKNESS OF ABSORBER SHEET
C   K      = THERMAL CONDUCTIVITY OF ABSORBER
C   ALPHA  = ABSORPTIVITY OF ABSORBER
```

```
C      THE FOLLOWING INFORMATION MUST BE ACCURATE. AS A CHECK, DOES
C    ( # OF BENDS IN COLLECTOR)*(H + HC) = DISTANCE BETWEEN INLET AND
C    OUTLET AT COLLECTOR?
C
C    UP      = DISTANCE FROM TANK BOTTOM TO COLLECTOR INLET PIPE
C    DOWN    = DISTANCE FROM TANK TOP TO COLLECTOR OUTLET PIPE
C    BE      = CIRCUMFERENTIAL LENGTH OF A BEND IN THE COLLECTOR TUBES
C    TFB     = DISTANCE FROM INLET TO FIRST BEND IN COLLECTOR TUBE
C    TLB     = TUBE LENGTH BETWEEN BENDS IN COLLECTOR
C    LIN     = LENGTH OF INLET PIPE FROM TANK TO COLLECTOR
C    LOUT    = LENGTH OF OUTLET PIPE FROM TANK TO COLLECTOR
C    DYIN    = VERTICAL LENGTH OF INLET PIPE
C    DYOUT   = VERTICAL LENGTH OF OUTLET PIPE
C    H       = VERTICAL DISTANCE ACROSS BEND IN COLLECTOR
C    HC      = VERTICAL DISTANCE FROM THE END OF ONE BEND TO THE
C              BEGINNING OF A SUCCEEDING BEND
C    HEIGHT  = HEIGHT OF TANK
C    SLOPE   = SLOPE OF COLLECTOR (RADIANS)
C
C    STORAGE TANK CHARACTERISTICS
C
C    US      = OVERALL LOSS COEFFICIENT FOR STORAGE TANK
C    DIAM    = DIAMETER OF TANK
C
C    TEST DATA
C
C    TIME    = TIME OF TEST
C    PERIOD  = LENGTH OF TIME INTERVALS (MINUTES)
C    INTRVL  = TOTAL NUMBER OF TIME INTERVALS
C    RADTN   = VALUE OF INTEGRATED NORMAL SOLAR RADIATION
C    TAMB    = AMBIENT TEMPERATURE
C    VEL     = WIND VELOCITY
C    MDL     = LOAD FLOW RATE
C    TLOAD   = TEMPERATURE OF RETURN FLUID
C    TST(N)  = INITIAL TEMPERATURES OF FOUR TANK NODES
C    TCO(N)  = INITIAL TEMPERATURES OF FOUR COLLECTOR NODES
C
C    MISCELLANEOUS
C
C    SIGMA   = BOLTZMAN'S CONSTANT
C    SECTNS  = DESIRED NUMBER OF SECTIONS COLLECTOR TUBE IS TO BE DIVIDED
C    MATRIX  = 1 FOR THE MATRIX SOLUTION TO THE DIFFERENTIAL
C              EQUATION, 0 FOR THE CRANK-NICHOLSON
C    TERMS   = DESIRED NUMBER OF TERMS FOR THE MATRIX SOLUTION
C    SHADE   = FRACTION OF RADIATION REDUCED FROM SHADING
C    FK      = FRICTION FACTOR ASSOCIATED WITH BENDS,TEES,ETC.
C    IGATE   = # OF GATE VALVES IN INLET PIPE
C    ITEE    = # OF TEES IN INLET PIPE
C    ILONGC  = # OF LONG ELBOWS IN INLET PIPE
C    ISTC    = # OF SHORT ELBOWS IN INLET PIPE
C    NGATE   = # OF GATE VALVES IN OUTLET PIPE
C    NLONGC  = # OF LONG ELBOWS IN OUTLET PIPE
C    NSTC    = # OF SHORT ELBOWS IN OUTLET PIPE
C    EG      = EQUIVALENT LENGTH OF A GATE VALVE
C    ET      = EQUIVALENT LENGTH OF A TEE
C    ELC     = EQUIVALENT LENGTH OF A LONG ELBOW
C    ESTC    = EQUIVALENT LENGTH OF A SHORT ELBOW
C
C
C
```

```
      C
     1      DIMENSION RADTN(144),TAMB(144),VEL(144),MDLO(144),TCO(4),TST(4),
            1 DTS(4,4),TFOLD(101),X(101),TF(101),TCOLD(4)
     2      DIMENSION DERT(4),TSTOLD(4),AA(4),A(4,4),F(4,1)
     3      REAL KL,L,LP,KINS,K,MCP,MCG,MCPAN,MDC,MDL,MDCO
     4      REAL MCINS,MDLO,LENGTH,MDCL,MASS,MCPST,LIN,LOUT
     5      INTEGER SECTNS,TIME,PERIOD,TERMS
     6      READ, T,EC,REFIDX,W,UC,B,DI,LP,DE,PER,DEP,
            1 MCP,MCG,MCPAN,MCINS,CA,EMISP,EMISG,EMISPN,AC,CV,KINS,XINS
     7      READ, TUBLEN,K,DELTA,ALPHA,US,DIAM,CP,SIGMA,
            1 PERIOD,TIME,INTRVL,SECTNS,VF,SHADE
     8      READ, UP,DOWN,BE,TFB,TLB,LIN,LOUT,DYIN,DYOUT,H,HC,HEIGHT,
            1  SLOPE
     9      READ, FK,IGATE,ITEE,ILONGC,ISTC,NGATE,NLONGC,NSTC,
            1  EG,ET,ELC,ESTC
    10      READ,(RADTN(I),I=1,INTRVL)
    11      READ, (VEL(I),I=1,INTRVL)
    12      READ, (MDLO(I),I=1,INTRVL)
    13      READ, (TAMB(I),I=1,INTRVL)
    14      READ, (TST(N),N=1,4)
    15      READ, TLOAD,(TCO(I),I=1,4)
    16      READ, MATRIX,TERMS
    17      DATA PI,PS/3.14159,62.0/
    18      DELTAT=PERIOD/60.
    19      DO 5 NN=1,4
    20      DO 5 JJ=1,4
    21    5 DTS(NN,JJ)=0.0
    22      M=SECTNS+1
    23      MM=M+1
    24      DO 10 NN=1,MM
    25   10 TFOLD(NN)=TCO(2)
    26      TFEND=TCO(2)
    27      LENGTH=TUBLEN/(FLOAT(SECTNS))
    28      X(1)=0.0
    29      DO 15 J=2,M
    30   15 X(J)=X(J-1)+LENGTH
    31      VOLUME=PI*DIAM*DIAM*HEIGHT/4.0
    32      MASS=PS*VOLUME
    33      MCPST=MASS/4.0
    34      AST=PI*DIAM*HEIGHT/4.0
    35      FLAG=0.
    36      ELOAD=0.0
    37      RT=0.0
    38      QUT=0.0
    39      DIST=0.0
    40      DISTO=0.0
    41      IPAGE=18
    42      MDC=0.0
    43      KNT=0
    44      PIPE=LIN
    45      TMTS=(TST(1)+TST(2)+TST(3)+TST(4))/4.
    46      MDCL=MDC
    47      TA1=TAMB(1)
    48      TIN=TA1
    49      CALL PRELIM(T,EC,REFIDX,ALPHA,AP,AB)
    50      I=1
    51      IHOUR=TIME/100
    52      IHOUR=IHOUR*100
    53   20 RI=RADTN(I)
    54      TA=TAMB(I)
```

```
      V=VEL(I)
      IF (KNT .EQ. 1) TIN=TST(4)
      TINOLD=TIN
      MDL=MDLO(I)*8.3/DELTAT
      CALL QABSOR(RI,AP,DELTAT,AB,SHADE,S,SB)
      CALL COPY1(TCO,TCOLD,4)
      CALL COPY1(TST,TSTOLD,4)
   30 MDCO=MDC
      IF (MATRIX .EQ. 0) GO TO 70
      CALL AMAX(MCP,MCG,MCINS,MCPAN,AC,S,SB,VF,SIGMA,V,CV,EMISG,
     1 EMISP,EMISPN,KINS,XINS,CP,TA,TIN,TFEND,TCOLD,MDC,A,F)
      CALL SOLVE(A,F,TCOLD,TERMS,DELTAT,TCO)
        GO TO 80
   70 CALL CNSOL(MCP,MCG,MCINS,MCPAN,AC,S,SB,VF,SIGMA,V,CV,MDC,EMISG,
     1 EMISP,EMISPN,KINS,XINS,CP,TA,TIN,TFEND,TCOLD,DELTAT,TCO)
   80 CALL ULOSS(TCO,TCOLD,TA,SIGMA,EMISG,EMISPN,V,PER,DEP,AC,
     1 CV,KINS,XINS,EMISP,TPA,UL)
      CALL FPRIME(UL,K,DELTA,LP,B,DI,TPA,DE,UC,FP)
      CALL TCDIST(DELTAT,W,CA,X,MDC,CP,TA1,I,TST,FP,TA,S,M,TF,UL,
     1  PIPE,DI,LENGTH,DIST,KNT,TIN,TFEND,TFOLD)
      CALL ADPRED(DELTAT,DTS,TSTOLD,TST)
      CALL DERVT(TST,MCPST,AST,MDC,CP,TFEND,MDL,US,TLOAD,TA,DERT)
      CALL ADCORR(DELTAT,DTS,DERT,TSTOLD,TST)
      CALL MFLOW(SECTNS,LENGTH,TF,TST,TIN,UP,DOWN,BE,TFB,TLB,
     1 LIN,LOUT,DYIN,DYOUT,H,HC,DI,SLOPE,FK,HEIGHT,IGATE,ITEE,ILONGC,
     2 ISTC,NGATE,NLONGC,NSTC,EG,ET,ELC,ESTC,MDC)
      IF (MDC-MDCO .EQ. 0.0) GO TO 60
      IF (ABS((MDC-MDCO)*2./(MDC+MDCO)) .GE. .02) GO TO 30
   60 CALL DERVT(TST,MCPST,AST,MDC,CP,TFEND,MDL,US,TLOAD,TA,DERT)
      CALL NEWVAL(DTS,DERT)
      TIME=TIME+PERIOD
      ICHECK=TIME-IHOUR-60
      IF (ICHECK .LT. 0) GO TO 50
      TIME=TIME+40
      IF(TIME.NE.1300.) GO TO 55
      TIME=0100.
      IHOUR=0
   55 IHOUR=IHOUR+100
   50 TMT=(TST(1)+TST(2)+TST(3)+TST(4))/4.
      GPH=MDC/8.3
      RI=AC*RI
      RT=RT+RI
      TRISE=((TF(M)+TFOLD(M))-(TIN+TINOLD))*.5
      QU=.5*(MDCL+MDC)*CP*TRISE*DELTAT
      QUT=QUT+QU
      ELOAD=ELOAD+(MDLO(I)*8.3*((.5*(TSTOLD(1)+TST(1)))-TLOAD))*CP
      EFF=(QU/RI)*100.
      IF(EFF.GE.100.) FLAG=1.
      MDCL=MDC
      DIST=DISTO+(4.*MDC*DELTAT/(PS*DI*DI*PI))
      IF (DIST .GE. PIPE) KNT=1
      DISTO=DIST
      IPAGE=IPAGE+1
      IF(IPAGE.NE.19) GO TO 57
      IPAGE=2
      WRITE(6,93)
      WRITE(6,94)
      WRITE(6,92)
      WRITE(6,91)
   57 CONTINUE
```

```
109          WRITE(6,90) TIME,MDLO(I),GPH,TIN,TF(M),TRISE,
            1 (TST(J),J=1,4),TMT,RI,QU,EFF
110          CALL COPY1(TF,TFOLD,M)
111          I=I+1
112          IF (I .LE. INTRVL) GO TO 20
113          EFFD=100.*QUT/RT
114          EFFS=(MASS*(TMT-TMTS)+ELOAD)/RT
115          EFFS=100.*EFFS
116          WRITE(6,95)
117          WRITE(6,96) RT,QUT,EFFD
118          WRITE(6,97) EFFS
119          IF(FLAG.EQ.1.) WRITE(6,99)
120          WRITE(6,98)
121       95 FORMAT('+',2X,127('-')//)
122       96 FORMAT('+',28X,'T O T A L S     F O R     T H E     D A Y :',
            1 26X,F8.1,3X,F8.1,6X,F4.1/////)
123       97 FORMAT('+',28X,'S Y S T E M     E F F I C I E N C Y     F O R
            1T H E     D A Y :',5X,F4.1,1X,'%')
124       90 FORMAT(' ',3X,I4,2(4X,F4.1),4X,F5.1,4X,F5.1,4X,F4.1,5(4X,F5.1),
            1   5X,F6.1,5X,F6.1,6X,F4.1//)
125       91 FORMAT('0',2X,127('-')//)
126       92 FORMAT(' ',3X,'(HRS)',3X,'(GAL)',3X,'(GPH)',4X,'('F)',5X,
            1   '('F)',4X,'('F)',5(5X,'('F)'),6X,'(BTU)',5X,'(BTU)',6X,
            2   '(%)')
127       93 FORMAT('1',3X,'REAL',4X,'LOAD',4X,'MASS',7X,'COLLECTOR',6X,
            1   'TEMP.',4X,4('TANK',5X),'MEAN',16X,'USEFUL',3X,'COLLECTOR')
128       94 FORMAT(' ',3X,'TIME',2(4X,'FLOW'),4X,'INLET',4X,'OUTLET',3X,
            1   'RISE',7X,'1',8X,'2',8X,'3',8X,'4',6X,'TANK',3X,'INSOLATION',
            2   4X,'GAIN',4X,'EFFICIENCY')
129       98 FORMAT('1')
130       99 FORMAT(10(/)'+',28X,'**** COLLECTOR EFFICIENCY HAS EQUALLED OR EX
            1CEEDED 100%.  THIS CONDITION'  /' ',34X,'CAN EXIST OVER A SMALL TI
            2ME INTERVAL DUE TO THE CAPACITANCE EFFECTS'/' ',34X,'OF THE COLLEC
            3TOR.  THIS MAY OCCUR WHEN THE ABSORBER HAS REACHED AN'/' ',34X, 'O
            4PERATING TEMPERATURE AND THE INCIDENT RADIATION SUDDENLY DROPS.')
131          STOP
132          END
     C
133          SUBROUTINE PRELIM(T,EC,REFIDX,ALPHA,AP,AB)
     C       THIS CALCULATES THE EFFECTIVE ABSORPTANCE OF THE COVER PLATE
     C       AND ABSORBER PLATE
134          REF=((REFIDX-1.0)/(REFIDX+1.0))**2.
135          EKL=EXP(-EC*T)
136          TAU=(1.-REF)*(1.-REF)*EKL
137          TAU=TAU/(1.-(REF*REF*EKL*EKL))
138          AB=(1.-REF)*(1.-EKL)/(1.-(REF*EKL))
139          AB=AB+AB*(TAU-(TAU*ALPHA/(1.-REF*(1.-ALPHA))))
140          AP=TAU*ALPHA/(1.-REF*(1.-ALPHA))
141          RETURN
142          END
     C
143          SUBROUTINE QABSOR(RI,AP,DELTAT,AB,SHADE,S,SB)
144          S=RI*AP*(1.-SHADE)/DELTAT
145          SB=RI*AB/DELTAT
146          RETURN
147          END
     C
```

```
148           SUBROUTINE COPY1(A,B,LL)
149           DIMENSION A(LL),B(LL)
150           DO 10 N=1,LL
151        10 B(N)=A(N)
152           RETURN
153           END
      C
154           SUBROUTINE ADPRED(H,DT,TOLD,T)
      C       THIS IS THE ADAMS MOULTON PREDICTOR
155           DIMENSION T(4),DT(4,4),TOLD(4)
156           DO 10 N=1,4
157        10 T(N)=TOLD(N)+H*(55.*DT(N,1)-59.*DT(N,2)+37.*DT(N,3)-9.*DT(N,4))/24
158           RETURN
159           END
      C
160           SUBROUTINE ADCORR(H,DT,DER,TOLD,T)
      C       THIS IS THE ADAMS MOULTON CORRECTOR
161           DIMENSION T(4),DER(4),DT(4,4),TOLD(4)
162           DO 10 N=1,4
163        10 T(N)=TOLD(N)+H*(9.*DER(N)+19.*DT(N,1)-5.*DT(N,2)+DT(N,3))/24.
164           RETURN
165           END
      C
166           SUBROUTINE NEWVAL(DT,DER)
      C       THIS RESETE THE VALUES OF THE DERIVATIVES FOR THE NEXT
      C          ADAMS MOULTON STEP
167           DIMENSION DT(4,4),OLD(4,4),DER(4)
168           DO 30 N=1,4
169           DO 30 J=1,4
170        30 OLD(N,J)=DT(N,J)
171           DO 10 N=1,4
172        10 DT(N,1)=DER(N)
173           DO 20 N=1,4
174           DO 20 J=2,4
175        20 DT(N,J)=OLD(N,J-1)
176           RETURN
177           END
      C
178           SUBROUTINE AMAX(MCP,MCG,MCINS,MCPAN,AC,S,SB,VF,SIGMA,V,CV,
             1 EMISG,EMISP,EMISPN,KINS,XINS,CP,TA,TIN,TFEND,TCOLD,MDC,A,F)
      C       THIS SETS UP THE A MATRIX FOR USE IN SOLVING THE
      C       DIFFERENTIAL EQUATIONS
179           DIMENSION TCOLD(4),A(4,4),F(4,1)
180           REAL MDC,KINS,MCP,MCG,MCINS,MCPAN
181           DR=459.67
182           DO 10 I=1,4
183           F(I,1)=0.0
184           DO 10 J=1,4
185           A(I,J)=0.0
186        10 CONTINUE
187           HPG=CV*ABS(TCOLD(2)-TCOLD(1))**.25
188           H1R=SIGMA*(TCOLD(1)+TCOLD(2)+2.*DR)*((TCOLD(2)+DR)**2.+
             1      (TCOLD(1)+DR)**2.)
189           H1R=H1R/((1./EMISP)+(1./EMISG)-1.)
190           H1=H1R*VF+HPG
191           H2=EMISG*SIGMA*(TCOLD(1)+TA+2.*DR)*((TCOLD(1)+DR)**2.+
```

```
     1      (TA+DR)**2.)
192          HWIND=1.+.3*V
193          H2=H2+HWIND
194          H3R=SIGMA*EMISPN*(TCOLD(4)+TA+2.*DR)*((TCOLD(4)+DR)**2.+
     1       (TA+DR)**2.)
195          A(1,1)=-(H1+H2)*AC/MCG
196          A(1,2)=H1*AC/MCG
197          A(2,1)=(H1R+HPG)*AC/MCP
198          A(2,2)=-(HPG+H1R+(2.*KINS/XINS))*AC/MCP
199          A(2,3)=2.*KINS*AC/(XINS*MCP)
200          A(3,2)=2.*KINS*AC/(XINS*MCINS)
201          A(3,3)=-2.*A(3,2)
202          A(3,4)=A(3,2)
203          A(4,3)=A(3,2)*MCINS/MCPAN
204          A(4,4)=-((2.*KINS/XINS)+HWIND+H3R)*AC/MCPAN
205          F(1,1)=(H2*TA+SB)*AC/MCG
206          F(2,1)=(AC*S-MDC*CP*(TFEND-TIN))/MCP
207          F(4,1)=AC*TA*(HWIND+H3R)/MCPAN
208          RETURN
209          END
     CC

210          SUBROUTINE SOLVE(A,F,TCOLD,K,DT,TCO)
211          DIMENSION A(4,4),F(4,1),XO(4,1),EAT(4,4),X(4,1),
     1 SUM(4,1),EATXO(4,1),EATSUM(4,1),TCOLD(4),TCO(4)
212          DO 10 I=1,4
213       10 XO(I,1)=TCOLD(I)
214          CALL EATINT(A,F,DT,K,EAT,SUM)
215          CALL MULT(EAT,XO,EATXO,4,4,1)
216          CALL MULT(EAT,SUM,EATSUM,4,4,1)
217          CALL ADD(EATXO,EATSUM,X,4,1)
218          DO 20 I=1,4
219       20 TCO(I)=X(I,1)
220          RETURN
221          END
     C

222          SUBROUTINE EATINT(A,F,DT,K,EAT,SUM)
223          DIMENSION A(4,4),F(4,1),Q(4,4),AN(4,4),AT(4,4),SUM(4,1),
     1 ANF(4,1),TEMP(4,4),AF(4,1),EAT(4,4)
224          DO 10 I=1,4
225          DO 10 J=1,4
226          EAT(I,J)=0.0
227          Q(I,J)=0.0
228          AN(I,J)=A(I,J)
229          IF (I .EQ. J) Q(I,J)=1.0
230       10 CONTINUE
231          CALL SCALAR(DT,F,SUM,4,1)
232          CALL SCALAR(DT,A,AT,4,4)
233          CALL ADD(Q,AT,EAT,4,4)
234          CALL MULT(A,F,AF,4,4,1)
235          COEF=-DT*DT/2.
236          CALL SCALAR(COEF,AF,AF,4,1)
237          CALL ADD(AF,SUM,SUM,4,1)
238          COEF=-COEF
239          KK=K-2
240          DO 20 N=1,KK
241          CALL MULT(A,AN,TEMP,4,4,4)
242          DO 99 III=1,4
243          DO 99 LLL=1,4
```

```
244      99  AN(III,LLL)=TEMP(III,LLL)
245          IF (N .GT. 1) COEF=DT/(N+1)
246          CALL SCALAR(COEF,AN,AN,4,4)
247          CALL ADD(AN,EAT,EAT,4,4)
248          CALL MULT(TEMP,F,ANF,4,4,1)
249          COEF=(COEF*DT/(N+2))*((-1.)**(N+1))
250          CALL SCALAR(COEF,ANF,ANF,4,1)
251          CALL ADD(ANF,SUM,SUM,4,1)
252      20  CONTINUE
253          RETURN
254          END
     C
255          SUBROUTINE SCALAR(SCALE,X,Z,L,M)
256          DIMENSION X(L,M),Z(L,M)
257          DO 10 I=1,L
258          DO 10 J=1,M
259      10  Z(I,J)=SCALE*X(I,J)
260          RETURN
261          END
     C
262          SUBROUTINE MULT(X,Y,Z,L,M,N)
263          DIMENSION X(L,M),Y(M,N),Z(L,N)
264          DO 10 I=1,L
265          DO 10 J=1,N
266          Z(I,J)=0.0
267          DO 20 K=1,M
268      20  Z(I,J)=Z(I,J)+X(I,K)*Y(K,J)
269      10  CONTINUE
270          RETURN
271          END

272          SUBROUTINE ADD(X,Y,Z,L,M)
273          DIMENSION X(L,M),Y(L,M),Z(L,M)
274          DO 10 I=1,L
275          DO 10 J=1,M
276      10  Z(I,J)=X(I,J)+Y(I,J)
277          RETURN
278          END
     C
279          SUBROUTINE CNSOL(MCP,MCG,MCINS,MCPAN,AC,S,SB,VF,SIGMA,V,CV,MDC,
            1   EMISG,EMISP,EMISPN,KINS,XINS,CP,TA,TIN,TFEND,TCOLD,DELTAT,TCO)
     C      THIS SUBROUTINE CALCULATES THE NODAL TEMPERATURES AT 'T+DELTA T'
     C      GIVEN THE TEMPERATURES AT 'T'.  IT UTILIZES THE IMPLICIT CRANK -
     C      NICHOLSON TECHNIQUE AND THE RECURSION FORMULA FOR SOLVING THE
     C      RESULTING SET OF SIMULTANEOUS LINEAR EQUATIONS.
280          DIMENSION TCO(4),TCOLD(4),TCOD(4,1),TC(4,1),A(4,4),ATCO(4,1),
            1   F(4,1),AP(4,4),FP(4,1),FF(4,1)
281          REAL IDENT(4,4),MDC,MCP,MCG,MCINS,MCPAN,KINS
282           DATA IDENT/1.,0.,0.,0.,0.,1.,0.,0.,0.,0.,1.,0.,0.,0.,0.,1./
283          CALL AMAX(MCP,MCG,MCINS,MCPAN,AC,S,SB,VF,SIGMA,V,CV,EMISG,
            1 EMISP,EMISPN,KINS,XINS,CP,TA,TIN,TFEND,TCOLD,MDC,A,F)
284          DO 10 I=1,4
285      10  TCOD(I,1)=TCOLD(I)
286          DELTAH=.5*DELTAT
287          CALL SCALAR(DELTAH,A,A,4,4)
288          CALL MULT(A,TCOD,ATCO,4,4,1)
289          CALL SCALAR(DELTAT,F,FF,4,1)
```

```
290           CALL ADD(TCOD,ATCO,ATCO,4,1)
291           CALL ADD(ATCO,FF,FF,4,1)
292           Z=-1.
293           CALL SCALAR(Z,A,A,4,4)
294           CALL ADD(IDENT,A,A,4,4)
295           CALL RECUR(A,FF,TC)
296           DO 20 I=1,4
297       20  TCOLD(I)=TC(I,1)
298           CALL AMAX(MCP,MCG,MCINS,MCPAN,AC,S,SB,VF,SIGMA,V,CV,EMISG,
                 1   EMISP,EMISPN,KINS,XINS,CP,TA,TIN,TFEND,TCOLD,MDC,AP,FP)
299           CALL ADD(F,FP,FP,4,1)
300           CALL SCALAR(DELTAH,FP,FP,4,1)
301           CALL ADD(ATCO,FP,FP,4,1)
302           CALL SCALAR(DELTAH,AP,AP,4,4)
303           CALL SCALAR(Z,AP,AP,4,4)
304           CALL ADD(IDENT,AP,AP,4,4)
305           CALL RECUR(AP,FP,TC)
306           DO 30 I=1,4
307       30  TCO(I)=TC(I,1)
308           RETURN
309           END
      C
310           SUBROUTINE RECUR(A,F,T)
      C     THIS SUBROUTINE CALCULATES THE MATRIX EQUATION A*T=F
      C     BY THE RECURSION FORMULA
311           DIMENSION A(4,4),F(4,1),T(4,1),AA(4),B(4),C(4),BETA(4),GAM(4)
312           DO 10 I=1,3
313           B(I)=A(I,I)
314           AA(I+1)=A(I+1,I)
315       10  C(I)=A(I,I+1)
316           B(4)=A(4,4)
317           BETA(1)=B(1)
318           GAM(1)=F(1,1)/BETA(1)
319           DO 20 I=2,4
320           BETA(I)=B(I)-(AA(I)*C(I-1))/BETA(I-1)
321       20  GAM(I)=(F(I,1)-AA(I)*GAM(I-1))/BETA(I)
322           T(4,1)=GAM(4)
323           DO 30 I=1,3
324           K=4-I
325       30  T(K,1)=GAM(K)-(C(K)*T(K+1,1))/BETA(K)
326           RETURN
327           END
      C
328           SUBROUTINE ULOSS(TCO,TCOLD,TA,SIGMA,EMISG,EMISPN,V,PER,DEP,AC,
                1 CV,KINS,XINS,EMISP,TPA,UL)
329           DIMENSION TCO(4),TCOLD(4),TAVE(4)
330           REAL KINS
331           DO 10 N=1,4
332       10  TAVE(N)=(TCO(N)+TCOLD(N))/2.
333           TPA=TAVE(2)
334           DIFF=(TAVE(2)-TA)
335           IF (DIFF .LT. 1.) GO TO 50
336           QRAD=SIGMA*((TAVE(2)+459.67)**4.-(TAVE(1)+459.67)**4.)
337           QRAD=QRAD/((1./EMISP)+(1./EMISG)-1.)
338           QCON=ABS(TAVE(2)-TAVE(1))
339           IF (QCON .LT. .001) GO TO 40
340           QCONV=(QCON**.25)*CV*(TAVE(2)-TAVE(1))
341           GO TO 45
```

```
342      40  QCONV=0.
343       45 QTOP=QRAD+QCONV
344          QREAR=2.*KINS*(TAVE(2)-TAVE(3))/XINS
345          QEDGE=.08*PER*DEP*(TAVE(2)-TA)/AC
346          QTOTAL=QTOP+QREAR+QEDGE
347          UL=QTOTAL/ABS(TAVE(2)-TA)
348          IF (UL .GT. 0.0) GO TO 60
349      50  UL=4.*SIGMA*(TA+459.67)**3/((1./EMISP)+(1./EMISG)-1.)
350          UL=UL+(.08*PER*DEP/AC)
351          UL=UL+(2.*KINS/XINS)
352      60  RETURN
353          END
         C
354          SUBROUTINE FPRIME(UL,K,DELTA,LP,B,DI,TPA,DE,UC,FP)
         C    THIS CALCULATES THE FIN EFFECIENCY FACTOR
355          REAL K,LP
356          IF (UL .LE. 0.0) GO TO 10
357          F=(TANH(SQRT(UL/(K*DELTA))*LP))/(SQRT(UL/(K*DELTA))*LP)
358          HF=4.3636*COND(TPA)/DI
359          FP=(B/((B-DE)*F))+(B*UL/UC)
360          FP=1./((1./FP)+(DE/B))
361          FP=FP+(B*UL/(3.14159*DI*HF))
362          FP=1./FP
363          GO TO 20
364       10 FP=1.0
365       20 RETURN
366          END
         C
367          FUNCTION COND(T)
         C    CALCULATE CONDUCTIVITY OF WATER AT SOME TEMP.
368          DATA A,B,C/-.138926E-5,.196771E-2,-.302238/
369          COND=(A*(T+459.67)+B)*(T+459.67)+C
370          RETURN
371          END
         C
372          SUBROUTINE TCDIST(DELTAT,W,CA,X,MDC,CP,TA1,I,TST,FP,TA,S,M,TF,UL,
            1  PIPE,DI,LENGTH,DIST,KNT,TIN,TFEND,TFOLD)
         C    THIS CALCULATES THE TEMP. DISTRIBUTION IN THE COLLECTOR
373          REAL MDC,LENGTH,LIN
374          DIMENSION TST(4) ,X(100),TF(100),TFOLD(100)
         C    **** FOR TWO SINUSOIDAL COLLECTORS IN PARALLEL,
         C         CHANGE 1 IN NEXT CARD TO 2
375          MDC=MDC/1.
376          DO 260 J=1,M
377          VALU=X(J)-((MDC*CP*DELTAT)/(W*CA))
378          IF (VALU .LT. 0.) GO TO 10
379          IF(I.GT.1) GO TO 70
380          TPLUS=TA1
381          TMINUS=TA1
382          GO TO 80
383      70  TPLUS=TFOLD(IFIX(VALU/LENGTH+2.0))
384          TMINUS=TFOLD(IFIX(VALU/LENGTH+1.00))
385      80  FRAC=VALU-X(IFIX(VALU/LENGTH+1.0))
386          VALUF=FRAC*(TPLUS-TMINUS)/LENGTH+TMINUS
387      90  RO=-FP*UL*DELTAT/CA
388          TF(J)=(EXP(RO))*(VALUF-(S/UL)-TA)+(S/UL)+TA
389          GO TO 260
```

```
390      10  IF (KNT .EQ. 1) GO TO 20
391          VALUF=TST(4)
392          PV=PIPE*VALU
393          IF (DIST .LT. PV) VALUF=TA1
394          GO TO 30
395      20  VALUF=TST(4)
396      30  TIME=X(J)*DELTAT/(X(J)-VALU)
397          RO=-FP*UL*TIME/CA
398          TF(J)=(EXP(RO))*(VALUF-(S/UL)-TA)+(S/UL)+TA
399      260 CONTINUE
400      120 TFEND=TF(M)
         C       **** FOR TWO SINUSOIDAL COLLECTORS IN PARALLEL,
         C            CHANGE 1 IN NEXT CARD TO 2
401          MDC=MDC*1.
402          RETURN
403          END
         C

404          SUBROUTINE DERVT(TST,MCPST,AST,MDC,CP,TFEND,MDL,US,TLOAD,TA,DERT)
         C       THIS CALCULATES DERIVATIVES OF THE TANK NODES
405          REAL MCPST,MDC,MDL
406          DIMENSION TST(4),DERT(4)
407          DERT(1)=((MDC*CP*(TFEND-TST(1)))-(MDL*CP*(TST(1)-TST(2)))-
            1 (AST*US*(TST(1)-TA)))/MCPST
408          DO 10 J=2,3
409       10 DERT(J)=((MDC*CP*(TST(J-1)-TST(J)))-(MDL*CP*(TST(J)-
            1 TST(J+1)))-(AST*US*(TST(J)-TA)))/MCPST
410          DERT(4)=((MDC*CP*(TST(3)-TST(4)))-(MDL*CP*(TST(4)-TLOAD))-
            1 (AST*US*(TST(4)-TA)))/MCPST
411          RETURN
412          END
         C

413          SUBROUTINE MFLOW(SECTNS,LENGTH,TF,TST,TIN,UP,DOWN,BE,L,LP,
            1 LIN,LOUT,DYIN,DYOUT,H,X,DI,SLOPE,FK,HEIGHT,IGATE,ITEE,
            2 ILONGC,ISTC,NGATE,NLONGC,NSTC,EG,ET,ELC,ESTC,MDC)
414          INTEGER SECTNS
415          REAL MDC,MDD
416          REAL TF(101),TST(4)
417          REAL L,LENGTH,LP,LOUT,LIN
418          DATA PI,PS,GRAV/3.141593,62.42,32.17/
419          DATA A,B,C/-.696536E-4,.659389E-1,46.8964/
420          DATA IPASS/1/
421          RO(DUMMY)=(A*(DUMMY+459.67)+B)*(DUMMY+459.67)+C
422          K=L/LENGTH
423          M=SECTNS-K
424          S=X/LP
425          SLOP=SIN(SLOPE)
426          HT=0.
427          F2S=0.
428          NS=1
429          NF=K
430       500 DO 520 J=NS,NF
431          DY=X/(2*LP)*LENGTH*SLOP
432          T=TF(J)
433          HT=HT-RO(T)*DY
434       520 CONTINUE
435          IF(J.GE.SECTNS) GO TO 600
436          J=K+1
         C       CALCULATION OF HT IN CURVED SECTIONS STARTS HERE
```

```
437     550  J=J+1
438          DY=(H+(2*LENGTH-BE)*S)*SLOP
439          T=TF(J)
440          HT=HT-RO(T)*DY
     C       CALCULATE FRICTION LOSS SUM TERM FOR CURVES
441          F2S=F2S+1./RO(T)**2
442          J=J+1
443          IF(J.LT.M) GO TO 560
444          NS=J
445          NF=SECTNS
446          GO TO 500
447     560  IF(J.EQ.(K+3)) EXCESS=L-LP
448          EXCESS=EXCESS+LP+BE
     C       CALCULATION OF HT FOR STRAIGHT SECTION
449     570  DY=S*LENGTH*SLOP
450          T=TF(J)
451          HT=HT-RO(T)*DY
452          J=J+1
     C       TEST TO SEE IF IT IS IN A BEND
453          IF((J*LENGTH-EXCESS).GT.LP) GO TO 550
454          GO TO 570
455     600  CONTINUE
     C       ADD TO HT THE CONTRIBUTION FRON THE TANK AND THE PIPES
456          T=TIN
457          HT=HT+RO(T)*DYIN
458          T=TF(SECTNS)
459          HT=HT-RO(T)*DYOUT
460          DY=HEIGHT/4.
461          TT=TST(1)
462          HT=HT+.5*(RO(T)+RO(TT))*((DY/2.)-DOWN)
463          DO 650 N=1,3
464          T=TST(N)
465          TT=TST(N+1)
466       650 HT=HT+.5*(RO(T)+RO(TT))*DY
467          TT=TST(4)
468          T=TIN
469          HT=HT+.5*(RO(T)+RO(TT))*((DY/2.)-UP)
470          HT=HT/PS
471          IF (HT .LE. 0.0) GO TO 580
     C       BEGIN CALCULATION OF FRICTION FACTORS FO & FT
472          F1S=0.
473          DO 620 J=1,SECTNS
474          T=TF(J)
475          F1S=F1S+VIS(T)*LENGTH/RO(T)**2
476     620  CONTINUE
     C       **** FOR TWO SINUSOIDAL COLLECTORS IN PARALLEL,
     C            CHANGE 1 IN NEXT CARD TO 2
477          FTEMP=F1S/1.
478          F1S=0.0
479          T=TF(1)
480          IF(IPASS.NE.1) GO TO 630
481          CALL EQUIVL(IGATE,ITEE,ILONGC,ISTC,NGATE,NLONGC,NSTC,
            1 EG,ET,ELC,ESTC,EQIN,EQOUT)
482          IPASS=2
     C       INCREASE F1S TO INCLUDE FRICTION IN THE INLET AND OUTLET PIPES
483          LIN=LIN+EQIN
484          LOUT=LOUT+EQOUT
485       630 F1S=F1S+VIS(T)*LIN/RO(T)**2
486          T=TF(SECTNS)
487          F1S=F1S+VIS(T)*LOUT/RO(T)**2
```

```
488           F1S=F1S+FTEMP
      C       **** FOR TWO SINUSOIDAL COLLECTORS IN PARALLEL,
      C            CHANGE 1 IN NEXT CARD TO 4
489           F2S=F2S/1.
490           FO=128./((DI**4)*PI*GRAV)*F1S
491           FT=8.*FK/(PI*PI*GRAV*(DI**4.))*F2S
492           MDC=(SQRT(FO*FO+4.*FT*HT)-FO)/(2*FT)
493           MDC =3600.*MDC
494           GO TO 590
495         580 MDC=0.0
496         590 CONTINUE
497           RETURN
498           END
      C

499           FUNCTION VIS(TEMP)
      C       CALCULATES THE ABSOLUTE VISCOSITY OF WATER AT TEMPERATURE 'T'
500           DATA ABSV20/1.002/
501           TC=(TEMP-32.0)/1.8
502           IF(TC.GE.20.) GO TO 700
503           T=(TC-20)
504           X=1301./((.00585*T+8.1855)*T+998.333)-3.30233
505           VIS=(10.**X)*.000672
506           RETURN
507          700  X= (1.3272*(20.-TC)-.001053*(TC-20.)**2)/(TC+105.)
508           VIS=(ABSV20*10.**X)*.000672
509           RETURN
510           END
      C

511           SUBROUTINE EQUIVL(IGATE,ITEE,ILONGC,ISTC,NGATE,NLONGC,NSTC,
             1 EG,ET,ELC,ESTC,EQIN,EQOUT)
      C       THIS SUBROUTINE CALCULATES THE EQUIVALENT LENGTHS OF PIPE
      C          CORRESPONDING TO THE ELBOWS,GATES, AND TESS IN THE INLET AND
      C          OUTLET PIPES.  IT RETURNS 2 VARIABLES, 1 FOR INLET AND 1 FOR
      C          THE OUTLET TO BE USED IN CALCULATING THE FIRCTION IN THE PIPES.
512           EQIN=IGATE*EG+ITEE*ET+ILONGC*ELC+ISTC*ESTC
513           EQOUT=NGATE*EG+NLONGC*ELC+NSTC*ESTC
514           RETURN
515           END
      C

      $ENTRY
```

REAL TIME (HRS)	LOAD FLOW (GAL)	MASS FLOW (GPH)	COLLECTOR INLET (°F)	COLLECTOR OUTLET (°F)	TEMP. RISE (°F)	TANK 1 (°F)	TANK 2 (°F)	TANK 3 (°F)	TANK 4 (°F)	MEAN TANK (°F)	INSOLATION (BTU)	USEFUL GAIN (BTU)	COLLECTOR EFFICIENCY (%)
910	0.0	0.3	75.0	76.0	0.5	75.0	75.0	75.0	75.0	75.0	78.5	0.1	0.1
920	0.0	1.2	75.0	79.1	2.6	75.0	75.0	75.0	75.0	75.0	235.2	2.7	1.1
930	0.0	2.4	75.0	84.0	6.6	75.1	75.0	75.0	75.0	75.0	390.9	16.4	4.2
940	0.0	3.7	75.0	90.2	12.1	75.4	75.0	75.0	75.0	75.1	544.9	51.2	9.4
950	0.0	5.0	75.0	97.4	18.8	76.1	75.0	75.0	75.0	75.3	696.6	113.8	16.3
1000	0.0	6.3	75.0	105.5	26.5	77.3	75.1	75.0	75.0	75.6	845.2	207.0	24.5
1010	0.0	7.3	75.0	112.8	34.1	79.1	75.3	75.0	75.0	76.1	990.3	320.3	32.3
1020	0.0	7.8	75.0	116.3	39.5	81.3	75.6	75.1	75.0	76.8	1131.2	412.2	36.4
1030	0.0	8.3	75.0	119.8	43.1	83.8	76.1	75.1	75.0	77.5	1267.1	479.0	37.8
1040	0.0	8.8	75.0	123.3	46.5	86.4	76.7	75.2	75.0	78.3	1397.7	549.2	39.3
1050	0.0	9.2	75.0	126.4	49.8	89.2	77.5	75.4	75.1	79.3	1522.3	618.8	40.6
1100	0.0	9.6	75.1	129.3	52.8	92.2	78.5	75.6	75.1	80.3	1640.3	685.1	41.8
1110	0.0	9.9	75.1	132.0	55.6	95.2	79.8	75.9	75.2	81.5	1751.4	747.9	42.7
1120	0.0	10.2	75.2	134.5	58.1	98.3	81.1	76.2	75.2	82.7	1854.9	806.8	43.5
1130	0.0	10.4	75.2	136.7	60.4	101.5	82.7	76.7	75.3	84.1	1950.5	861.6	44.2
1140	0.0	10.7	75.3	138.8	62.4	104.6	84.5	77.3	75.5	85.5	2037.7	911.9	44.7
1150	0.0	10.9	75.5	140.7	64.2	107.6	86.4	78.0	75.7	86.9	2116.2	956.9	45.2

REAL TIME (HRS)	LOAD FLOW (GAL)	MASS FLOW (GPH)	COLLECTOR INLET (°F)	COLLECTOR OUTLET (°F)	TEMP. RISE (°F)	TANK 1 (°F)	TANK 2 (°F)	TANK 3 (°F)	TANK 4 (°F)	MEAN TANK (°F)	INSOLATION (BTU)	USEFUL GAIN (BTU)	COLLECTOR EFFICIENCY (%)
1200	0.0	11.1	75.7	142.7	66.0	110.6	88.4	78.9	75.9	88.4	2185.7	1001.4	45.8
1210	0.0	11.2	75.9	144.4	67.6	113.5	90.5	79.8	76.3	90.0	2245.8	1042.2	46.4
1220	0.0	11.3	76.3	145.5	68.7	116.4	92.7	80.9	76.6	91.7	2296.2	1067.8	46.5
1230	0.0	11.3	76.6	146.6	69.4	119.0	95.0	82.1	77.1	93.3	2336.9	1084.4	46.4
1240	0.0	11.4	77.1	147.6	70.0	121.6	97.3	83.4	77.6	95.0	2367.5	1098.6	46.4
1250	0.0	11.4	77.6	148.4	70.4	124.0	99.6	84.8	78.2	96.6	2388.0	1106.3	46.3
100	0.0	11.3	78.2	149.0	70.5	126.2	102.0	86.2	78.9	98.3	2398.3	1107.2	46.2
110	0.0	11.3	78.9	149.5	70.4	128.3	104.3	87.8	79.6	100.0	2398.3	1102.6	46.0
120	0.0	11.2	79.6	149.8	70.0	130.2	106.5	89.4	80.5	101.7	2388.0	1091.9	45.7
130	0.0	11.1	80.5	150.0	69.5	132.0	108.8	91.0	81.3	103.3	2367.5	1074.7	45.4
140	0.0	11.0	81.3	150.0	68.7	133.6	110.9	92.7	82.3	104.9	2336.9	1052.1	45.0
150	0.0	10.9	82.3	149.9	67.7	135.0	113.0	94.4	83.3	106.4	2296.2	1024.5	44.6
200	0.0	10.7	83.3	149.6	66.5	136.3	114.9	96.1	84.4	107.9	2245.8	991.2	44.1
210	0.0	10.5	84.4	149.2	65.0	137.4	116.8	97.8	85.5	109.4	2185.7	952.6	43.6
220	0.0	10.4	85.5	148.9	63.6	138.3	118.6	99.5	86.6	110.7	2116.2	917.6	43.4
230	0.0	10.2	86.6	148.4	62.1	139.1	120.2	101.1	87.7	112.0	2037.7	883.5	43.4
240	0.0	10.0	87.7	148.0	60.5	139.8	121.8	102.7	88.9	113.3	1950.5	844.3	43.3

REAL TIME (HRS)	LOAD FLOW (GAL)	MASS FLOW (GPH)	COLLECTOR INLET (°F)	COLLECTOR OUTLET (°F)	TEMP. RISE (°F)	TANK 1 (°F)	TANK 2 (°F)	TANK 3 (°F)	TANK 4 (°F)	MEAN TANK (°F)	INSOLATION (BTU)	USEFUL GAIN (BTU)	COLLECTOR EFFICIENCY (%)
250	0.0	9.6	88.9	146.6	58.4	140.4	123.2	104.3	90.0	114.5	1854.9	790.6	42.6
300	0.0	9.2	90.0	145.0	55.8	140.8	124.5	105.8	91.2	115.6	1751.4	723.9	41.3
310	0.0	8.8	91.2	143.4	53.1	141.0	125.7	107.2	92.3	116.5	1640.3	658.9	40.2
320	0.0	8.3	92.3	141.7	50.2	141.1	126.7	108.5	93.4	117.4	1522.3	593.9	39.0
330	0.0	7.8	93.4	139.6	47.2	141.0	127.6	109.7	94.4	118.2	1397.7	527.0	37.7
340	0.0	7.2	94.4	136.9	43.8	140.8	128.4	110.8	95.4	118.9	1267.1	454.1	35.8
350	0.0	6.5	95.4	134.5	40.3	140.5	129.1	111.8	96.3	119.4	1131.2	381.8	33.8
400	0.0	5.8	96.3	131.6	36.8	140.1	129.6	112.7	97.1	119.9	990.3	313.5	31.7
410	0.0	4.9	97.1	128.4	32.9	139.6	130.0	113.4	97.8	120.2	845.3	244.3	28.9
420	0.0	3.9	97.8	124.8	28.8	139.1	130.4	114.0	98.4	120.5	696.6	174.9	25.1
430	0.0	2.5	98.4	120.7	24.4	138.6	130.5	114.5	98.8	120.6	544.9	107.9	19.8
440	0.0	0.7	98.8	116.4	19.8	138.3	130.6	114.7	99.0	120.6	390.9	44.9	11.5
450	0.0	0.0	99.0	111.0	14.7	138.2	130.6	114.7	99.0	120.6	235.2	7.5	3.2
500	0.0	0.0	99.0	104.4	8.7	138.1	130.6	114.6	99.0	120.6	78.5	0.0	0.0
			TOTALS FOR THE DAY:								73338.4	30206.7	41.2

SYSTEM EFFICIENCY FOR THE DAY: 40.7 %

FOOTNOTES

[1]H. C. Hottel and B. B. Woertz, "The Performance of Flat Plate Solar Heat Collectors," Transactions of the American Society of Mechanical Engineers 64 (February 1942): 91-104.

[2]H. Tabor, "Solar Energy Collector Design," Transactions of the Conference on the Use of Solar Energy 2 (1958): 1-23.

[3]D. J. Close, "The Performance of Solar Water Heaters with Natural Circulation," Solar Energy 6 (1962): 33-40.

[4]C. L. Gupta and H. P. Garg, "System Design in Solar Water Heaters with Natural Circulation," Solar Energy 12 (1960): 163-182.

[5]Thomas L. Hartman, III, "Computer Aided Analysis of Flat Plate Solar Collectors" (Masters thesis, Florida Technological University, 1975).

[6]Austin Whillier and G. Saluja, "The Thermal Performance of Solar Water Heaters," Solar Energy 9 (1965): 21-26.

[7]S. A. Klein, J. A. Duffie, and W. A. Beckman, "Transient Considerations of Flat Plate Solar Collectors," Transactions of the American Society of Mechanical Engineers Journal of Engineering for Power 96 (April 1974): 109.

[8]Raymond W. Bliss, "The Derivation of Several 'Plate Efficiency Factors' Useful in the Design of Flat Plate Solar Heat Collectors," Solar Energy 3 (1959): 55-64.

[9]John A. Duffie and William A. Beckman, Solar Energy Thermal Processes (New York: Wiley Interscience, 1974), pp. 108-115.

[10]Hartman, "Computer Aided Analysis of Flat Plate Solar Collectors," pp. 19-27.

[11]Hottel and Woertz, "The Performance of Flat Plate Solar Heat Collectors," pp. 91-104.

[12]Duffie and Beckman, Solar Energy Thermal Processes, p. 15.

[13]Klein et al., "Transient Considerations of Flat Plate Solar Collectors," p. 111.

[14]Bliss, "The Derivation of Several 'Plate Efficiency Factors' Useful in the Design of Flat Plate Solar Heat Collectors," p. 60.

[15]S. I. Abdel-Khalik, "Heat Removal Factor for a Flat Plate Solar Collector with a Serpentine Tube," Solar Energy 18 (1976): 59-64.

[16]R. Siegel and J. Howell, Thermal Radiation Heat Transfer (New York: McGraw-Hill, 1972), p. 785.

[17]U.S., Congress, House, Committee on Science and Technology, Hearings before the Subcommittee on Energy Research, Development and Demonstration. 94th Cong., 1st sess., 1975, p. 382.

[18]Ibid., p. 382.

[19]Ibid., p. 383.

[20]Close, "The Performance of Solar Water Heaters with Natural Circulation," p. 36.

[21]Chemical Rubber Company Handbook of Chemistry and Physics, 49th ed., s.v. "The Viscosity of Water from $0^{\circ}C$ to $100^{\circ}C$."

[22]Close, "The Performance of Solar Water Heaters with Natural Circulation," pp. 33-40.

[23]Jeffrey B. Pearce, "Analytical and Experimental Investigation of Pumped Solar Hot Water Systems" (Masters thesis, Florida Technological University, 1976).

[24]Frank Ayres, Theory and Problems of Differential Equations (New York: Shaum Publishing Co., 1952), p. 238.

[25]U.S., Congress, House, Committee on Science and Technology, Hearings before the Subcommittee on Energy Research, Development and Demonstration, p. 382.

[26]Ibid., p. 382.

[27]Ayres, Theory and Problems of Differential Equations, p. 157.

[28]Richard Bronson, Matrix Methods (New York: Academic Press, 1970), pp. 153-155.

[29]Ibid., p. 122.

[30]T. R. McCalla, Introduction to Numerical Methods and Fortran Programming (New York: John Wiley and Sons, 1967).

[31]C. F. Gerald, Applied Numerical Analysis (Reading, Massachusetts: Addison-Wesley Publishing Co., 1970).

[32]Ibid., p. 127.

[33]Glen E. Meyers, Analytical Methods in Conduction Heat Transfer (New York: McGraw-Hill, 1971), pp. 275-287.

BIBLIOGRAPHY

Abdel-Khalik, S. I. "Heat Removal Factor for a Flat Plate Solar Collector with a Serpentine Tube." Solar Energy 18 (1976): 59-64.

Ayres, Frank. Theory and Problems of Differential Equations. New York: Shaum Publishing Co., 1952.

Bliss, Raymond. "The Derivation of Several 'Plate Efficiency Factors' Useful in the Design of Flat Plate Solar Heat Collectors." Solar Energy 3 (1959): 55-64.

Bronson, Richard. Matrix Methods. New York: Academic Press, 1970.

Chemical Rubber Company Handbook of Chemistry and Physics, 49th ed. S.v. "The Viscosity of Water from 0°C to 100°C."

Close, D. J. "The Performance of Solar Water Heaters with Natural Circulation." Solar Energy 6 (1962): 33-40.

Duffie, John A., and Beckman, William A. Solar Energy Thermal Processes. New York: Wiley Interscience, 1974.

Gerald, C. F. Applied Numerical Analysis. Reading, Massachusetts: Addison-Wesley Publishing Co., 1970.

Gupta, C. L., and Garg, H. P. "System Design in Solar Water Heaters with Natural Circulation." Solar Energy 12 (1968): 163-182.

Hartman, Thomas L. III. "Computer Aided Analysis of Flat Plate Solar Collectors. Masters thesis, Florida Technological University, 1975.

Hottel, H. C., and Woertz, B. B. "The Performance of Flat Plate Solar Heat Collectors." Transactions of the American Society of Mechanical Engineers 64 (February 1942): 91-104.

Klein, S. A.; Duffie, J. A.; and Beckman, W. A. "Transient Considerations of Flat Plate Solar Collectors." Transactions of the American Society of Mechanical Engineering Journal of

Engineering for Power 96 (April 1974): 109-112.

McCalla, T. R. Introduction to Numerical Methods and Fortran Programming. New York: John Wiley and Sons, 1967.

Meyers, Glen E. Analytical Methods in Conduction Heat Transfer. New York: McGraw-Hill, 1971.

Pearce, Jeffrey B. "Analytical and Experimental Investigation of Pumped Solar Hot Water System." Masters thesis, Florida Technological University, 1976.

Seigel, Robert, and Howell, John. Thermal Radiation Heat Transfer. New York: McGraw-Hill, 1972.

Tabor, H. "Solar Energy Collector Design." Transactions of the Conference on the Use of Solar Energy 2 (1958): 1-23.

U.S. Congress. House. Committee on Science and Technology. Hearings before the Subcommittee on Energy Research, Development and Demonstration, 94th Cong., 1st sess., 1975.

Whillier, Austin, and Saluja, G. "The Thermal Performance of Solar Water Heaters." Solar Energy 9 (1965): 21-26.